ZONGULDAK BÜLENT ECEVİT UNIVERSITY

GRADUATE SCHOOL OF NATURAL AND APPLIED SCIENCES

LEGENDRIAN WHITEHEAD LINKS

DEPARTMENT OF MATHEMATICS

DOCTOR OF PHILOSOPHY THESIS

ECE GÜLŞAH ÇOLAK

December 2021

ZONGULDAK BÜLENT ECEVİT UNIVERSITY

GRADUATE SCHOOL OF NATURAL AND APPLIED SCIENCES

LEGENDRIAN WHITEHEAD LINKS

DEPARTMENT OF MATHEMATICS

DOCTOR OF PHILOSOPHY THESIS

Ece Gülşah ÇOLAK

ADVISOR: Prof. Dr. Yusuf KAYA

CO-ADVISOR: Prof. Dr. John B. ETNYRE

ZONGULDAK

December 2021

APPROVAL OF THE THESIS:

The thesis entitled "Legendrian Whitehead Links" and submitted by Ece Gülşah ÇOLAK has been examined and accepted by the jury as a Doctor of Philosophy thesis in Department of Mathematics, Graduate School of Natural and Applied Sciences, Zonguldak Bülent Ecevit University. 17/12/2021

Advisor: Prof. Dr. Yusuf KAYA   ....
Zonguldak Bülent Ecevit University, Faculty of Arts and Science, Department of Mathematics

Member: Prof. Dr. Burak ÖZBAĞCI   ....
Koç University, College of Science, Department of Mathematics

Member: Prof. Dr.Yüksel SOYKAN   ....
Zonguldak Bülent Ecevit University, Faculty of Arts and Science, Department of Mathematics

Member: Prof. Dr. Sinem ONARAN   ....
Hacettepe University, Faculty of Science, Department of Mathematics

Member: Assist. Prof. Dr. Can Murat DİKMEN   ....
Zonguldak Bülent Ecevit University, Faculty of Arts and Science, Department of Mathematics

---

Approved by the Graduate School of Natural and Applied Sciences.   ..../..../202..

Prof. Dr. Ahmet ÖZARSLAN
Director

"With this thesis it is declared that all the information in this thesis is obtained and presented according to academic rules and ethical principles. Also as required by the academic rules and ethical principles all works that are not result of this study are cited properly."

Ece Gülşah ÇOLAK

ABSTRACT

Doctor of Philosophy Thesis

LEGENDRIAN WHITEHEAD LINKS
Ece Gülşah ÇOLAK

Zonguldak Bülent Ecevit University
Graduate School of Natural and Applied Sciences
Department of Mathematics

Thesis Advisor: Prof. Dr. Yusuf KAYA
Thesis Co-Advisor: Prof. Dr. John B. ETNYRE
December 2021, 85 pages

In this thesis we classify Legendrian positive Whitehead links in S^3 with the standard tight contact structure, (S^3, ξ_{std}), up to Legendrian isotopy. By using the convex surface theory on contact $3-$manifolds we show how one can destabilize Legendrian positive Whitehead links in (S^3, ξ_{std}) until each component of it has Thurston-Bennequin number is -1. We also show that there are two Legendrian representatives of the positive Whitehead link with maximal Thurston-Bennequin number, $tb = -2$ and the same rotation number, $r = 0$. In addition to these, we show that the components can be interchanged by a Legendrian isotopy and the two different representatives of the positive Whitehead link with maximal Thurston-Bennequin number become the same after one single (positive or negative) stabilization. These results exhibit that Legendrian positive Whitehead links in (S^3, ξ_{std}) are not Legendrian simple.

Keywords: Contact structures, Legendrian knots, convex surfaces, bypass, Legendrian isotopy.

Science Code: 403.04.01

ÖZET

Doktora Tezi

LEGENDRE WHITEHEAD LİNKLERİ

Ece Gülşah ÇOLAK

Zonguldak Bülent Ecevit Üniversitesi
Fen Bilimleri Enstitüsü
Matematik Anabilim Dalı

Tez Danışmanı: Prof. Dr. Yusuf KAYA
Tez Eş Danışmanı: Prof. Dr. John B. ETNYRE
Aralık 2021, 85 sayfa

Bu tez çalışmasında, standart tayt kontak yapılı $3-$boyutlu S^3 küresi içerisindeki Legendre pozitif Whitehead linkleri Legendre izotopisi altında sınıflandırdık. Kontak $3-$manifoldlarda konveks yüzey teorisini kullanarak (S^3, ξ_{std}) içerisindeki Legendre pozitif Whitehead linklerinin her bir bileşeninin Thurston-Bennequin sayısının -1 olana kadar nasıl destabilize olabildiğini gösterdik. Ayrıca, $tb = -2$ olacak şekilde maksimum Thurston-Bennequin sayısına sahip $r = 0$ olacak şekilde aynı rotasyon sayılı positive Whitehead linkin iki tane Legendre temsilcisi olduğunu gösterdik. Bunların yanında linkin bileşenlerinin bir Legendre izotopi altında yer değiştirebileceğini ve maksimum Thurston-Bennequin sayısına sahip iki farklı temsilcinin tek bir stabilizasyon (pozitif veya negatif) altında aynı olduklarını ispatladık. Tüm bu sonuçlar, (S^3, ξ_{std}) içerisindeki Legendre pozitif Whitehead linklerinin yalın Legendre olmadığını göstermektedir.

ÖZET (devam ediyor)

Keywords: Kontak yapılar, Legendre düğümler, konveks yüzeyler, baypas, Legendre izotopi.

Science Code: 403.04.01

ACKNOWLEDGEMENTS

TABLE OF CONTENTS

LIST OF FIGURES

CHAPTER 1

INTRODUCTION

This thesis research lies in the areas of contact geometry, low-dimensional topology, and the knot theory. The geometry of contact structures can be used to answer significant problems in topology. In the other direction, topological methods have an important role in contact geometry. Huygens' (1690) principle in geometric optics can be considered as containing fundamental ideas of contact geometry, but contact structures on manifolds were first introduced by Sophus Lie (1872), under the influence Felix Klein, for the study of partial differential equations. Later, they arose again in the field of thermodynamics, geometric optics, and control theory and contact geometry showed up as its own specific field in the beginning of 1950s. More recently, they have been seen to have relations with low-dimensional topology, which is why we are interested in considering Legendrian links in $3-$dimensional contact manifolds. These special subclasses of links, which have many applications, have some certain properties regarding the contact structure and exhibit the topology and geometry of the underlying $3-$manifold. The main problem in the Legendrian Link Theory is given a topological link type in a contact $3-$manifold, to classify Legendrian links in this link type up to Legendrian isotopy. Thurston-Bennequin (tb) and the rotation number (r) invariants are two classical invariants for Legendrian links.

Some work about the classification of Legendrian links has been established by Eliashberg and Fraser (1995), [8], for Legendrian unknots, Etnyre and Honda (2001), [12], for Legendrian torus knots and figure eight knots in any tight contact manifold, Ding and Geiges (2007), [5], for Legendrian cable links, Dalton (2008), [4], for Legendrian torus links, Etnyre, LaFountain and Tosun (2012), [14], for Legendrian cable of positive torus knots, Etnyre et al. (2013), [15], for Legendrian positive twist knots, Tosun (2013), [30], for Legendrian $(p, q)-$cable knots, Etnyre and Vertesi (2017), [13], for Legendrian satellites, in the standard tight contact $3-$sphere. Onaran (2018), [28], worked on Legendrian torus

knots in Lens spaces and Geiges and Onaran (2020), [19], worked on Legendrian Hopf links in any contact structure on contact $3-$sphere. Classical invariants of Legendrian links distinguish different classes of them, but two Legendrian links which have the same classical invariants do not need to be Legendrian isotopic according to the Chekanov-Eliashberg's examples [2, 7]. In this thesis, our goal is to classify Legendrian positive Whitehead Links in the standard tight contact $3-$sphere.

Definition 1.1 *A **Whitehead Link** is a combination of two projections of the unknot.*

(a)   (b)
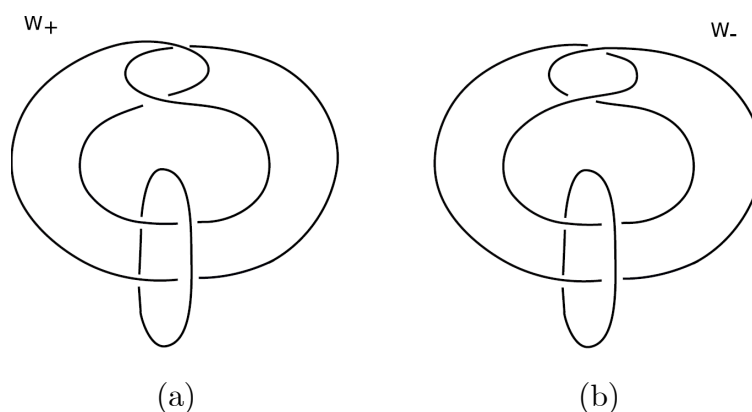
Figure 1.1 a) A Link diagram of the positive Whitehead link (mirror of the Whitehead link), b) A Link diagram of the (negative) Whitehead link.

We will denote the Whitehead link as W_- and the mirror of Whitehead link as W_+ because of the negative crossing and positive crossing in the diagram of the component with crossings, respectively. The Whitehead link was known long ago, but named after J.W.Whitehead, who employed this link in the construction of the Whitehead manifold which is an open, contractible $3-$manifold, that is not homeomorphic to $\mathbb{R}^3$.

Another diagram of the Whitehead link is represented as in Figure 1.2, which is topologically isotopic to W_-.
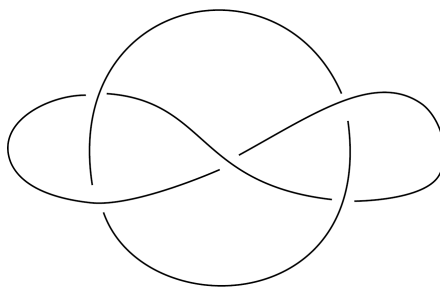
Figure 1.2 Another link diagram of the Whitehead link.

An upper bound on the tb invariant for Legendrian links in terms of the Kauffman polynomials of the links was first observed by Lee Rudolph [27]. For concerned inequailty related to bound on tb, some alternative proofs with different approaches were exhibited in [3, 16, 17]. This inequailty states that tb is not bigger than the minimal degree in the variable x of the Kauffman polynomial:

$$tb \leq -\max \deg_x K.$$

We obtain from [21] that $tb(W_-) \leq -5$ for any Legendrian representation of W_- since the Kauffman polynomial of W_- is given by

$$
\begin{aligned}
K_{W_-}(x,y) \ = \ & yx^5 - 2x^4 - (2y^3 + 6y)x^3 + (-y^4 - y^2 + 6 + y^{-2})x^2 \\
& + (3y^3 + 9y + 2y^{-1})x + (y^4 + y^2 - 5 - 2y^{-2}) \\
& - (y^3 + 4y - 2y^{-1})x^{-1} + (2 + y^{-2})x^{-2}.
\end{aligned}
$$

Hence, we cannot realize W_- with components consisting of Legendrian unknots with maximal tb. This was first observed by Mohnke in [21].

Figure 1.3 illustrates Legendrian fronts of these two Whitehead links in the same knot type, respectively, which have the same total tb and r. In this figure, the components have different tb and r invariants: we have $tb(M_1) = -1$, $tb(M_2) = -4$ and $tb(L_1) = -3$, $tb(L_2) = -2$.
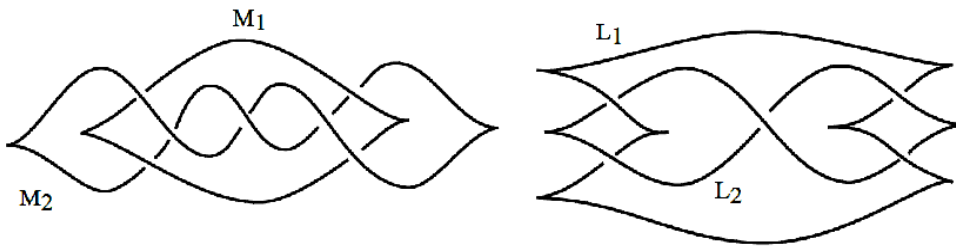
Figure 1.3 Two fronts of Legendrian Whitehead links with maximal $tb = -5$.

The Kauffman polynomial gives only a trivial bound for the mirror of Whitehead link W_+. It can be represented as a Legendrian link of Legendrian unknots each of which has $tb = -1$.

In general, very little is known related to realizing Legendrian links with given Legendrian knot components and the restrictions on Thurston-Bennequin invariants. In this thesis, we will try to find the complete classification of the Legendrian Positive Whitehead links

by using the strategy in Chapter 3 and convex surface theory which we will consider in Chapter 2. In Chapter 4, we will obtain the following results.

Theorem 1.1 (Classification Theorem) *There are two Legendrian representatives of oriented positive Whitehead link W_+ with maximal Thurston-Bennequin number shown in the Figure 1.4 and they become the same after a single (positive or negative) stabilization. All other representatives destabilize to one of the maximal Thurston-Bennequin number representatives and are determined by the Thurston-Bennequin number and the rotation number. Moreover, the components shown in Figure 1.5 can be interchanged by a Legendrian isotopy.*
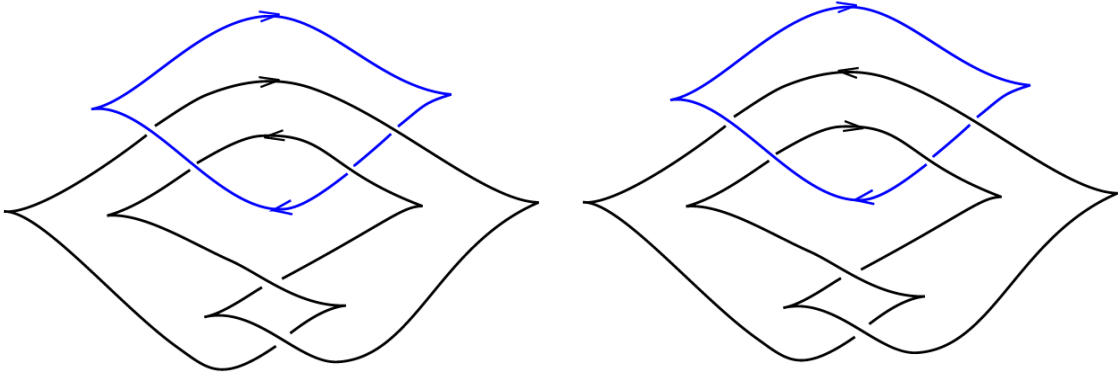
Figure 1.4 The two Legendrian representatives of W_+ with maximal $tb = -2$ and components both having $tb = -1$, $r = 0$.

The Classification theorem follows from the next 4 results.

Theorem 1.2 *Given a Legendrian positive Whitehead link W_+, then this link can be destabilized until each component has $tb = -1$.*

Theorem 1.3 *There is a unique Legendrian representative of W_+ with maximal Thurston–Bennequin number, $tb = -2$ if orientations are ignored. This representative has rotation number $r = 0$.*

Theorem 1.4 *Given the Legendrian link L in the knot type W_+ with $tb = -2$, the components of L can be interchanged by Legendrian isotopy as indicated in Figure 1.5 taking orientations on the components into account.*
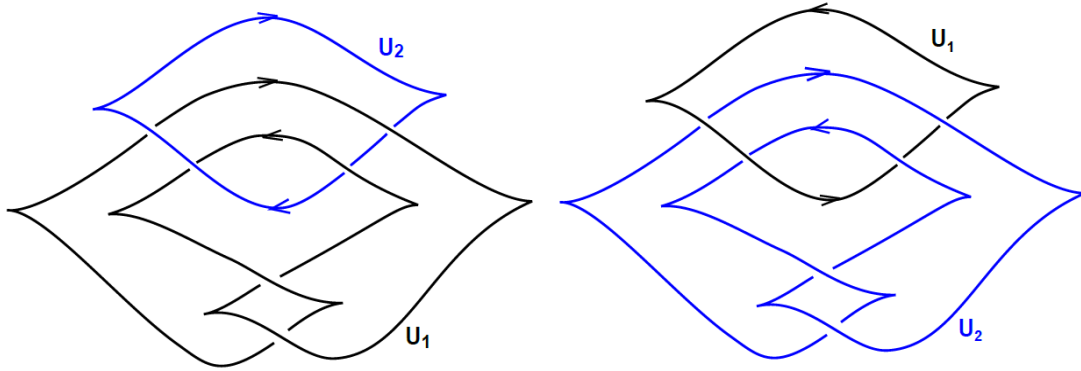
Figure 1.5 Legendrian isotopic two Legendrian W_+ with $tb = -2$.

Theorem 1.5 *There are two Legendrian representatives of positive Whitehead link W_+ with maximal Thurston-Bennequin number shown in the Figure 1.4 and they become the same after a single (positive or negative) stabilization.*

Two key lemmas in the proof of these theorems are the following.

Lemma 1.6 *Given any Legendrian L in the knot type W_+ such that $L = U_1 \cup U_2$, the U_2 component of L can be destabilized in the complement of U_1 until it has $tb = -1$.*

The dividing set on A mentioned in the next lemma is defined in chapter 4.

Lemma 1.7 *When $tb(U_2) = -1$ then we can assume the dividing set on A is in Figure 1.6.*
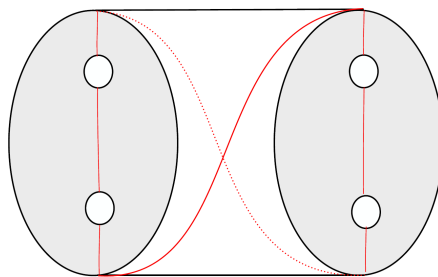
Figure 1.6 The dividing curve on A when $tb(U_2) = -1$.

The classification of the Legendrian negative Whitehead links is an important problem too, which we work on for future research.

CHAPTER 2

BACKGROUND

In this chapter, we review some of the definitions and theorems which are needed throughout the thesis and mainly use the sources [10], [11], [18] and [29].

2.1 CONTACT STRUCTURES

Although contact structures are defined for odd-dimensional manifolds, we will only consider contact structures on $3-$manifolds.

Definition 2.1 *A contact structure ξ on an oriented $3-$manifold M is given by a field of hyperplanes (i.e. a codimension-1 sub-bundle of the tangent bundle TM) which is nowhere integrable. The pair (M,ξ) is called a contact $3-$manifold.*

Locally a hyperplane field can always be written as the kernel of a non-vanishing $1-$form α, i.e., for every point in M, there is a neighborhood U and a $1-$form α defined on U such that $\xi_x = \ker(\alpha_x)$ for all $x \in U$. The $1-$form α satisfies the Frobenius integrability condition $\alpha \wedge d\alpha = 0$ iff ξ is an integrable hyperplane field. From this point of view, ξ is a contact structure on M if any locally $1-$form α defining ξ satisfies $\alpha \wedge d\alpha \neq 0$. The condition $\alpha \wedge d\alpha \neq 0$ (non-integrability) is independent of choosing α and implies that ξ is not everywhere tangent to any surface along an open subset of the surface. So one may think that the hyperplanes twist too much to be tangent to surfaces as is seen in Figure 2.1. If ξ is orientable, it is possible to write $\xi = \ker(\alpha)$ globally.

Example 2.1 *The standard contact structure on $\mathbb{R}^3$ is given by*

$$\xi_{st} = \ker(dz - ydx) = span\left\{\frac{\partial}{\partial y}, \frac{\partial}{\partial x} + y\frac{\partial}{\partial z}\right\}$$

with Cartesian coordinates (x, y, z). The plane fields along $xz-$plane are all parallel to $xy-$plane. We have a horizontal plane at the origin and as we move along the $y-$axis the

7

planes twist around the $y-$axis in a left hand manner. Moving through the y axis from origin to infinity the planes will make a $\pi/2$ twist.
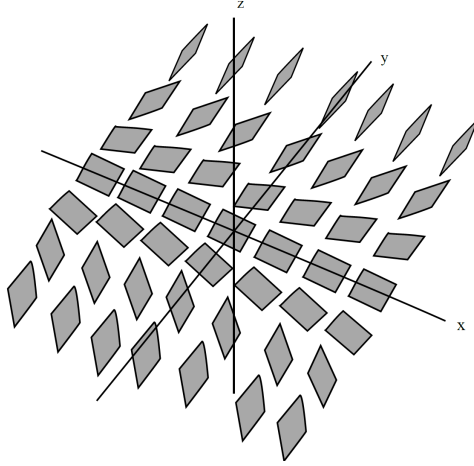
Figure 2.1 The standard contact structure ξ_{st} on $\mathbb{R}^3$.

Definition 2.2 *Two contact structures ξ_0 and ξ_1 on manifolds M_0 and M_1, respectively are contactomorphic if there is a diffeomorphism $f : M_0 \to M_1$ such that $Tf(\xi_0) = \xi_1$, where $Tf : TM_0 \to TM_1$ indicates the differential of f.*

There are many contact structures on $\mathbb{R}^3$, but **Darboux's theorem** says that all of them locally look like (locally contactomorphic to) the standard contact structure. More precisely, near any point, a contact form α on $\mathbb{R}^3$ can be expressed as $dz - ydx$ by means of a change of coordinates, i.e., a local diffeomorphism. This is the one important difference between contact geometry and Riemannian geometry. If there are differences between contact structures, then they must be found at the global level, like topological invariants.

There are two types of contact structures on $3-$manifolds. If there is a disk $D \subset M$ embedded such that $T_pD = \xi_p$ for $\forall p \in \partial D$ then D is called an overtwisted disk and ξ is called an overtwisted contact structure. If the contact structure is not overtwisted then it is tight. The contact manifold $(\mathbb{R}^3, \xi_{st})$ is **tight** [1].

Example 2.2 *The contact manifold $(\mathbb{R}^3, \xi_{ot} = \ker(\alpha = \cos r dz + r \sin r d\theta))$ with cylindrical coordinates is overtwisted, and $D = \{(r, \theta, z) \mid z = 0, \ r \leq \pi\}$ is an overtwisted disk. See Figure 2.2.*

8
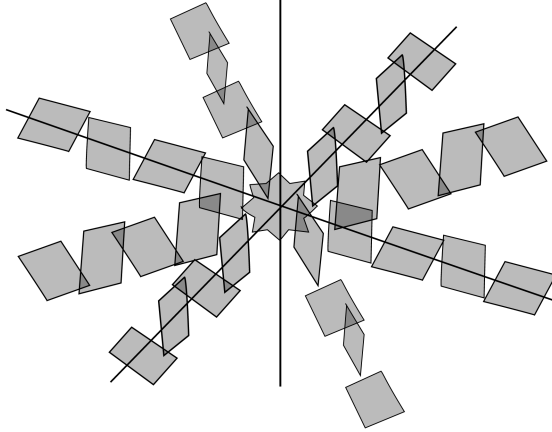
Figure 2.2 The contact structure ξ_{ot} on $\mathbb{R}^3$.

It follows from [1] that the contact structures ξ_{st} and ξ_{ot} on $\mathbb{R}^3$ are not contactomorphic.

Example 2.3 *The standard tight contact structure on $3-$sphere S^3 in $\mathbb{R}^4$ is given by $\xi_{std} = \ker\left(\alpha = (x_1 dy_1 - y_1 dx_1 + x_2 dy_2 - y_2 dx_2)\mid_{S^3}\right)$ with Cartesian coordinates (x_1, y_1, x_2, y_2) in $\mathbb{R}^4$. The contact structure on S^3 with one point removed is contactomorphic to $(\mathbb{R}^3, \xi_{st})$. For a proof of this contactomorphism, one can check [18].*

Theorem 2.1 *(Eliashberg 1992, [6]) There is a unique tight contact structure on S^3 up to isotopy.*

Theorem 2.1 and Theorem 2.2 will be useful in proving there is a unique representation of the link W_+ with maximal tb.

Let $Diff_0\left(S^3\right)$ be the group of orientation-preserving diffeomorphisms of S^3 that fix the plane $\xi_{std}(p)$ where p is a fix point in S^3, and let $Diff_{\xi_{std}}$ be the group of diffeomorphisms of S^3 that preserve ξ_{std}.

Theorem 2.2 *(Eliashberg 1992, [6]) The natural inclusion of $Diff_{\xi_{std}} \hookrightarrow Diff_0\left(S^3\right)$ is a weak homotopy equivalence.*

From this, any contactomorphism of (S^3, ξ_{st}) is contact isotopic to the identity. Specifically, we will use the fact that if there is a contactomorphism of (S^3, ξ_{st}) taking a Legendrian link L to L', then L and L' are Legendrian isotopic.

2.2 LEGENDRIAN KNOTS AND LINKS

We mainly use [10], [11], [18] and [29] in this section.

Definition 2.3 *A **Legendrian knot** K in a contact manifold (M^3, ξ) is an embedded S^1 that is always tangent to $\xi : T_p K \subset \xi_p$, for $p \in K$. A **Legendrian link** is a disjoint union of Legendrian knots.*

We will represent Legendrian knots and links in $(\mathbb{R}^3, \xi_{st})$ via the *front projection* which is

$$\Pi : \mathbb{R}^3 \to \mathbb{R}^2 \ : \ (x, y, z) \to (x, z).$$

The image, $\Pi(K)$, of K, is called **front projection** of K. A Legendrian link will generically have an immersed front projection with semi-cubical cusps and no vertical tangencies; conversely, any such projection can be uniquely lifted to a Legendrian link using $y = dz/dx$ which result in the fact that at each crossing the slope of overcrossing is smaller than the undercrossing in the link diagram.

Example 2.4 *Figure 2.3 illustrates front diagrams for Legendrian knots and links realizing the unknot and Hopf link.*

(a)	(b)
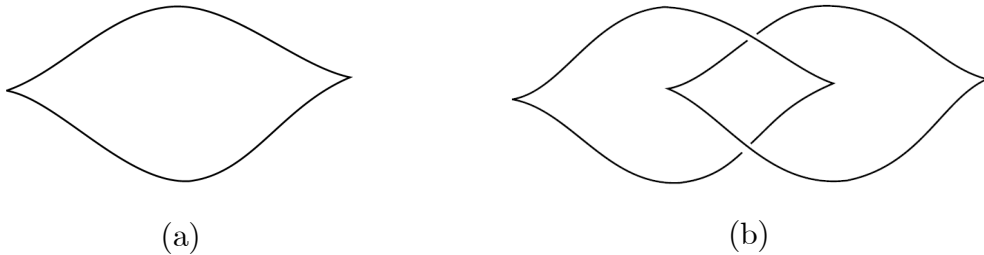
Figure 2.3 a) Front of a Legendrian unknot, b) Front of a Legendrian Hopf link.

Every knot type has a Legendrian realization. Two Legendrian knots K_0 and K_1 are **Legendrian isotopic** if there is an isotopy through Legendrian knots between them; and are **ambient contact isotopic** if there is a $1-$parameter family ϕ_t, $t \in [0, 1]$ of contactomorphisms of the ambient contact manifold such that $\phi_0 = id$ and $\phi_1(K_0) = K_1$.

Theorem 2.3 *The classification of Legendrian knots up to Legendrian isotopy in (S^3, ξ_{st}) is equivalent to the classification up to contact isotopy.*

Theorem 2.4 *Two front diagrams represent Legendrian isotopic Legendrian knots if and only if they are related by ambient isotopy in $\mathbb{R}^2$ and a sequence of moves shown in Figure 2.4.*
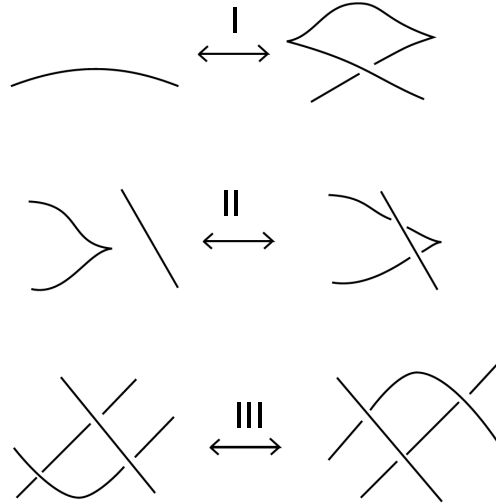
Figure 2.4 Legendrian Reidemeister Moves, as well as the rotation of each by 180° around all the coordinate axes.

We will use Legendrian Reidemester moves for proving that two representations (symmetric with each other) of the Legendrian Whitehead Mirror are Legendrian isotopic.

The classical invariants of Legendrian knots are the topological knot type, the **Thurston-Bennequin invariant** $tb(K)$, and the **rotation number** $r(K)$. The Thurston-Bennequin invariant $tb(K)$ measures the twisting of contact planes around K with respect to the framing induced by a Seifert surface (surface whose boundary is K). The rotation number $r(K)$ for oriented null homologous knots (bounds an embedded oriented surface) counts the number of times the direction of K rotates around in a trivialization of the contact planes on a Seifert surface for K. One can compute $tb(K)$ and $r(K)$ via the front projection of K as follows:

$$
\begin{aligned}
tb(K) &= \text{writhe}\left(\Pi\left(K\right)\right) - \frac{1}{2}(\text{number of cusps in } \Pi\left(K\right)), \\
r(K) &= \frac{1}{2}(\text{number of down cusps } - \text{ number of up cusps}),
\end{aligned}
$$

where writhe of $\Pi\left(K\right)$ is the sum of the signs of the crossings of $\Pi\left(K\right)$. Right and left handed crossing, illustrated in Figure 2.5, contribute $+$ and $-$ to writhe of $\Pi\left(K\right)$, respectively.

11

(a)   (b)
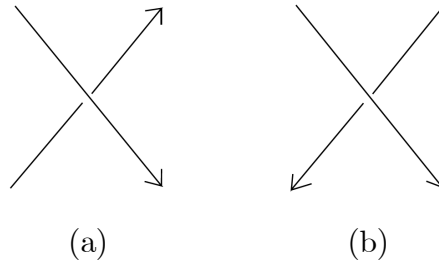
Figure 2.5 a) A right handed crossing, b) A left handed crossing.

For a link $L = K_1 \cup K_2$, $tb(L) = tb(K_1) + tb(K_2) + 2lk(K_1, K_2)$, where $lk(K_1, K_2)$ is the linking number of K_1 and K_2. In this thesis, $tb(L) = tb(U_1) + tb(U_2)$ for any Legendrian L in the link type W_+ such that $L = U_1 \cup U_2$ since $lk(K_1, K_2) = 0$. It does not depend on the orientation of the components.

One can distinguish links which are not Legendrian isotopic from different value of the invariants. Given a Legendrian knot K there is a way to get another Legendrian knot in the same topological knot type, which is not Legendrian isotopic to K. This operation is called **stabilization**, which corresponds to adding a zig-zag to the front projection of the knot in $(\mathbb{R}^3, \xi_{st})$. If down cusps are added then it is a *positive stabilization* $S_+(K)$, and if up cusps are added then it is a *negative stabilization* $S_-(K)$ (see Figure 2.6).
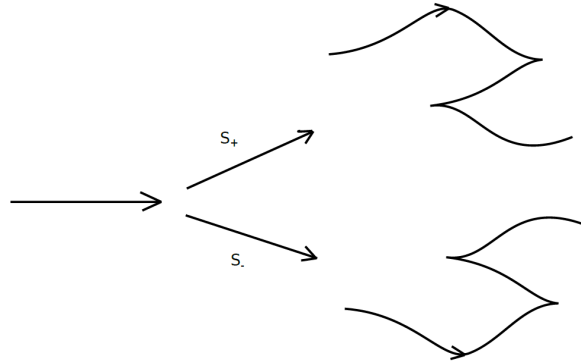
Figure 2.6 Stabilizations in the front projection.

Stabilizations for Legendrian knots can be defined in any contact manifold by Darboux's Theorem because stabilizations are done locally. It can be also noted that after stabilizations the classical invariants change as follows: $tb(S_\pm(K)) = tb(K) - 1$ and $r(S_\pm(K)) = r(K) \pm 1$. Hence, although the knot and its stabilization are in the same topological knot type, they are not Legendrian isotopic. By stabilizing, one can obtain an infinite number of Legendrian realizations of a knot in its knot type with arbitrarily negative Thurston-Bennequin invariants.

Lemma 2.5 *Stabilization is a well-defined operation and* $S_+(S_-(K)) = S_-(S_+(K))$.

Since the stabilization operation is well-defined it does not matter where the stabilization is done. In the opposite direction, K **destabilize**s if there is a Legendrian knot K' such that $K = S_\pm(K')$. In any tight contact structure there is an upper bound on Thurston-Bennequin invariant coming from *Bennequin Inequality* [6] which says that $tb(K) + |r(K)| \leq -\chi(\Sigma)$, where Σ is a Seifert surface for K. Hence, it is not necessarily easy to destabilize a knot while it is easy to stabilize. This led one to think about the importance of finding the maximal Thurston-Bennequin invariant denoted by $\overline{tb}(\mathcal{K})$ of Legendrian knots topological isotopic to $\mathcal{K}$ or simply written as maximal tb:

$$\overline{tb}(\mathcal{K}) = \max\{tb(K) \mid K \in \mathcal{L}(\mathcal{K})\},$$

where $\mathcal{K}$ denotes a topological knot type and $\mathcal{L}(\mathcal{K})$ denotes set of all Legendrian knots in this knot type up to Legendrian isotopy. This is an invariant of the topological knot type.

One can ask whether or not two knots in the same topological knot type are Legendrian isotopic when they have same Thurston-Bennequin and rotation number. If this so, these knots are called **Legendrian simple**. Determining when a knot is Legendrian simple is one of the main problems of the Legendrian Knot Theory.

2.3 CONVEX SURFACE THEORY

We will introduce in this section the tools from convex surface theory to the study of Legendrian links in the standard tight contact structure on S^3. We mainly use [11], [12], [15], [18], [22], [23] and [24] as a source to exhibit some definitions and theorems in convex surface theory.

If Σ is a surface in (M, ξ) then $\xi \cap T\Sigma$ is a singular line field on Σ and may be integrated to a singular foliation Σ_ξ called the **characteristic foliation**. It is singular at points where $\xi = T\Sigma$.

Characteristic foliations on surfaces in contact 3–manifolds are a very important tool for the classification of contact structures on 3−manifolds.

Theorem 2.6 *(Giroux, [22]) Let Σ_1 and Σ_2 be closed surfaces in contact $3-$manifolds (M_1, ξ_1) and (M_2, ξ_2) (with ξ_1, ξ_2 cooriented), and $\phi : \Sigma_1 \to \Sigma_2$ a diffeomorphism with $\phi(\Sigma_{1\xi_1}) = \Sigma_{2\xi_2}$ as oriented characteristic foliations. Then there is a contactomorphism $\psi : N(\Sigma_1) \to N(\Sigma_2)$ of suitable neighborhoods $N(\Sigma_1)$ and $N(\Sigma_2)$ of Σ_1 and Σ_2 with $\phi(\Sigma_1) = \Sigma_2$ and such that $\psi|_{\Sigma_1}$ is isotopic to ϕ via an isotopy preserving the characteristic foliation.*

From this theorem, the contact structure near a surface is determined by its characteristic foliation; and to work with a foliation on a surface is easier than a whole contact structure. A vector field υ in (M, ξ) is called **contact** if its flow preserves ξ, i.e. if $\xi = \ker \alpha$ then $\mathcal{L}_v \alpha = f\alpha$, where $f : M \to \mathbb{R}$ is a function on M. This condition is independent of the choice of contact form α defining a given ξ. A surface Σ in (M, ξ) is **convex** if there exists a contact vector field v transverse to Σ. Equivalently, Σ is convex exactly when there is a neighborhood $N = \Sigma \times I$ in M such that ξ is invariant in the I-direction. The **dividing set** of Σ is a family of disjoint embedded curves $\Gamma_\Sigma = \{p \in \Sigma \mid v(p) \in \xi_p\}$, i.e. Γ_Σ is where ξ is tangent to I. The isotopy type of Γ_Σ is independent of choice of v so the dividing set is well defined up to isotopy. Let $\mathcal{F}$ be a singular foliation on an orientable surface Σ. A multi-curve Γ is said to divide $\mathcal{F}$ if Γ is transverse to $\mathcal{F}$, $\Sigma \backslash \Gamma$ is the disjoint union of two (possibly disconnected) surfaces Σ_+ and Σ_- with $\partial \overline{\Sigma_+}$ and $\partial \overline{\Sigma_-} = \Gamma$, and there is a vector field u and volume form ω on Σ so that u is tangent to $\mathcal{F}$, $\pm \mathcal{L}_u \omega > 0$ on $\Sigma_\pm$, and $u|_\Gamma$ points out of Σ_+.

Theorem 2.7 *(Giroux, [22]) Let Σ be an orientable surface in (M, ξ) with Legendrian boundary (possibly empty). Then Σ is a convex surface if and only if Σ_ξ has dividing curves. Moreover, if Σ is convex Γ_Σ will divide Σ_ξ.*

We define the **twisting number** $tw_\Sigma(\gamma)$ of a closed Legendrian curve γ with respect to the framing induced by Σ to be the number of counterclockwise (right) 2π twists of ξ along γ, relative to Σ. In particular, if γ is a connected component of the boundary of a compact surface Σ, $T\Sigma$ gives a natural framing, and if Σ is a Seifert surface of γ, then $tw_\Sigma(\gamma)$ is the Thurston–Bennequin invariant $tb(\gamma)$.

Theorem 2.8 *(Giroux, [22]) Any closed surface is $C^\infty-$close to a convex surface.*

We can perturb any closed surface by a $C^\infty-$isotopy so that the surface is convex. Later, Kanda [23] proved that this result is true with another conditions as follows:

Theorem 2.9 *(Kanda, [23]) Any surface with Legendrian boundary satisfying $tw_\Sigma(\gamma) \leq 0$ for all boundary components γ of Σ may be C^0 small perturbed near the boundary and then C^∞ small perturbed on the interior to make convex.*

Let v be a contact vector field for (M, ξ) that is transverse to a surface Σ and let Γ be the dividing curves on Σ. An isotopy $F : \Sigma \times [0, 1] \to M$ of Σ is called *admissible* if $F(\Sigma \times \{t\})$ is transversal to v for all t.

Theorem 2.10 *(Giroux Flexibility Theorem, [22]) Let Σ be a closed surface or a surface with Legendrian boundary. Let Γ be the dividing set for Σ_ξ and $\mathcal{F}$ be another singular foliation on Σ divided by Γ. Then there is an admissible isotopy $F : \Sigma \times [0, 1] \to M$ of Σ such that $F(\Sigma \times \{0\}) = \Sigma$, $F(\Sigma \times \{1\})_\xi = \mathcal{F}$ and the isotopy is fixed on Γ.*

This theorem shows that dividing curves Γ_Σ on a convex surface contains the important information of a contact structure in a neighborhood of a convex surface, so we can focus only the dividing set instead of whole characteristic foliation which will be very useful to prove Theorem 4.1.

The following is Grioux's criterion for determining which convex surfaces have neighborhoods being tight:

Theorem 2.11 *(Giroux's criterion) If $\Sigma \neq S^2$ is a convex surface (closed or compact with Legendrian boundary) in (M, ξ), then Σ has a tight neighborhood if and only if Γ_Σ has no homotopically trivial closed curves. If $\Sigma = S^2$, Σ has a tight neighborhood if and only if $\#\Gamma_\Sigma = 1$.*

Therefore, we see that when ξ is tight and $\Sigma \neq S^2$, then none of the dividing curves Γ_Σ bounds an embedded disk in Σ. From the Giroux's Criterion, if Σ is a torus, Γ_Σ will consist of an even number $2n > 0$ of parallel essential curves. On a convex torus Σ, we can choose a proper identification of Σ with $\mathbb{R}^2/\mathbb{Z}^2$ such that Γ_Σ has even number $(2n)$ parallel essential curves (one can find a suitable parametrization for making these curves' slope 0) and from Giroux Flexibility Theorem, the characteristic foliation Σ_ξ has $2n$ curves of singularities (one in aech component of $\Sigma \backslash \Gamma_\Sigma$) which are called *Legendrian divides,* and the rest of the leaves in T_ξ is non-singular closed curves which are called *Legendrian ruling curves.* We call such a convex Σ is in **standard form.** From Giroux

Flexibility Theorem, any convex torus can be isotoped by an admissible isotopy into standard form.

A **standard neighborhood** of a Legendrian knot K is a solid torus $N(K)$ having convex boundary with two dividing curves of slope $1/tb(K)$. We will usually take the boundary of $N(K)$ to be a convex torus in standard form. This neighborhood is uniquely determined by K up to isotopy through such neighborhoods [24].

A useful formulation of Giroux Flexibility Theorem is called Legendrian Realization Principle which is due to Kanda [23]:

Theorem 2.12 *(Legendrian Realization Principle) Consider a closed curve C on a closed convex surface or a convex surface Σ with Legendrian boundary. Assume $C \pitchfork \Gamma_\Sigma$ and every component of $\Sigma \setminus C$ nontrivially intersects Γ_Σ. Then there exists an admissible isotopy $F_t = F(\cdot, t)$, $t \in [0, 1]$ so that $F_0 = id$, $F_t(\Sigma)$ are all convex, $F_1(\Gamma_\Sigma) = \Gamma_{F_1(\Sigma)}$ and $F_1(C)$ is Legendrian.*

As a result, we can realize almost any curve as a Legendrian one.

Theorem 2.13 *(Relative Convex Realization Principle, Kanda [23]) If γ is a Legendrian curve in a surface Σ, and $tw_\Sigma(\gamma) \leq 0$ then Σ may be isotoped relative to γ so that it is convex. Moreover, if Σ is convex, then*

$$tw_\Sigma(\gamma) = -\frac{1}{2}\#(\gamma \cap \Gamma_\Sigma).$$

Here $\#(\gamma \cap \Gamma_\Sigma)$ indicates the unsigned intersection number of γ and Γ_Σ.

We will frequently need that a surface with Legendrian boundary can be made convex fixing the boundary. From the theorem above we have the next lemma for Legendrian knots.

Lemma 2.14 *(Kanda [23]) If Σ has a single Legendrian boundary component $\partial\Sigma = \gamma$ (Σ is a Seifert surface), then Σ may be made convex if and only if $tb(\gamma) \leq 0$. Moreover, if Σ is convex, then*

$$tb(\gamma) = -\frac{1}{2}\#(\gamma \cap \Gamma_\Sigma) \ and \ r(\gamma) = \chi(\Sigma_+) - \chi(\Sigma_-),$$

where Σ_+ and Σ_- are as in the definition of convexity.

We will often use this formula for the Thurston-Bennequin invariant in the next chapters to see how many times a component of the link intersect the dividing set.

We know describe a method for altering the dividing curves of a convex surface.

Definition 2.4 *Let α be a Legendrian arc in a given convex surface Σ so that α intersects Γ_Σ in three points p_1, p_2, p_3 (where p_1, p_3 are the end points of the arc). A **bypass** for Σ (along α), see Figure 2.7, is a convex disk D with Legendrian boundary such that*

1. $D \cap \Sigma = \alpha$,

2. $tb(\partial D) = -1$,

3. $\partial D = \alpha \cup \beta$,

4. $\alpha \cap \beta = \{p_1, p_3\}$ are corners of D and elliptic singularities of D_ξ.

5. There are 3 elliptic singularities (p_1, p_2, p_3) of D_ξ alternating in sign and along β there are singularities of the same sign of $\alpha \cap \beta$, alternating between elliptic or hyperbolic.
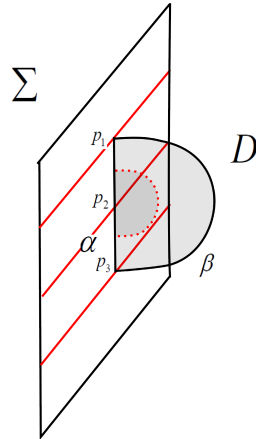
Figure 2.7 A piece of Σ, the dividing curves Γ_Σ (red straight lines) and the bypass disk D.

We call such an arc α on a surface Σ an **attaching arc**. Bypasses were first introduced in [24]. The most basic property of bypasses is how a convex surface changes when pushed across a bypass. Bypass attachment is very imporant operation in our work for obtaining a destabilization of our link.

A properly embedded arc $a \subset \Gamma_\Sigma$ in Σ is called *boundary parallel* if the closure of one of the components of $\Sigma \backslash a$ is a disk that contains no components of Γ_Σ in its interior, in other words, if $a \subset \Gamma_\Sigma$ cuts off a half-disk which has no other intersections with Γ_Σ. One may use the Legendrian realization principle to show that a boundary parallel dividing curve (that is not the only dividing curve on Σ) will give a bypass for $\partial \Sigma$, because it allows one to "bypass" some twisting as the following lemma indicates.

Lemma 2.15 *([11]) If the dividing curves Γ_Σ contain a boundary parallel arc, Γ_Σ not connected, γ is Legendrian, $\partial\Sigma = \gamma$ and $tb(\gamma) < 1$ then γ can be destabilized.*

Example 2.5 *In Figure 2.8, the curves of green, pink, blue and red colour are dividing curves on some surface and intersect the black curve which is $\partial\Sigma$ eight times. By 2.14, $tb(\partial\Sigma) = -\frac{1}{2}\#(\partial\Sigma \cap \Gamma_\Sigma)$, we have $tb(\partial\Sigma) = -4$. The red and green curves are boundary parallel curves and so they assign a bypass for $\partial\Sigma$.*
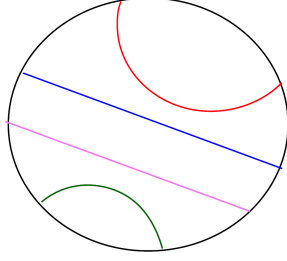
Figure 2.8 Boundary parallel curves (The green and the red one).

In the proofs in next chapters, we will find bypass in an annular region, so we need the next proposition. A slight perturbation of a convex surface will not change the isotopy type of the dividing curves, but moving the surface through a bypass may change the isotopy type of the dividing curves as follows:

Theorem 2.16 *(Honda [24]) Let D be a bypass for a given Σ along $\alpha \subset \Sigma$. Inside any open neighborhood of $\Sigma \cup D$ there is a (one-sided) neighborhood $N = \Sigma \times [0,1]$ of $\Sigma \cup D$ with $\Sigma = \Sigma \times \{0\}$ (if Σ is oriented, orient N so that $\Sigma = -\Sigma \times \{0\}$ as oriented manifolds) such that Γ_Σ is related to $\Gamma_{\Sigma \times \{1\}}$ as shown in Figure 2.9.*

(a) (b)
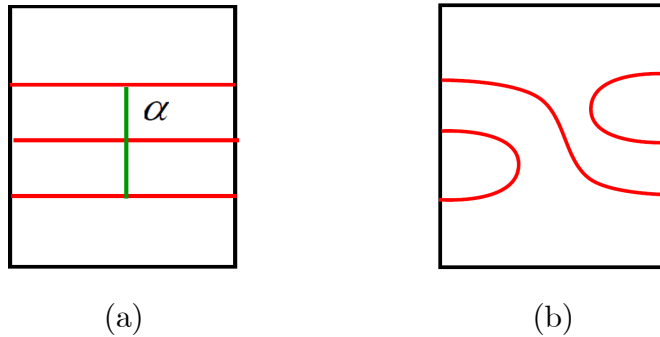
Figure 2.9 Result of a bypass attachment: (a) original surface Σ with attaching arc α, (b) the surface $\Sigma' = \Sigma \times \{1\}$. The dividing curves Γ_Σ and $\Gamma_{\Sigma'}$ are shown in red.

Figure 2.9 shows the result when one attaches the bypass from the front, for attaching a bypass from the back the orientation of $[0, 1]$ in Theorem 2.16 needs to be changed. The result of a bypass attachment from the back is the mirror of Figure 2.9.

We will mainly use Theorem 2.16 to alter the dividing curves with bypasses in order to find a destabilization of each component of W_+ in Theorem 4.1.

If a bypass exist then the others can be found by rotating the attaching arc of a bypass. This is the concept of Lemma 2.17.

Lemma 2.17 *([25])Suppose that there is a disk D in a convex surface Σ which $D \cap \Gamma_\Sigma$, α and α' are as illustrated in Figure 2.10. If a bypass exists for Σ along an attaching arc α from the front, then there exists also a bypass for Σ along an attaching arc α' from the front.*
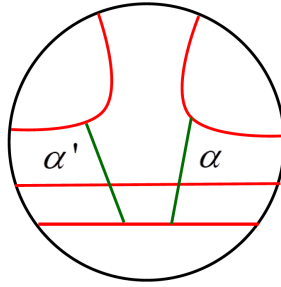
Figure 2.10 Bypass rotation.

The next lemma shows how the dividing sets of two convex surfaces which meet along a Legendrian corner behave.

Lemma 2.18 *([24])(Edge Rounding Lemma)Let Γ_{Σ_1} and Γ_{Σ_2} be the dividing curves of convex surfaces Σ_1 and Σ_2, respectively, and $\partial\Sigma_1 = \partial\Sigma_2$ is Legendrian. Assume Σ_1 and Σ_2 in $\mathbb{R}^3$ is modeled by $\{(x, y, z) : x = 0, \ y \geq 0\}$ and $\{(x, y, z) : y = 0, \ x \geq 0\}$. Then we may form a surface Σ_3 from $\Sigma = \Sigma_1 \cup \Sigma_2$ (join along $x = y = 0$) by replacing in a small neighborhood N_ε of $\Sigma_1 \cap \Sigma_2$ with the intersection of N_ε with $\{(x, y, z) : (x - \delta)^2 + (y - \delta)^2 = \delta^2\}$. For a suitably chosen δ, the resulting surface Σ_3 is a surface of class of C^1 with dividing curve as illustrated in Figure 2.11, but Σ_3 can be smoothed by a small isotopy so that the dividing curves are as shown in Figure 2.11.*

(a)   (b)
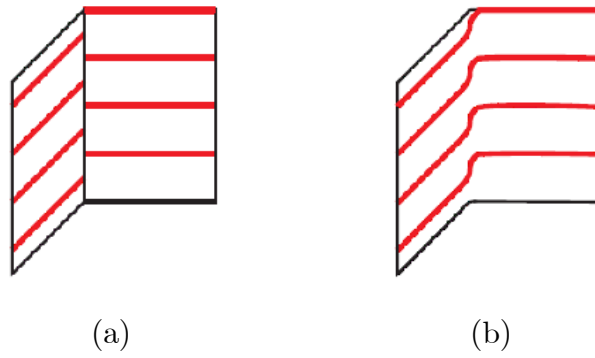
Figure 2.11 Rounding a corner between two convex surfaces. a) $\Sigma_1 \cup \Sigma_2$, b) Σ_3. Red lines are dividing curves.

While moving from Σ_1 to Σ_2, the dividing curves move up (down) if Σ_2 is to the right (left) of Σ_1.

CHAPTER 3

SOME CLASSIFICATION RESULTS

We give the known classification results of Legendrian unknot and twist knots in this chapter.

From Lemma 2.5, if the following steps can be carried out then one can classify Legendrian knots in a knot type $\mathcal{K}$ with a useful strategy:

1. All Legendrian knots in $\mathcal{L}(\mathcal{K})$ can be destabilized except those with maximal tb.

2. Classify Legendrian knots in $\mathcal{L}(\mathcal{K})$ with maximal tb.

3. Understand when Legendrian knots become the same under stabilization.

If $\mathcal{K}$ has a unique Legendrian representation with maximal tb then the last step in the strategy is unnecessary.

In the next sections Figure 3.1, Figure 3.3 and Figure 3.4 is called the *mountain range* associated to the knot type. Here, the numbers in the mountain range indicate the number of Legendrian knots with corresponding invariants, if the number is 1 then there is a unique Legendrian representative with these corresponding invariants. The lines indicate positive stabilization if it has negative slope and indicate negative stabilization if it has positive slope.

3.1 THE UNKNOT

Theorem 3.1 *(Eliashberg and Fraser 1995, [8]) In any tight contact* $3-$*manifold, two oriented Legendrian unknots are Legendrian isotopic if and only if their Thurston-Bennequin invariants and rotation numbers agree. All Legendrian unknots are stabilizations of the unique one with* $tb = -1$ *and* $r = 0$ *(see (a) in Figure 2.3).*
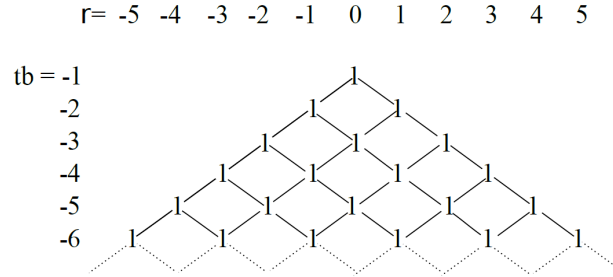
Figure 3.1 Mountain range for Legendrian unknots.

We call then the unknot is Legendrian simple, because it is determined by its tb and r.

3.2 LEGENDRIAN NONSIMPLE KNOTS AND TWIST KNOTS

A twist knot is a twisted Whitehead double of the unknot which is shown as $K = K_m$ in Figure 3.2. In this figure, there are m right-handed half twists in the box if $m \geq 0$, and $|m|$ left-handed half twists if $m < 0$.
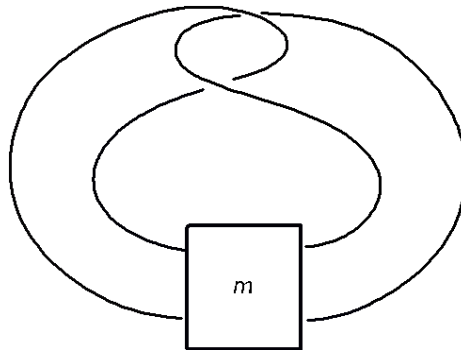
Figure 3.2 The twist knot K_m.

It is sufficient to classify Legendrian unknots only by checking their classical invariants. Hovewer, it is not true that classical invariants always suffice to classify Legendrian knots. If Legendrian knots in a given topological knot type are determined up to Legendrian isotopy by their classical invariants then the knot type is said to be *Legendrian simple*; otherwise it is *Legendrian nonsimple.* In 1997, Chekanov [2] gave the first example of a Legendrian nonsimple knot type: $K_{-4} = m\,(5_2)$. In 2001, Epstein, Fuchs, and Meyer [9] generalized the result by showing that there are at least n different Legendrian representatives with maximal tb of the twist knot K_{-2n} with crossing number $2n + 1$. In 2013, Etnyre, Ng and Vertesi gave the complete classification of Legendrian representatives of positive twist knots as follows:

Theorem 3.2 *(Etnyre, Ng and Vertesi 2013, [15]) Let $K = K_m$ be twist knot of Figure 3.2 with m half twists. Classification of Legendrian twist knots in (S^3, ξ_{st}) :*

1. *For $m \geq -2$ even, there is a unique representative of K_m with maximal Thurston–Bennequin number, $tb = -m - 1$. This representative has rotation number $r = 0$, and all other Legendrian knots of type K_m destabilize to the one with maximal Thurston–Bennequin number.*

2. *For $m \geq 1$ odd, there are exactly two representatives with maximal Thurston–Bennequin number, $tb = -m - 5$. These representatives are distinguished by their rotation numbers, $r = \pm 1$, and a negative stabilization of the $r = 1$ knot is isotopic to a positive stabilization of the $r = -1$ knot. All other Legendrian knots destabilize to at least one of these two.*

3. *For $m \leq -3$ odd, K_m has $(-m + 1)/2$ Legendrian representatives with $(tb, r) = (-3, 0)$. All other Legendrian knots destabilize to one of these. After any positive number of stabilizations (with a fixed number of positive and negative stabilizations), these $(-m + 1)/2$ representatives all become isotopic.*

4. *For $m \leq -2$ even with $m = -2n$, K_m has $n^2/2$ different Legendrian representations with $(tb, r) = (1, 0)$. All other Legendrian knots destabilize to one of these. These Legendrian knots fall into $n/2$ different Legendrian isotopy classes after any given positive number of positive stabilizations, and $n/2$ different Legendrian isotopy classes after any given positive number of negative stabilizations. After at least one positive and one negative stabilization (with a fixed number of each), the knots all become Legendrian isotopic.*

This teorem is depicted in Figure 3.3. Since all numbers in the mountain ranges in Figure 3.3 (a) and (b) are 1, these knot types are Legendrian simple. In addition, K_{-3} is Legendrian simple.

r= -3 -2 -1 0 1 2 3

tb = -2n-1
   -2n-2
   -2n-3
   -2n-4

(a)

r= -4 -3 -2 -1 0 1 2 3 4

tb = -2n-4
   -2n-5
   -2n-6
   -2n-7

(b)

r= -3 -2 -1 0 1 2 3

tb = -3
   -4
   -5
   -6

(c)

r= -3 -2 -1 0 1 2 3

tb = 1
   0
   -1
   -2

(d)
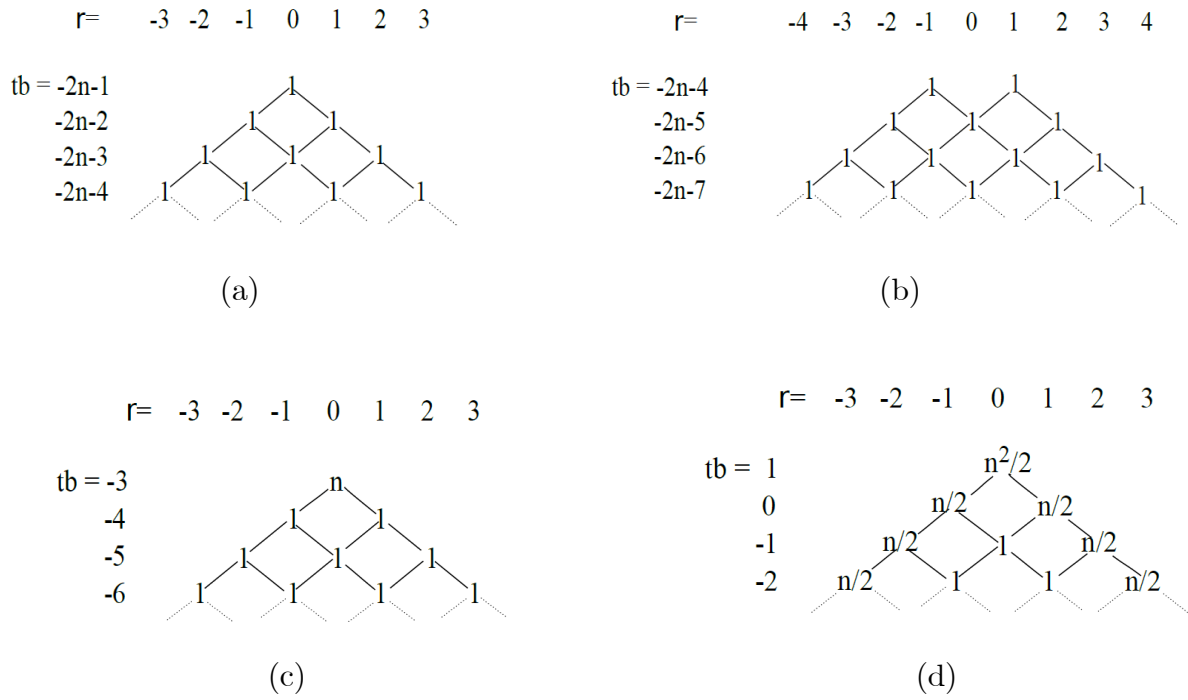
Figure 3.3 Legendrian mountain range for a) K_{2n} $(n \geq -1)$, b) K_{2n-1} $(n \geq 1)$, c) K_{-2n-1} $(n \geq 1)$, d) K_{-2n} $(n \geq 1)$.

There are many works about the classification of Legendrian knots, but very little known of Legendrian links. We can ask whether Legendrian Whitehead links are Legendrian simple or not. We will answer it for Legendrian positive Whitehead links in the next chapter.

24

CHAPTER 4

THE PROBLEM: LEGENDRIAN WHITEHEAD LINKS

In the light of the classification of Legendrian positive twist knots stated in section 3.2, we will give the complete classification of Legendrian positive Whitehead links by using the strategy in Chapter 3 and the convex surface theory.

4.1 MAIN PROBLEM: LEGENDRIAN POSITIVE WHITEHEAD LINKS (LEGENDRIAN WHITEHEAD MIRROR)

One of the components of the positive Whitehead link is a special case of the twist knot K_m. When $m = 0$, K_0 is the one of the component of W_+ which is a topologically the unknot. See Figure 4.1. The link type W_+ may be considered as $W = O_1 \cup O_2$, where O_1 is taken as K_0.
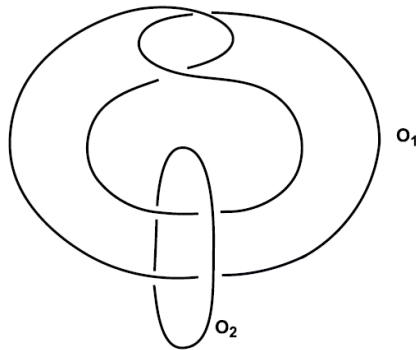
Figure 4.1 Positive Whitehead link $W = O_1 \cup O_2$ in the link type of W_+.

We write a Legendrian representative of W as $L = U_1 \cup U_2 \in \mathcal{L}(W_+)$.

Recall, in this work, we aim to prove our main theorem.

Theorem 1.1 There are two Legendrian representatives of positive Whitehead link W_+ with maximal Thurston-Bennequin number shown in the Figure 4.2 and they become the same after a single (positive or negative) stabilization. All other representatives

destabilize to one of the maximal Thurston-Bennequin number representatives and are determined by the Thurston-Bennequin number and the rotation number. Moreover, the components shown in Figure 4.3 can be interchanged by a Legendrian isotopy.
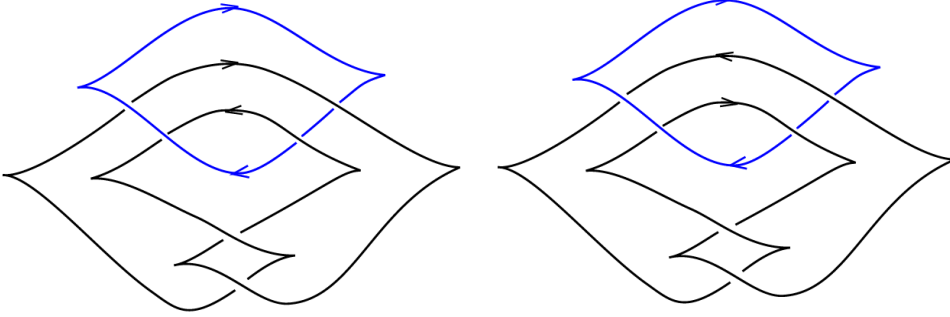
Figure 4.2 The two Legendrian representatives of W_+ with maximal $tb = -2$ and components both having $tb = -1$, $r = 0$.

This theorem follows from the following 4 results.

Theorem 1.2 Given a Legendrian positive Whitehead link W_+, then this link can be destabilized until each component has $tb = -1$.

Theorem 1.3 There is a unique Legendrian representative of W_+ with maximal Thurston–Bennequin number, $tb = -2$ if orientations are ignored. This representative has rotation number $r = 0$.

Theorem 1.4 Given the Legendrian link L in the link type W_+ with $tb = -2$, the components of L can be interchanged by Legendrian isotopy as indicated in Figure 4.3 taking orientations on the components into account.
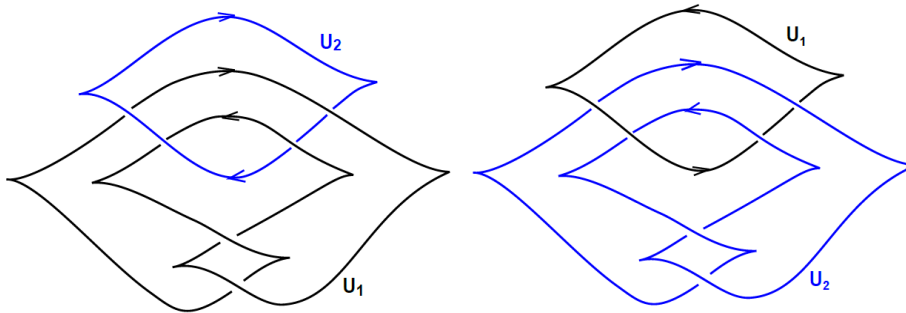
Figure 4.3 Legendrian isotopic two Legendrian W_+ with $tb = -2$.

Proof of Theorem 1.4 After we apply several Legendrian Reidemeister Moves (Theorem 2.4), we obtain that they are Legendrian isotopic. See Figure 4.4. In the proof, we draw U_1 in black and U_2 in blue.
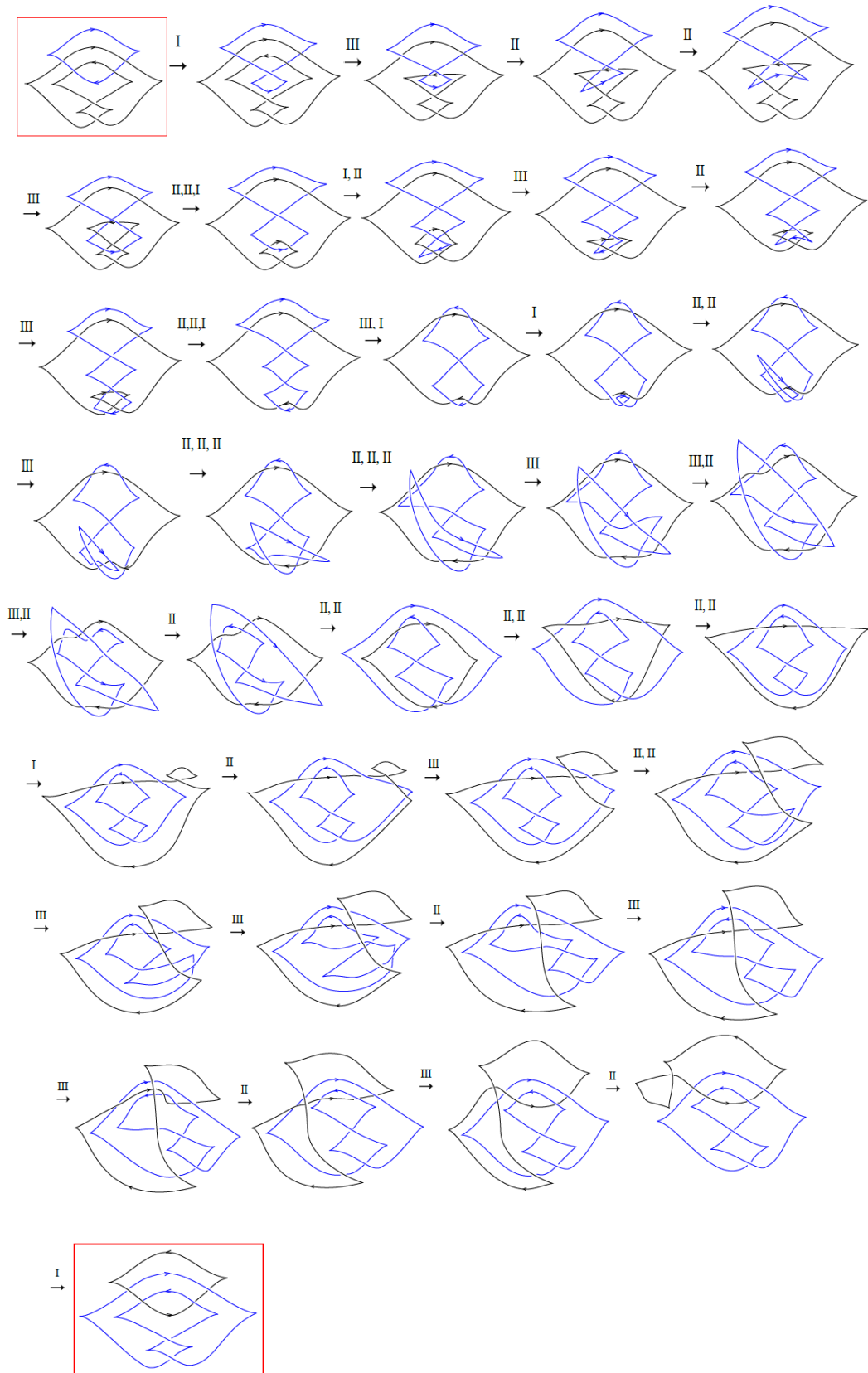
Figure 4.4 Legendrian isotopy interchanging the components.

27

Theorem 1.5 There are two Legendrian representatives of positive Whitehead link W_+ with maximal Thurston-Bennequin number shown in the Figure 4.2 and they become the same after a single (positive or negative) stabilization.

Proof of the Theorem 1.5 By Theorem 1.3, we know that any maximal Thurston-Bennequin number representative of W_+ is given as in Figure 4.2. In Figure 4.4 we obtain that we are able to interchange the components of W_+ with maximal Thurston–Bennequin number and reverse the orientations on the components by a Legendrian isotopy. In the diagram, we see $L = U_1 \cup U_2$ is Legendrian isotopic to $L' = U_2 \cup -U_1$, where $-U_1$ is U_1 with reversed orientation. By using the same Legendrian Reidemeister moves, we have that $-U_1 \cup -U_2$ is Legendrian isotopic to $-U_2 \cup U_1$, $U_2 \cup -U_1$ is Legendrian isotopic to $-U_1 \cup -U_2$ and $-U_2 \cup U_1$ is Legendrian isotopic to $U_1 \cup U_2$. Similarly, by using the same Legendrian Reidemester moves, we have that $U_1 \cup -U_2$ is Legendrian isotopic to $-U_2 \cup -U_1$, $-U_1 \cup U_2$ is Legendrian isotopic to $U_2 \cup U_1$, $U_2 \cup U_1$ is Legendrian isotopic to $U_1 \cup -U_2$ and $-U_2 \cup -U_1$ is Legendrian isotopic to $-U_1 \cup U_2$. However, two oriented Whitehead links $U_1 \cup U_2$ and $-U_1 \cup U_2$ are not Legendrian isotopic by [26]. Finally, we have two equivalence classes of Legendrian positive Whitehead links with $\max tb = -2$ and $r = 0$ as shown in Figure 4.2 via Theorem 1.3. Now, we will see that these two representatives are Legendrian isotopic after a single (positive or negative) stabilization. Let us positive stabilize U_1. After we apply several Legendrian Reidemeister Moves (Theorem 2.4) as seen in Figure 4.5, we obtain that $St_+(U_1) \cup U_2$ is Legendrian isotopic to $St_+(-U_1) \cup U_2$.
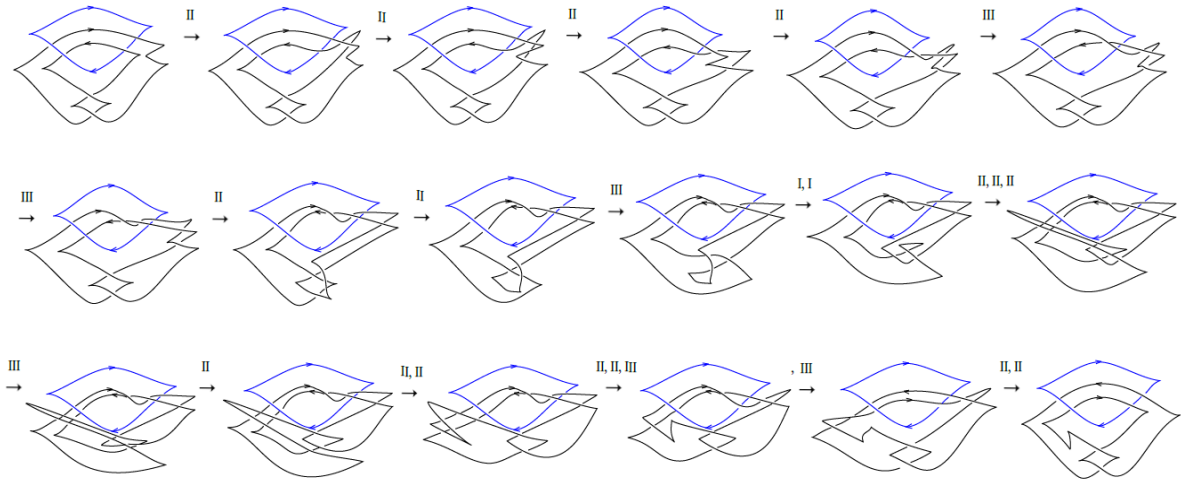
Figure 4.5 $St_+(U_1) \cup U_2$ is Legendrian isotopic to $St_+(-U_1) \cup U_2$.

It does not matter at what point the stabilization of U_1 is done via Lemma 2.5. Hence, when U_1 is stabilized along two different points, the results are Legendrian isotopic. In the proof, we draw U_1 in black and U_2 in blue. We conclude that $St_+(U_1 \cup U_2)$ is Legendrian isotopic to $St_+(-U_1 \cup U_2)$ while $U_1 \cup U_2$ is not Legendrian isotopic to $-U_1 \cup U_2$.

Now, let us negative stabilize U_1. Using the relation $St_-(U_1) = -St_+(-U_1)$ between the negative and the positive stabilization of a knot we can take $St_-(U_1)$ as the component in black of the last link in Figure 4.5 with reversed orientation and we can obtain that $St_-(U_1) \cup U_2$ is Legendrian isotopic to $St_-(-U_1) \cup U_2$ when we apply the Legendrian Reidemeister moves in the reverse order of the moves in Figure 4.5. Hence, we conclude that $St_-(U_1 \cup U_2)$ is Legendrian isotopic to $St_-(-U_1 \cup U_2)$ while $U_1 \cup U_2$ is not Legendrian isotopic to $-U_1 \cup U_2$. $\qquad\square$

Now, here we prepare for the proof of Theorems 1.2 and 1.3, and get help from [15]. Let S be the sphere shown in Figure 4.6. The Whitehead link $W_+ = O_1 \cup O_2$ is smoothly isotopic to the union of K_0 and B. Notice that K_0 intersects C on S in four points that divide K_0 into four unknotted pieces. We label the points $1, 2, 3,$ and 4 as in Figure 4.6 and we see the closed curve B on S seperates the points $1, 2$ from $3, 4$ in the figure. The sphere separates S^3 into two balls B_{in} and B_{out}, such that: K_0 intersects B_{out} in a vertical 2–braid with two negative half-twists, which are denoted $K_{out} = K_0 \cap B_{out}$, and K_0 intersects K_{in} in a horizontal 2–braid, which we denote $K_{in} = K_0 \cap B_{in}$.
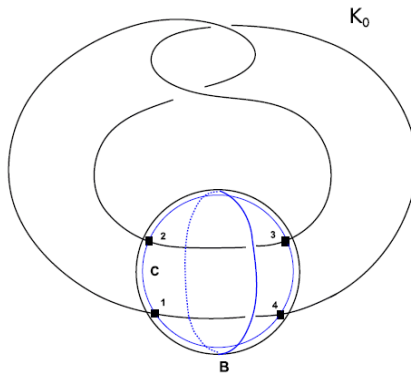
Figure 4.6 Model of the knot K_0.

Given a Legendrian representative $L = U_1 \cup U_2$ of W_+, there is a smooth isotopy $\phi : S^3 \to S^3$ taking K_0 to U_1 and B to U_2. The sphere S goes to $\phi(S)$ and we can assume that it is convex by Theorem 2.8. We would like to show that each component U_i can destabilize

to have $tb = -1$. For notational convenience, we will denote the image of S after the isotopy by S, we will also think of U_1 as K_0 and U_2 as B. Let $tb(U_i) = -n_i$, $i \in \{1, 2\}$.

Lemma 1.6 The Legendrian knot B can be destabilized in the complement of K_0 until it has $tb = -1$.

Proof of Theorem 1.3 Given a Legendrian representative $L = U_1 \cup U_2$ of W_+ without maximal tb. Destabilize $B = U_2$ until $tb = -1$ from Lemma 1.6. Now since smoothly the roles of U_1 and $-U_2$ can be interchanged by Theorem 1.4, we can arrange that $U_1 = B$ and $U_2 = K_0$. Lemma 1.6 holds also when we take K_0 with reversed orientation and we can again apply Lemma 1.6 to destabilize U_1 until it has $tb = -1$. $\qquad\square$

To prove Lemma 1.6 we will now start to normalize the dividing curves on S. We can consider a standard neighborhood N of K_0 as a solid torus $S^1 \times D^2$ from the Legendrian Standard Neighborhood Theorem and the boundary intersect S in four Legendrian unknots as seen in Figure 4.7. The boundary ∂N is convex with dividing set having two parallel curves.
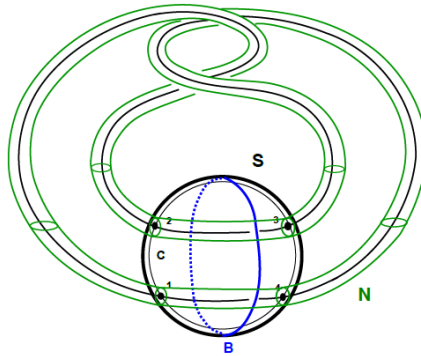
Figure 4.7 A model of $N = N(U_1)$.

Let P be the sphere with the interior of four disk removed $P = \overline{S \setminus N}$. Assume that U_2 has been taken maximal so that $tb(U_2) = -n$ for some $n > 0$. Let $N(U_2)$ be a standard neighborhood of U_2 disjoint from U_1. Set $Q = \overline{(S^3 - N(U_2))}$. The manifold Q is a solid torus $S^1 \times D^2$ having convex boundary with two dividing curves of slope $-n$. Here the curve on the boundary of a solid torus with slope n indicates the curve $p\lambda + q\mu$ with $\frac{p}{q} = n$ and λ, μ are elements of $H^2(\partial N(U_2), \mathbb{Z})$ such that μ is a meridian of $N(U_2)$ and λ is a longitude of $N(U_2)$. Then, we can take λ as a meridian of Q and μ as a

longitude of Q. We can assume the ruling curves on Q are meridional and choose two disks as modelled in Figure 4.8, namely D_1 and D_2 in Q bounded by these ruling curves. Precisely, $\partial Q \setminus (\partial D_1 \cup \partial D_2)$ contains two annuli A_1 and A_2 so that $A_1 \cup D_1 \cup D_2$ (after rounding corners by Lemma 2.18) shows the sphere S.
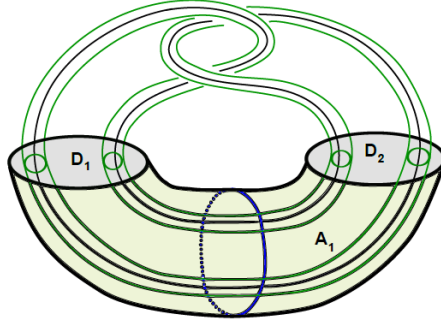
Figure 4.8 A model for S.

We can isotop each D_i such that a standard neighborhood N of U_1 intersects D_i along two disks with Legendrian boundary being meridional ruling curves on ∂N and D_i is convex by Theorem 2.8. Let $P_i = D_i \setminus N$. Accordingly P_i is a pair of pants with three boundary components, that we label $c_{i,1}$, $c_{i,2}$, $c_{i,3}$ so that $c_{i,3}$ is the boundary component contained in ∂Q and $c_{i,1}$, $c_{i,2}$ are ruling curves in ∂N. See Figure 4.9 for an illustration of P_i.
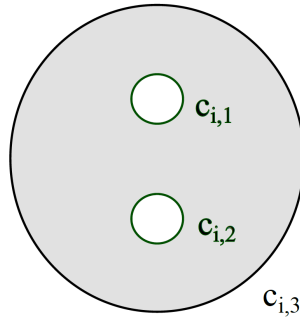
Figure 4.9 A model for P_i.

The dividing curves of P_i, $\Gamma_{P_i} = \Gamma_P \cap P_i$, intersects each of $c_{i,1}$ and $c_{i,2}$ exactly two times and intersects $c_{i,3}$ exactly $2n$ times. If Γ_{D_i} has more than two boundary parallel dividing curves then Γ_{P_i} has at least one boundary parallel dividing curve along $c_{i,3}$ and so U_2 can be destabilized in the complement of U_1 by using this boundary parallel dividing curve to form a bypass from Lemma 2.15. Since we have chosen that the maximal tb of U_2 is $-n$, D_i can have at most two boundary parallel dividing curves and thus Γ_{P_i} can be depicted in the next method as used in [15] and illustrated in Figure 4.10.

There is a coordinate system on D_i so that:

1. D_i is the unit disk in the xy plane;

2. $U_1 \cap D_i$ is $\{(0, \pm 1/2)\}$;

3. $C \cap D_i$ is the line segment $x = 0$;

4. P_i is the complement of small disks around $(0, \pm 1/2)$ in D_i.

Let $A_{i,j}$ be small annular neighborhoods of $c_{i,j}$ in P_i for $i \in \{1, 2\}$, $j \in \{1, 2, 3\}$ and let $P_i' = \overline{P_i \setminus A_{i,j}}$. The dividing curves on $\partial Q = \partial N(U_2)$ intersect D_i in $2n$ points by Lemma 2.14 since U_2 has been taken so that $tb(U_2) = -n$. For $n > 1$, the dividing set of P_i' can be considered to have n horizontal line segments in P_i', 2 of which in P_i' are given by the lines $y = \pm 1/2$. If we consider an identification between the closure of $A_{i,3}$ and the annulus $S^1 \times [0, 1]$ such that $\Gamma_{P_i} \cap (S^1 \times \{0\}) = \{p_1, ..., p_{2n}\}$, which has equally spaced points in $c_{i,3}$ and $\Gamma_{P_i} \cap (S^1 \times \{1\}) = \{p_1', ..., p_{2n}'\}$, which is the corresponding set to $\Gamma_{P_i} \cap (S^1 \times \{0\})$, in the other boundary component of $A_{i,3}$, then in $A_{i,3}$, Γ_{P_i} comprise of nonintersecting $2n$ segments which connect $p_1, ..., p_{2n}$ to $p_1', ..., p_{2n}'$ in some (cyclically permuted) order. Thus, the dividing curves in each $A_{i,j}$ can be considered as the obvious extension of the dividing curves in P_i' with some number of half-twists in $A_{i,1}$ and $A_{i,2}$ and some rigid rotation in $A_{i,3}$. In Figure 4.10 the light gray shaded region is P_i', the dark gray shaded region is $A_{i,3}$, the green shaded regions are $A_{i,1}$ and $A_{i,2}$, the union of all shaded regions is P_i, the blue vertical line is $C \cap P_i$, the red horizontal lines are the dividing curves on P_i, Γ_{P_i}, and the dividing curves in $A_{i,j}$ pass from $c_{i,j}$ to the other boundary component of $A_{i,j}$.
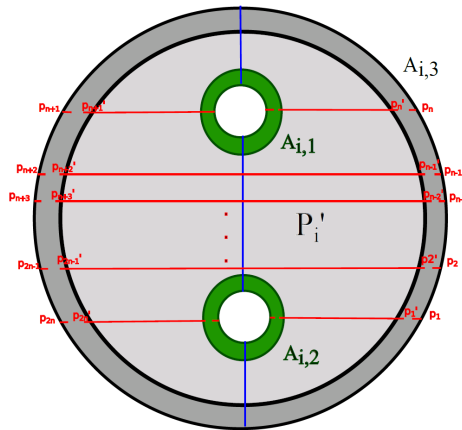
Figure 4.10 The disk D_i.

After we round the corners of $D_1 \cup D_2 \cup A_1$ by Lemma 2.18, we define A as the annulus $A_1 \cup A_{1,3} \cup A_{2,3}$. Since A_1 is a part of ∂Q, $\Gamma_{A_1} = A_1 \cap \Gamma_{\partial Q}$. There are $2n$ dividing curves passing from one boundary component to the other. Let Γ_A indicate the union of these dividing curves. We can again choose a product structure $S^1 \times [0,1]$ on the closure of A such that has the length of S^1 is $2n$, $\Gamma_A \cap (S^1 \times \{0\})$ and $\Gamma_A \cap (S^1 \times \{1\})$ each involves $2n$ equally spaced points, and Γ_A connects these two sets of points through $2n$ nonintersecting segments. From Giroux's criterion, the dividing set on the 2−sphere S in a tight contact structure must be connected, and thus the slope s of the curves in Γ_A must be relatively prime to n.
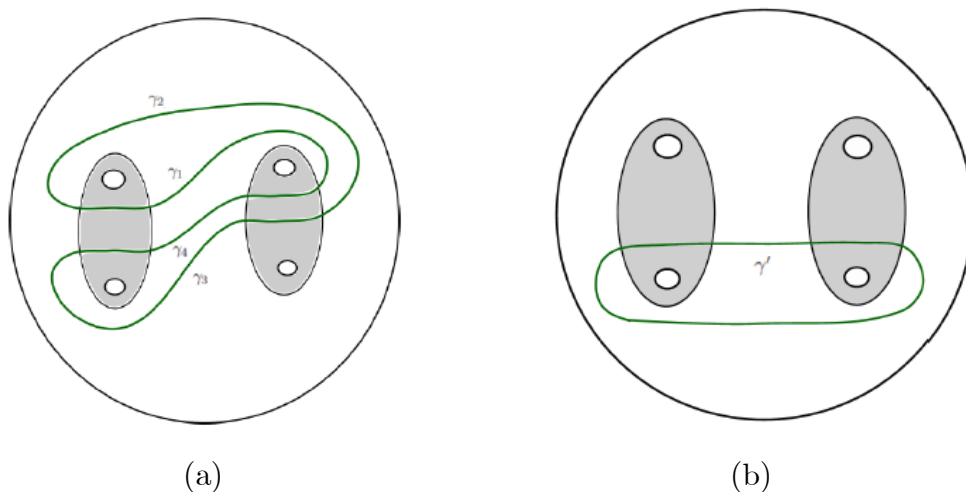
Figure 4.11 a) The curves $\gamma_1, \gamma_2, \gamma_3, \gamma_4$ obtaining from the intersection of the white annulus A and the green curve γ, b) The intersection of the white annulus A and the green curve γ'. The 2−sphere S with P_1' and P_2' shaded.

Now, we describe curves γ and γ' in S as shown in Figure 4.11 (a) and (b) on the left and the right, respectively. The curve γ bounds a disk called D_{out} in B_{out} and γ' bounds a disk called D_{in} in B_{in}, where D_{out} and D_{in} are disjoint from U_1. It can be assumed that the intersection of the dividing curves of S and both γ and γ' occurs only in A, and that the intersection of the curve γ and A is the union of the arcs $\gamma_1, \gamma_2, \gamma_3$ and γ_4 as shown in Figure 4.11. If γ is isotoped so that it intersects the P_i' in horizontal arcs, then using the above identification of the closure of A with $S^1 \times [0,1]$, the slopes of γ_i can be taken to be $2, 0, n, n-2$, respectively as illustrated in Figure 4.12. The curve γ' intersects A in two parallel linear arcs of slope 0.
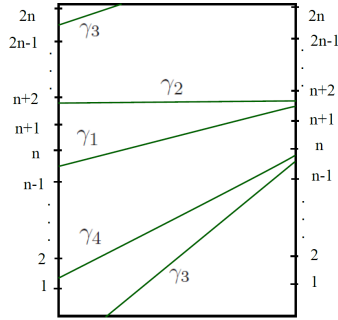
Figure 4.12 A model of the slopes of γ_i which are $2, 0, n, n-2$, respectively.

We can Legendrian realize γ and γ', and make D_{out} and D_{in} convex. In the case that $tb\,(\gamma)$ or $tb\,(\gamma')$ is not maximal, D_{out} or D_{in} has at least two boundary parallel dividing curves by Lemma 2.14 and thus there are at least two bypasses for $S \setminus N$ in the complement of U_1 by Lemma 2.15. Let c be the curve along which one of the bypasses is attached, which we will use in the proof of the Claims 4.1-4.3. In case that γ' bounds a disc in B_{in}, the bypass is attached from the back and therefore the resulting dividing curve of S is the mirror of the resulting dividing curve after attaching a bypass from the front. This can be seen in Figure 2.9.

First of all, we will find the configuration of the dividing curves on S in the next lemma. In order to prove this, we will use some results we have found in the proof of the Claim 4.3.

Lemma 1.7 When $tb(U_2) = -1$ then we can assume the dividing set on A is in Figure 4.13.
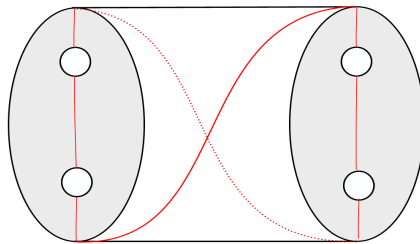
Figure 4.13 The dividing curve on A having slope of 1 when $tb(U_2) = -1$.

Proof of Theorem 1.2 We will use [15] as a guide to prove this theorem. Here we take the Legendrian knot K_0 to be U_1 and the Legendrian knot B to be U_2 as before. The standard model of K_0 was illustrated in Figure 4.6. Let $D = \{(x, y, z) \mid x^2 + z^2 \leq 1,\ y = 0\}$ be a convex disk in $\mathbb{R}^3 \subset S^3$. Let's take a standard neighborhood E of D in S^3, $E = \{(x, y, z) \mid x^2 + z^2 \leq 1,\ y^2 \leq 1\}$. Let F be the complement of the interior of E

in S^3 with corners rounded ($F = \overline{S^3 \setminus E}$). We know from Theorem 1.2 that U_2 destabilizes in the complement of U_1 until it has $tb = -1$. When $tb(U_2) = -1$ and U_2 does not destabilize, we have obtained in proof of Theorem 1.2, the slope of the dividing set on ∂B_{out} can be made 1 (it is Lemma 1.7) and thus it looks like Figure 4.13, indicated by the red curve. We want to prove that $U_1 \cap B_{out} = U_{1_{out}}$ (can be taken as $l_1' \cup l_2'$ which smoothly are as shown in Figure 4.15) is contactomorphic to two Legendrian arcs in F, namely l_1 (left) and l_2 (right) shown in Figure 4.14. The dividing curves on the boundary of the ball (∂F) in Figure 4.14 and the ones on ∂B_{out} in Figure 4.15 are diffeomorphic curves under the diffeomorphism of the ball.
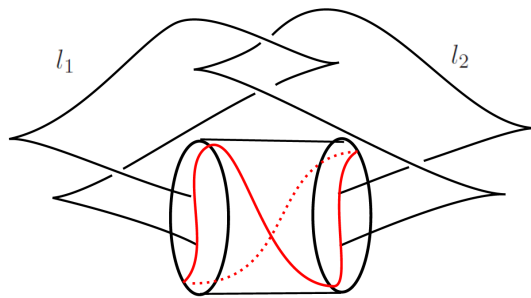
Figure 4.14 Model for a non-destabilizable tangle in B_{out}.
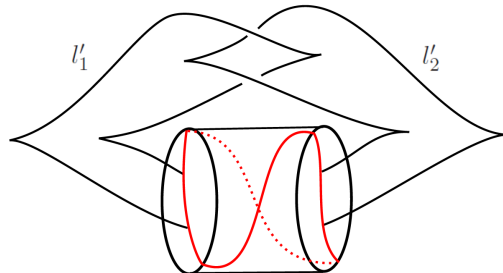
Figure 4.15 Model for the dividing set on ∂B_{out}.

We take product neighborhoods of l_1 and l_2, $N_1 = D^2 \times [0, 1]$ and $N_2 = D^2 \times [0, 1]$, respectively. We can assume each N_i intersects with ∂F in two disks, each of which intersects $\Gamma_{\partial F}$ in an arc. We can also assume that $\partial (N_i \cap \partial F)$ can take as the union of leaves of the characteristic foliation of ∂F and we can arrange that ∂N_i is convex by Theorem 2.8.

$H = F \setminus (N_1 \cup N_2)$ is a handlebody of genus 2 and the boundary of it is a surface with corners. The manifold after cutting H along properly embedded two disks D_1 and D_2 which are denoted in Figure 4.16 is a $3-$ball. The disks D_1 and D_2 are disjoint disks satisfying that $\partial D_i \subset \partial H$ and $Int(D_i) \subset Int(H)$ for $i \in \{1, 2\}$ ($Int(D_i)$ and $Int(H)$ indicate the interior of D_1 and H, respectively). In Figure 4.16 we see the boundary of

D_1 in H with the green curve and D_2 can be seen after reflecting the picture in a vertical line. We can isotop H into H^1 (H^1 is a standardly embedded handlebody of genus 2 in S^3 on the left hand side in Figure 4.16) by isotoping the handles of H^1 with N_1 and N_2 as illustrated in Figure 4.16. The disk D_1^1 bounded by the green curve and D_2^1 bounded by the curve reflected the green curve in a vertical line on the left hand side in Figure 4.16 (below) cut H^1 into a 3−ball. Thus, we see where the disks D_1 and D_2 come from isotoping the green curves from right to the left in Figure 4.16.
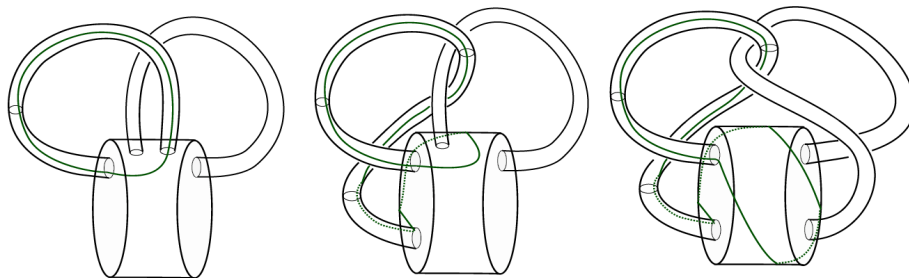
Figure 4.16 H^1 is on the left hand side and the disk D_1^1 in H^1 is bounded by the green curve. H is on the right hand side and the disk D_1 in H is bounded by the green curve.

Now, we will try to find how the contact structure on H and H' are determined and then we will prove the existence of a contactomorphism between F and B_{out} taking $l_1 \cup l_2$ to $l_1' \cup l_2' = U_{1_{out}}$. A contact structure on a neighborhood $N(\partial H)$ of ∂H is determined by the characteristic foliation on ∂H from Theorem 2.6. Thus, it can be found a bit smaller handlebody $\widehat{H}$ in H such that $\partial\widehat{H}$ is included in $N(\partial H)$ and is obtained by rounding the corners of ∂H. Let $\widehat{D}_i = D_i \cap \widehat{H}$. We can make $\widehat{D}_i$ convex and take L_i to be a Legendrian realization of $\partial\widehat{D}_i$ on $\partial\widehat{H}$ by Theorem 2.12.
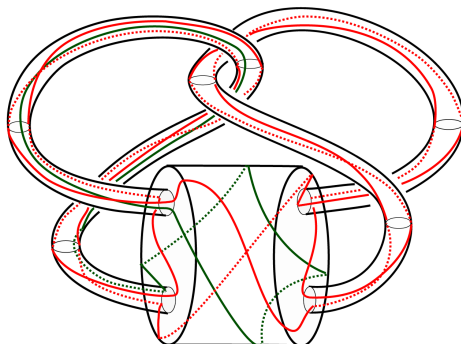
Figure 4.17 The red curves indicate the dividing curves.

The dividing set $\Gamma_{\widehat{D}_i}$ can be determined according to how $\partial\widehat{D}_i$ intersect $\Gamma_{\partial\widehat{H}}$. There are four points in the set of intersection of L_i and the dividing set $\Gamma_{\partial\widehat{H}}$. See Figure 4.17.

We observe that three of these points are in ∂N_i by noticing that $\partial \widehat{D}_i \cap \partial N_i$ intersects the dividing set efficiently and one point x of these points is in ∂F. Thus we have $tb(L_i) = -2$ by Lemma 2.14 and as we are in a tight contact structure $\Gamma_{\widehat{D}_i}$ is a collection of two boundary parallel arcs. Furthermore, these two boundary parallel arcs on $\widehat{D}_i$ do not straddle the point x. In order to prove this, let us suppose that one of these boundary parallel arcs straddles x. In this case, the other dividing arc on $\widehat{D}_i$ gives a bypass attached along ∂N_i. After we attach the bypass to $\partial \widehat{H}$, we have a genus $2-$surface Σ and a curve γ corresponding to L_i on $\partial \widehat{H}$. The bypass attachment operation gives that the new curve γ intersects the dividing arcs on Σ twice. One of the two dividing curves which does not consist x does not intersect the γ after bypass attachment and γ intersects the dividing set of Σ along only one dividing curve of Γ_Σ. After compressing the surface Σ along a meridional disk to N_{i+1} for $i \in \{1,2\}$ with the form that $N_3 = N_1$, we have a convex torus T (that is a genus $1-$ surface) on which γ sits. The curve γ does not bound a disk in the torus T, it is an essential curve in T and bounds a disk in the complement of T. Since γ intersects the dividing arcs on Σ along only one dividing curve of Γ_Σ, it can be isotoped to be disjoint from it. Hence γ can be Legendrian realized which results in an unknot with $tb = 0$, but this is a contradiction since we are in a tight contact manifold.

The dividing set on $\widehat{D}_i$ has now been completely determined, and thus the contact structure on H is completely determined by the characteristic foliation on ∂H (and after isotoping the boundary slightly, by $\Gamma_{\partial H}$) by Theorem 2.10. After we cut H along the disks D_1 and D_2, and round the edges we get a connected dividing set on F.

Now, we lead our attention to the knot U_1. We assume we have normalized U_1, N a neighborhood of U_1, and the sphere S as before while preparing the proof of the main theorem. Let l'_1 (left) and l'_2 (right) in Figure 4.15, be the Legendrian arcs which are the components of $U_1 \cap B_{out}$ and N'_1 and $N'_2$ the components of $N \cap B_{out}$. The set $H' = B_{out} \backslash (N'_1 \cup N'_2)$ is a handlebody of genus 2 and the boundary of it is a surface with corners. The manifold after cutting H' along properly embedded two disks D'_1 and D'_2 which are denoted in Figure 4.18 is a $3-$ball. D'_1 and D'_2 are disjoint disks satisying that $\partial D'_i \subset \partial H'$ and $Int(D'_i) \subset Int(H')$ for $i \in \{1,2\}$. In Figure 4.18 we see the boundary of D'_1 in H' with the green curve and D'_2 can be seen after reflecting the picture in a vertical line. H' can be isotoped into H^1 by isotoping the handles of H^1 with N'_1 and N'_2 as illustrated in Figure 4.18. We see where the disks D'_1 and D'_2 come from while isotoping the green

curves from right to the left in Figure 4.18. We can choose these two disks D'_1 and D'_2 as shown in Figure 4.18.
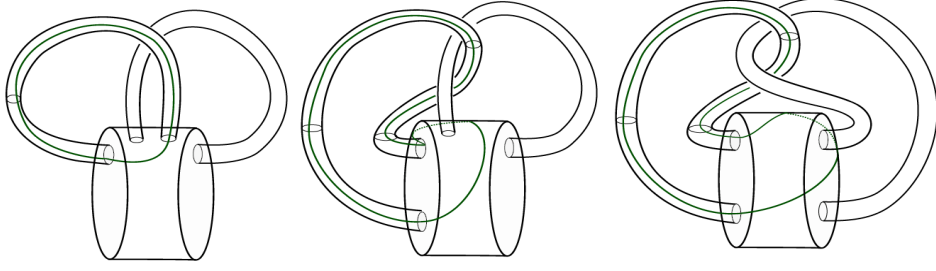
Figure 4.18 H' and H are on the left and right hand side, respectively. The disk D'_1 in H' is bounded by the green curve on the left hand side.

A contact structure on a neighborhood $N(\partial H')$ of $\partial H'$ is determined by the characteristic foliation on $\partial H'$. Thus, it can be found a bit smaller handlebody $\widehat{H'}$ in H' such that $\partial \widehat{H'}$ is included in $N(\partial H')$ and is obtained by rounding the corners of $\partial H'$. Let $\widehat{D'_i} = D'_i \cap \widehat{H'}$. We can make $\widehat{D'_i}$ convex and take L'_i to be a Legendrian realization of $\partial \widehat{D'_i}$ on $\partial \widehat{H'}$ by Theorem 2.12.
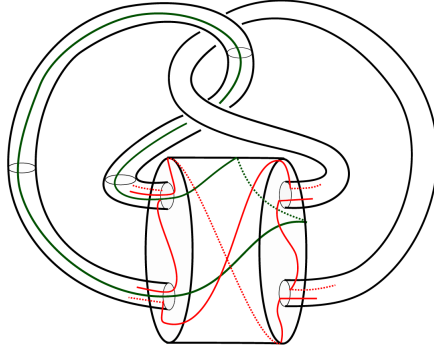
Figure 4.19 The red curves indicate the dividing curves.

There are two points in the set of intersection of L'_i and the dividing set $\Gamma_{\partial B_{out}}$. One of these points being near N'_i can be assumed to be on N'_i, the other one is on ∂B_{out} at some point y. While the intersection on $\partial \widehat{H'}$ is efficient, the intersection on $\partial(B_{out} \backslash N'_i)$ (a torus) is inefficient, the two intersection points in Figure 4.19 can be removed by isotopy. Since the intersection is inefficient, if $tb(L'_i) \leq -2$ then we get bypass for $\partial(B_{out} \backslash N'_i)$, but might be trivial bypass and trivial bypass does not change the dividing set [20]; if $tb(L'_i) \leq -3$ then there are at least two bypasses on $\widehat{D'_i}$ and one of these will destabilize L'_i. Thus, if $tb(L'_i) \leq -3$ then there is a bypass for $\partial \widehat{H'} \cap \partial N'_i$ along $\widehat{D'_i}$. This bypass on $\widehat{D'_i}$ can be considered to be a bypass along the boundary of the disk bounded by K_0 ([15], Claim 4.6) and it might give a destabilization of U_1.

By Theorem 4.1, we can assume U_1 and U_2 have $tb = -1$. When $tb(U_1) = -1$ and U_1 does not destabilize then $tb(L_i') = -2$, or -1. When $tb(L_i') = -2$, we have the disallowed bypass and the trivial bypass and since we are in a tight contact structure the bypass attachment must be trivial. When $tb(L_i') = -2$, the trivial bypass does not effect the dividing set and so L_i' does not destabilize. Thus, we obtain that $tb(L_i')$ is not -1. Hence L_i' intersects the dividing set for some point on $\partial N_i'$ apart from ∂B_{out}. Thus we may assume $tb(L_i') = -2$. $\Gamma_{\widehat{D_i'}}$ is a collection of two boundary parallel arcs as we are in a tight contact structure. These boundary parallel dividing curves do not straddle the point y.

Hence the dividing set on $\widehat{D_i'}$ has been determined, and thus the contact structure on H' is determined by the characteristic foliation on $\partial H'$ (and after isotoping the boundary slightly, by $\Gamma_{\partial H}$). After we cut H' along the disks D_1' and D_2', and round the edges we get a connected dividing set on B_{out}.

We can thus find a diffeomorphism $\phi : B_{out} \to F$ so that $\phi(\Gamma_{\partial B_{out}}) = \Gamma_{\partial F}$, $\phi(l_i') = l_i$, $\phi(D_i') = D_i$. This diffeomorphism can be isotoped to be a contactomorphism in a neighborhood of $(\partial F) \cup l_1 \cup l_2$ by Theorem 2.6. We also have determined the configuration of the dividing curves on D_i and D_i' above. Consequently, we can isotop ϕ to be a contactomorphism ψ from B_{out} to F taking $l_1' \cup l_2' = U_{1_{out}}$ to $l_1 \cup l_2$ and a ruling curve on ∂B_{out} isotopic to B to the some on ∂F. Therefore $l_1 \cup l_2$ is a non-destabilizable tangle in B_{out}.

We know the dividing set on ∂B_{out} when U_2 does not destabilize (Lemma 4.1) and we have found the data about contact structure on B_{out} when both U_1 and U_2 does not destabilize. We now look at the structure in B_{in}. The contactomorphism ψ from B_{out} to F in S^3 can be extended as a diffeomorphism to B_{in}. Because of the fact that unique tight contact structure on the $3-$ball up to isotopy by Theorem 2.1, we can isotop this diffeomorphism considering B_{out} to a contactomorphism on B_{in}. $U_{1_{in}}$ is a Legendrian $2-$braid, and we know that if there is not a destabilization of the $2-$braid, then it is obtained by putting two twists by [15]. Hence, we have a contactomorphism of S^3 taking $U_1 = U_{1_{in}} \cup U_{1_{out}}$ to the knot U_1' in Figure 4.20, and U_2 on ∂B_{out} to the knot U_2' on ∂F. It follows that given any L in the knot type W_+ such that $L = U_1 \cup U_2$ are contact isotopic to Figure 4.21 by Theorem 2.2. Since Legendrian isotopy in (S^3, ξ_{st}) is the same as an ambient contactomorphism from Theorem 2.3, these two links are Legendrian isotopic.
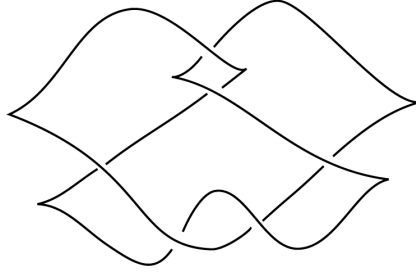
Figure 4.20 Legendrian knot U_1' being Legendrian isotopic to U_1.

Thus, when both U_1 and U_2 does not destabilize, there is a unique representative of the link as shown in Figure 4.21 with maximal Thurston-Bennquin invariant $tb = -2$ and rotation number $r = 0$ if orientations are ignored.
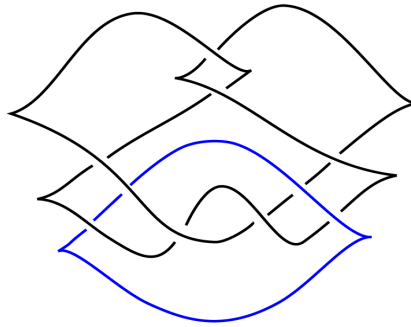
Figure 4.21 Legendrian positive Whitehead link with maximal tb.

In addition, after four Legendrian Reidemeister Moves (Theorem 2.4) we see that the link in Figure 4.21 is Legendrian isotopic to the link $U_1 \cup U_2$ shown in Figure 4.22.
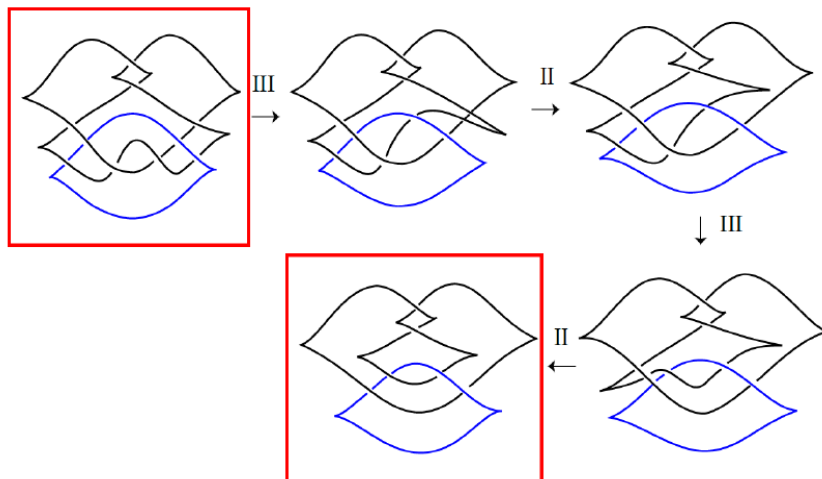
Figure 4.22 Legendrian isotopy between two different legendrian front of the positive Whitehead link W_+ with maximal tb.

$\square$

The link is realized by two $tb = -1$ Legendrian unknots. The number of the representatives will change when we take the orientations on this link in Figure 4.21 into account. However, this is in the concept of Theorem 1.5.

The proofs of Lemma 1.6 and 1.7 both follow from the proofs of the following claims. We here set the Legendrian class of W as $L = U_1 \cup U_2 \in \mathcal{L}(W_+)$, where $W = O_1 \cup O_2$ in the knot type W_+ with $O_1 = K_0$ and $O_2 = B$. Let $tb(U_i) = -n_i$, $i \in \{1, 2\}$. We will check all the cases to understand when U_2 destabilizes. In the rest of the work, red curves indicates dividing curves Γ_A and green curves indicates γ and γ', respectively.

Claim 4.1 *When $n_2 \geq 4$, U_2 destabilizes.*

Claim 4.2 *When $n_2 = 3$, U_2 destabilizes.*

Claim 4.3 *When $n_2 = 2$, U_2 destabilizes.*

Corollary 4.1 *When $tb(U_2) = -1$, the dividing set are in the forms of Figure 4.104 (b), 4.94 (a) and 4.96 (b) with slope -1, 0, 1, respectively.*

We will need Giroux's criterion theorem (Theorem 2.11) to detect bypasses for the next proofs. In particular, we will eliminate the bypasses which make the dividing set is disconnected in tight contact sphere.

Proof of Lemma 1.7 We have found as a corollary in searching the cases when U_2 destabilizes (concept of Theorem 1.2) that when $tb(U_2) = -1$ the dividing set is in the form of either Figure 4.103 (b), 4.93 (a) and 4.95 (b) which we redraw in Figure 4.23. The slope s of the dividing curves equals -1, 0 and 1 in Figure 4.23 (a), (b) and (c), respectively.

(a)   (b)   (c)
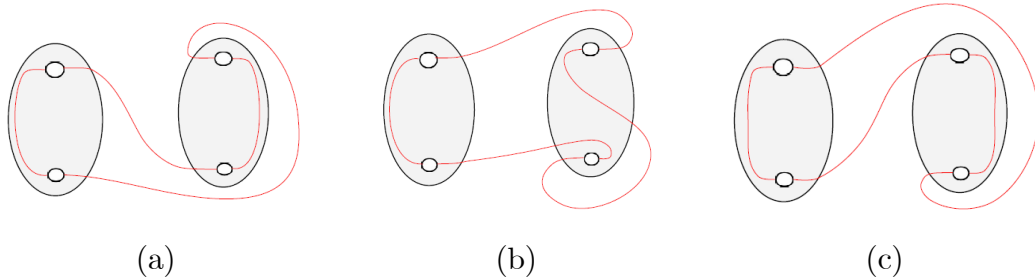
Figure 4.23 The dividing curves on A when $tb(U_2) = -1$.

When $s = 0$, we see that the intersection of the dividing set on A and the curve γ in green in Figure 4.24.
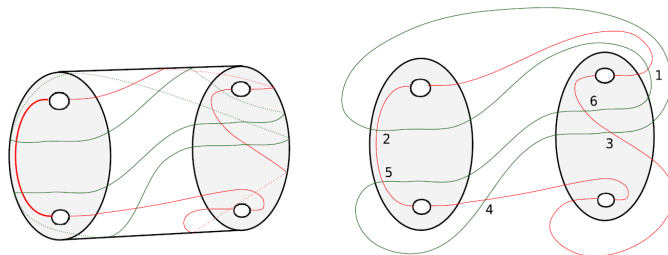
Figure 4.24 Γ_A when $s = 0$.

If we attach a bypass along $3 - 4 - 5$ and $6 - 1 - 2$, then we would obtain a convex sphere S with disconnected dividing set, contradicting tightness by Theorem 2.11. For the attaching arcs $1 - 2 - 3$, $2 - 3 - 4$, $4 - 5 - 6$ and $5 - 6 - 1$ when there is a bypass from the front, we also have a bypass on A along the arc $1' - 2' - 3'$, $2' - 3' - 4'$ and $5' - 6' - 1'$, respectively from Bypass Rotation (Lemma 2.17) as shown in Figure 4.25. After attaching the bypass along $1' - 2' - 3'$, $2' - 3' - 4'$, $4' - 5' - 6'$ and $5' - 6' - 1'$ we obtain that the resulting dividing curve are as seen in Figure 4.26 by Theorem 2.16 and the slope s of the dividing set on A increases by 1 in Figure 4.26. Hence, the new dividing curve on A has slope of 1.

(a)

(b)

(c)

(d)
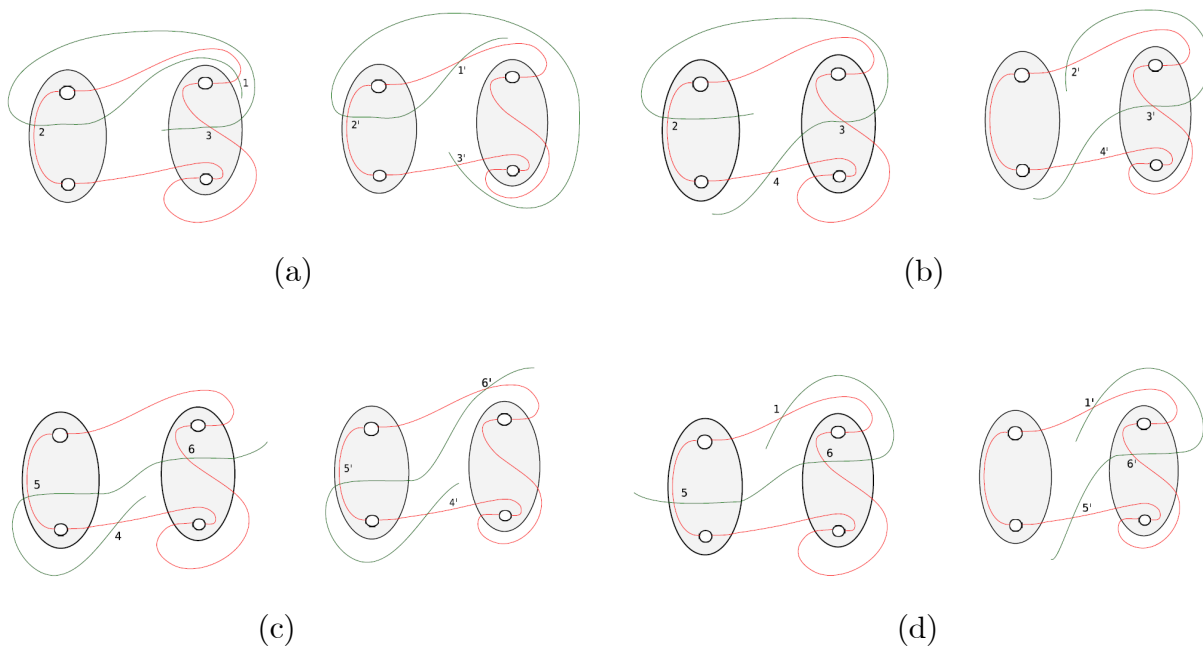
Figure 4.25 Getting a new bypass along a) $1' - 2' - 3'$, b) $2' - 3' - 4'$, c) $4' - 5' - 6'$, d) $5' - 6' - 1'$ after using bypass rotation when $s = 0$.

(a)   (b)   (c)   (d)
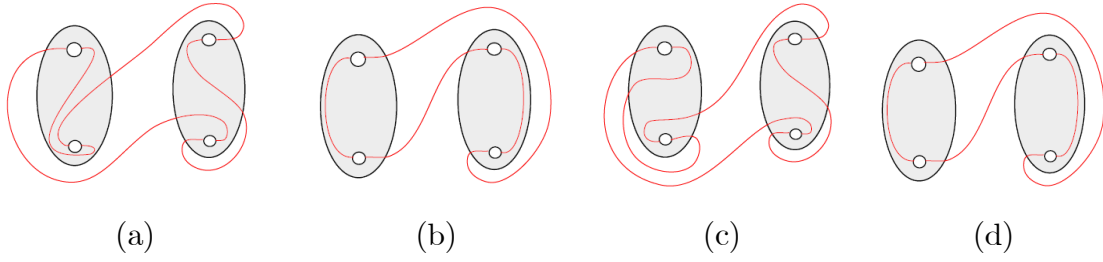
Figure 4.26 The dividing set on A after attaching the bypass along a) $1' - 2' - 3'$, b) $2' - 3' - 4'$, c) $4' - 5' - 6'$, d) $5' - 6' - 1'$ when $s = 0$.

Figure 4.26 (a) and Figure 4.26 (c) look different from Figure 4.26 (b) and Figure 4.26 (d), but they only differ by Dehn twists parallel to the inside boundary components. When $s = -1$, we see that the intersection of the dividing set on A and the curve γ in green in Figure 4.27.
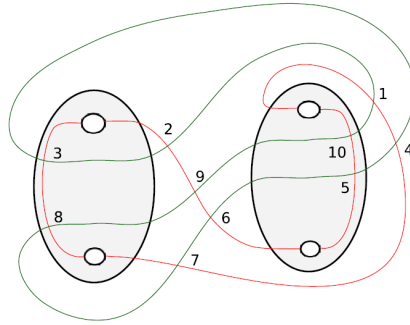
Figure 4.27 Γ_A when $s = -1$.

When we attach a bypass along the attaching arcs $2 - 3 - 4$, $4 - 5 - 6$, $7 - 8 - 9$ and $9 - 10 - 1$, then we have the resulting dividing curves on A are as seen in Figure 4.28 by Theorem 2.16 and the slope s increases by 1. Hence, the new dividing curve on A has slope of 0. When $s = 0$, we know the slope can increase by 1 as shown in Figure 4.26. If we attach a bypass along the other attaching arcs then we would obtain a convex sphere S with disconnected dividing set, contradicting tightness.

(a)   (b)   (c)   (d)
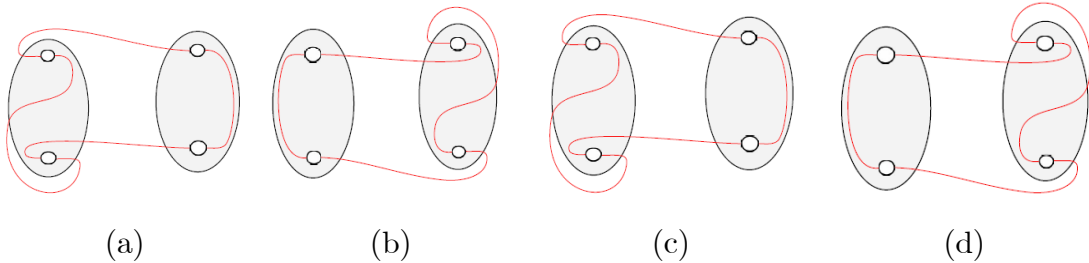
Figure 4.28 The dividing set on A after attaching the bypass along a) $2 - 3 - 4$, b) $4 - 5 - 6$, c) $7 - 8 - 9$, d) $9 - 10 - 1$ when $s = -1$.

$\square$

Proof of the Lemma 1.6 The proof follows from the proofs of the Claim 4.1, Claim 4.2 and Claim 4.3 which we will exhibit next. □

If a bypass along c from front destabilizes U_2, then there is no need to check the bypasses along c from back, or vice versa. However, we examined both of them in the following proofs when doing case by case analysis. We find sometimes the bypass is on one side, sometimes on the other side and sometimes both sides.

Proof of the Claim 4.1 Notice that if $c \cap (P_1' \cup P_2')$ has one component, we meet with the following situations for c in Figure 4.29 When we attach the bypass from the back, the subcases for $c \subset \gamma'$ are the mirrors of the subcases for γ.
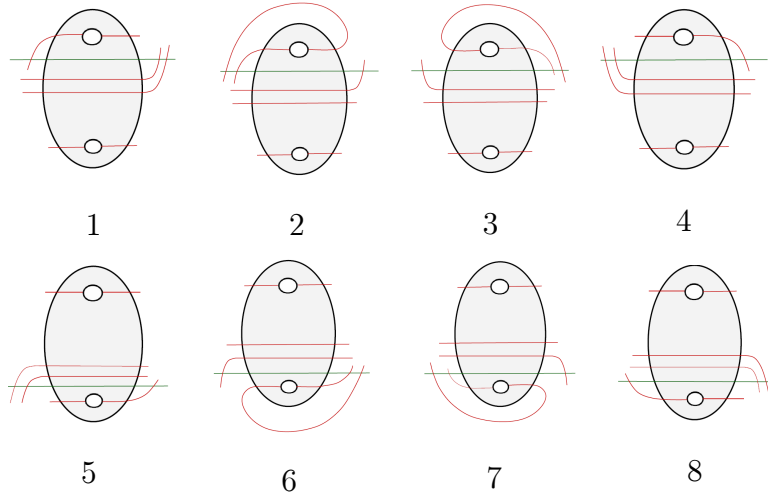
Figure 4.29 The 8 subcases if $c \cap (P_1' \cup P_2')$ has one component when $n_2 \geq 4$.

In the case when $n_2 \geq 4$ or $|s| > 7$ there will be a bypass c along γ and along γ'. We need to see how attaching it will affect the dividing curves on S. If $c \cap (P_1' \cup P_2') = \emptyset$, then when attaching the bypass to $A \subset S$, we can destabilize U_2 in the complement of U_1. If $c \cap (P_1' \cup P_2')$ has one component, the possibilities of c are shown in Figure 4.29. For $s > 7$, we must consider the 1st, 2nd, 5th, and 6th configurations in Figure 4.29. If c is a subset of γ we see that in cases 2 and 6 that the dividing set on S is disconnected after attaching the bypass. This contradicts the tightness of the contact structure so such bypasses never exist. In cases 1 and 5 we see that U_2 destabilizes. If c is a subset of $\gamma\prime$ then in all cases U_2 destabilizes for some slopes and for the other slopes in cases 2 and 6 we see that U_2 destabilizes. For $s < -7$ one can similarly see that either a bypass attachment leads to a disconnected dividing set for S, and so does not exist, or destabilizes U_2.

We are left to consider the case when $n_2 = 4$ and $s = 1, 2, 3, 5, 7, -1, -3, -5,$ or -7. We will do a case by case analysis of these.

1.1 Let $s = 1$.

1. Figure 4.30 illustrates a model of the case when $n_2 = 4$ and $s = 1$ for γ.
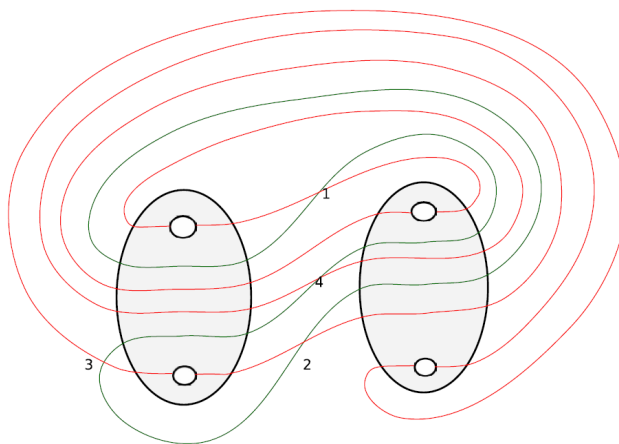
Figure 4.30 A model of the case when $n_2 = 4$ and $s = 1$ for γ.

All the cases when there could be bypasses c along γ in Figure 4.30 are represented as the result of attaching bypass in Figure 4.31 (a) and (b). We see that U_2 destabilizes in all these cases. If we attach a bypass along $1 - 2 - 3$ and $3 - 4 - 1$, then we would obtain a convex sphere S with disconnected dividing set, contradicting tightness. We meet the subcase 7 for a bypass along $2 - 3 - 4$ and $4 - 1 - 2$ is the case when $c \cap (P_1' \cup P_2')$ has two components. After the destabilization we see below that the n_2 becomes 3 and s is -1 and 1, respectively.

(a)   (b)

Figure 4.31 a) Γ_A after bypass along the arc $2 - 3 - 4$, b) Γ_A after bypass along the arc $4 - 1 - 2$.

2. Figure 4.32 illustrates a model of the case when $n_2 = 4$ and $s = 1$ for γ'.

Figure 4.32 A model of the case when $n_2 = 4$ and $s = 1$ for γ'.

Only one case when there could be bypasses c along γ' in Figure 4.32 is represented as the result of attaching bypass in Figure 4.33. We see that U_2 destabilizes in this case. If we attach a bypass along $1 - 2 - 3$ and $3 - 4 - 1$, then we would obtain a convex sphere S with disconnected dividing set, contradicting tightness. If we attach a bypass along $4 - 1 - 2$, then we do not have a destabilization of U_2. We meet the subcase mirror of 7 for a bypass along $2 - 3 - 4$. After the destabilization we see that the n_2 becomes 3 and s is still 1.

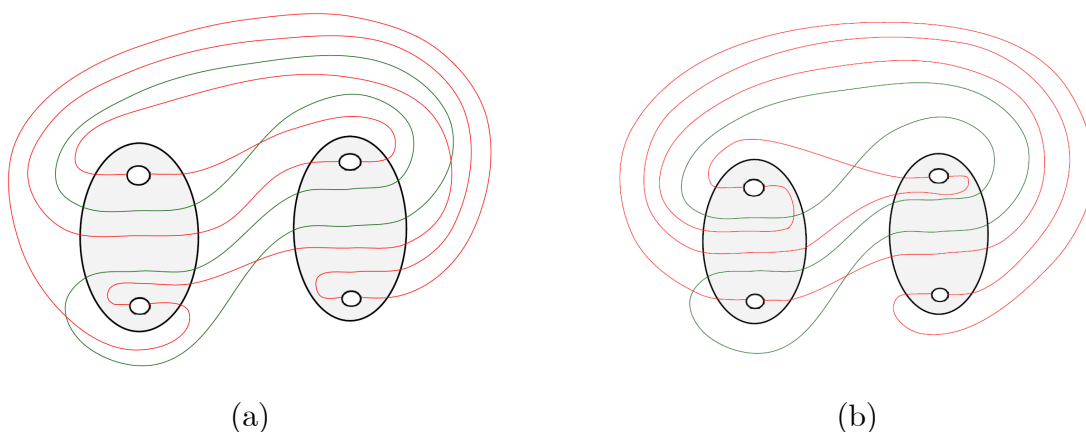**Figure 4.33** Γ_A after bypass along the arc $2 - 3 - 4$.

1.2 Let $s = 3$.

1. Figure 4.34 illustrate a model of the case when $n_2 = 4$ and $s = 3$ for γ.
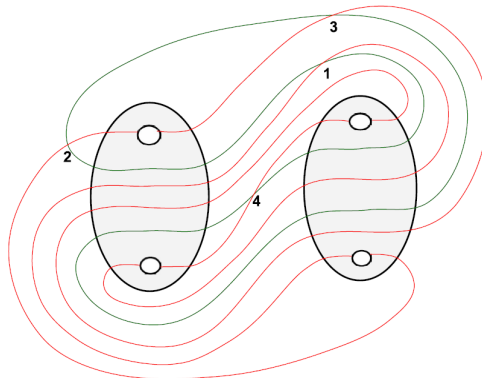
Figure 4.34 A model of the case when $n_2 = 4$ and $s = 3$ for γ.

All the cases when there could be bypasses c along γ in Figure 4.34 are represented as the result of attaching bypass in Figure 4.35 (a) and (b). If we attach a bypass along $1-2-3$ and $3-4-1$, then we would obtain a convex sphere S with disconnected dividing set, contradicting tightness. It is clearly seen in Figure 4.35 that U_2 was not destabilized since it has $tb = -5$.

(a)   (b)

Figure 4.35 a) Γ_A after bypass along $2-3-4$, b) Γ_A after bypass along $4-1-2$.

2. Figure 4.36 illustrates a model of the case when $n_2 = 4$ and $s = 3$ for γ'.
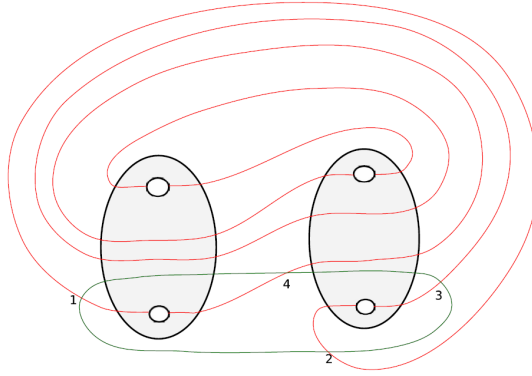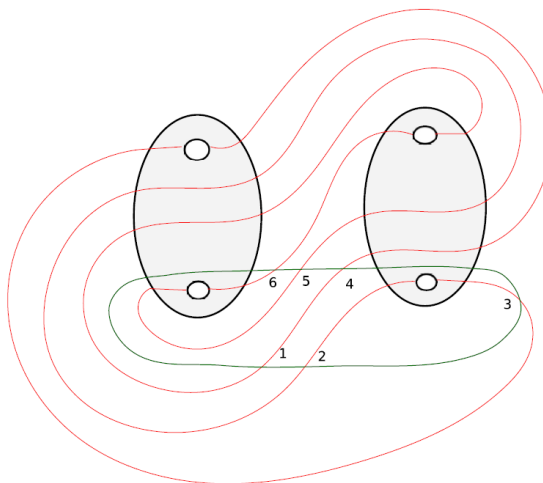

Figure 4.36 A model of the case when $n_2 = 4$ and $s = 3$ for γ'.

All the cases when there could be bypasses c along γ' in Figure 4.36 are represented as the result of attaching bypass in Figure 4.37 (a) and (b). We see that U_2 destabilizes in all these cases. If we attach a bypass along $1-2-3$, $3-4-5$, $4-5-6$ and $6-1-2$ then we would obtain a convex sphere S with disconnected dividing set, contradicting tightness. We meet the subcase mirror of 7 for both situations. After the destabilization we see that the n_2 becomes 3 and s is 3.

(a)   (b)

Figure 4.37 a) Γ_A after bypass along $2 - 3 - 4$, b) Γ_A after bypass along $5 - 6 - 1$.

1.3 Let $s = 5$.

1. Figure 4.38 illustrates a model of the case when $n_2 = 4$ and $s = 5$ for γ.

Figure 4.38 A model of the case when $n_2 = 4$ and $s = 5$ for γ.

Some cases when there could be bypasses c along γ in Figure 4.38 are represented as the result of attaching bypass in Figure 4.39 (a) and (b). We see that U_2 destabilizes in all these cases. If we attach a bypass along a curve $1 - 2 - 3$, $2 - 3 - 4$, $3 - 4 - 5$, $5 - 6 - 7$, $6 - 7 - 8$, $7 - 8 - 9$, $8 - 9 - 10$, $9 - 10 - 11$, $11 - 12 - 1$ and $12 - 1 - 2$ then we would obtain a convex sphere S with disconnected dividing set, contradicting tightness. After the destabilization along a curve $4 - 5 - 6$ and $10 - 11 - 12$ we see that the n_2 becomes 3 and s becomes 3.
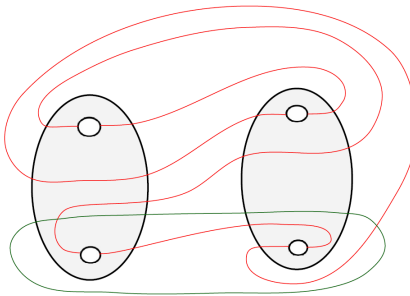
Figure 4.39 a) Γ_A after bypass along $4 - 5 - 6$, b) Γ_A after bypass along $10 - 11 - 12$.

2. Figure 4.40 illustrates a model of the case when $n_2 = 4$ and $s = 5$ for γ'.

Figure 4.40 A model of the case when $n_2 = 4$ and $s = 5$ for γ'.

Some cases when there could be bypasses c along γ' in Figure 4.40 are represented as the result of attaching bypass in Figure 4.41 (a) and (b). We see that U_2 destabilizes in all these cases. If we attach a bypass along $1 - 2 - 3$, $5 - 6 - 7$, $10 - 11 - 12$, and $11 - 12 - 1$, then we would obtain a convex sphere S with disconnected dividing set, contradicting tightness. If we attach a bypass along $2 - 3 - 4$, $4 - 5 - 6$ and $9 - 10 - 11$ which are the cases when $c \cap (P'_1 \cup P'_2)$ has no components, then we would obtain a destabilization of U_2 and after the destabilization we would see that the n_2 becomes 3 and s becomes 3. If we attach a bypass along $7 - 8 - 9$ which is the subcase mirror of 8, $3 - 4 - 5$ and $8 - 9 - 10$ which are the cases when $c \cap (P'_1 \cup P'_2)$ has no components, then we obtain a destabilization of U_2 and after the destabilization we see that the n_2 becomes 2 and s becomes 3. If we attach a bypass along $6 - 7 - 8$ which is the subcase mirror of 7, then we obtain a destabilization of U_2 and after the destabilization we see that the n_2 becomes 3 and s is still 5.
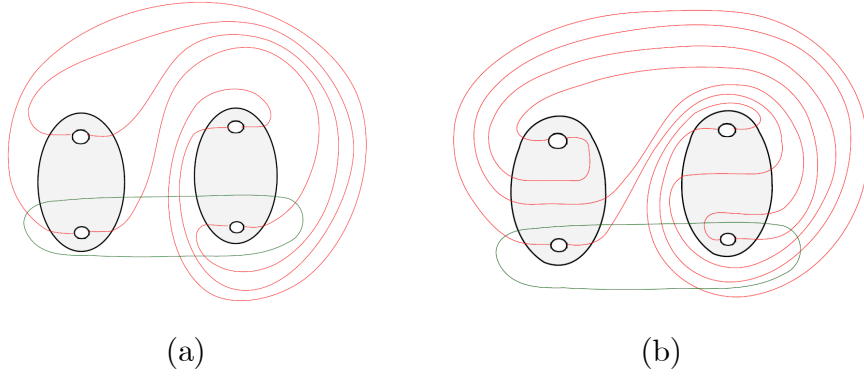
Figure 4.41 a) Γ_A after bypass along $3-4-5$, $7-8-9$, and $8-9-10$, b) Γ_A after bypass along $6-7-8$.
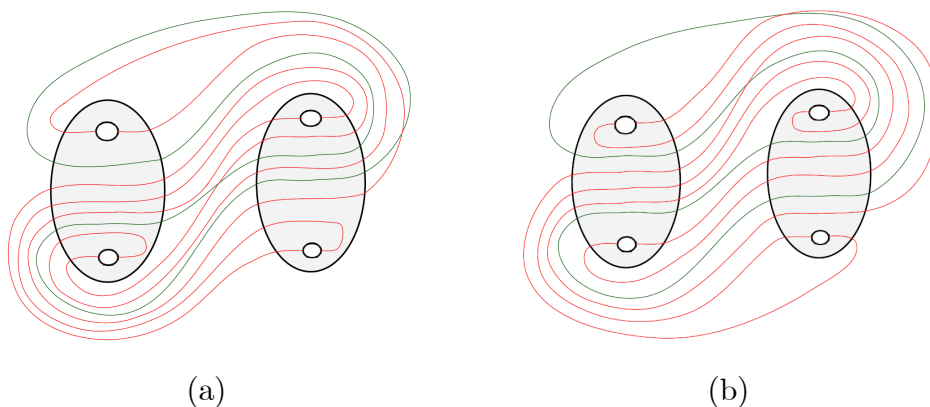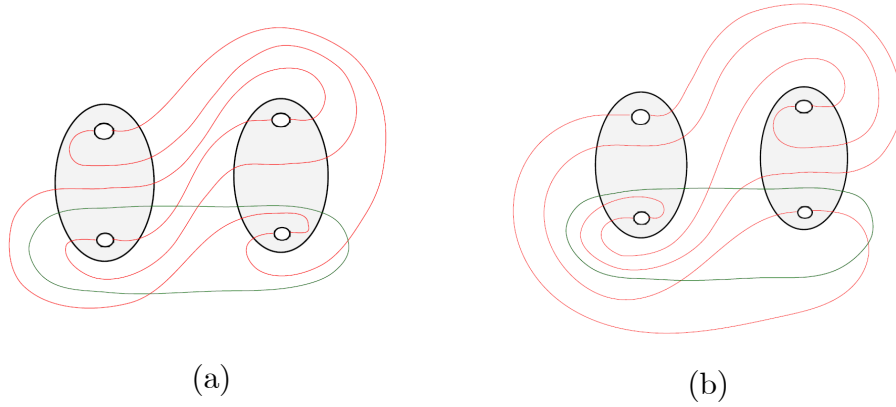
1.4 Let $s = 7$.

1. Figure 4.42 illustrates a model of the case when $n_2 = 4$ and $s = 7$ for γ.

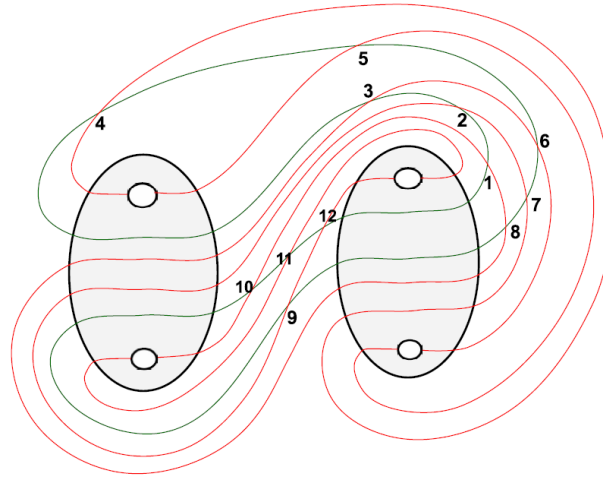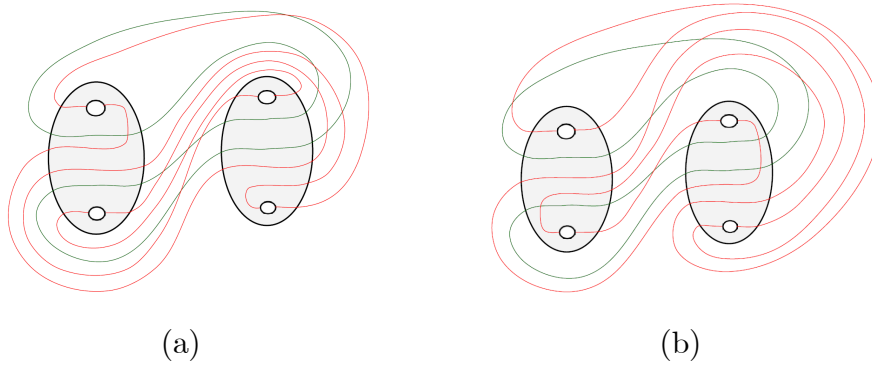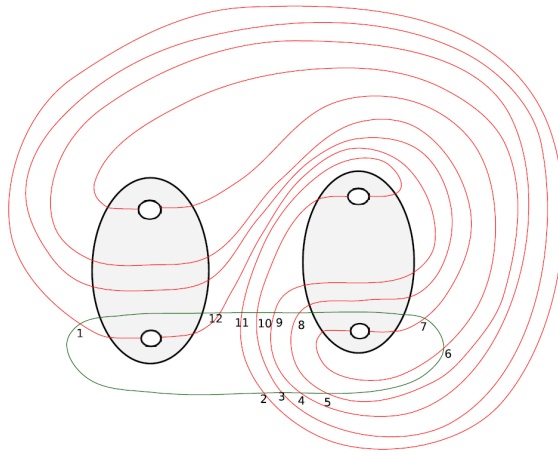**Figure 4.42** A model of the case when $n_2 = 4$ and $s = 7$ for γ.

Some cases when there could be bypasses c along γ in Figure 4.42 are represented as the result of attaching bypass in Figure 4.43 (a), (b) and (c). We see that U_2 destabilizes in all these cases. If we attach a bypass along $5-6-7$, $12-13-14$, and $21-22-1$, then we would obtain a convex sphere S with disconnected dividing set, contradicting tightness. If we attach a bypass along $7-8-9$, $14-15-16$, $19-20-21$ which are the cases when $c \cap (P_1' \cup P_2')$ has no components, then we would obtain a destabilization of U_2 and after the destabilization we would see that the n_2 becomes 2 and s becomes 3. If we attach a bypass along $4-5-6$, $11-12-13$, and $22-1-2$ which are the subcase 1, then we obtain a destabilization of U_2 and after the destabilization we see that the n_2 becomes 3 and s becomes 5.

50
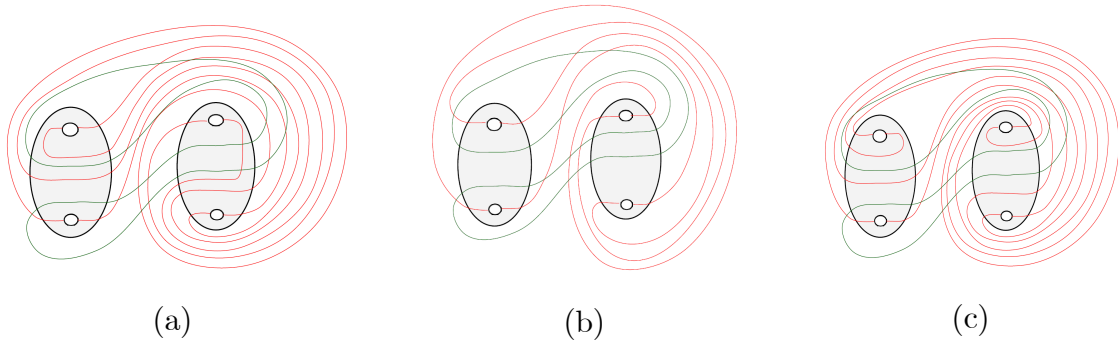
Figure 4.43 a) Γ_A after bypass along $4-5-6$, b) Γ_A after bypass along $7-8-9$, $14-15-16$ and $19-20-21$, c) Γ_A after bypass along $22-1-2$.

2. Figure 4.44 illustrates a model of the case when $n_2 = 4$ and $s = 7$ for γ'.

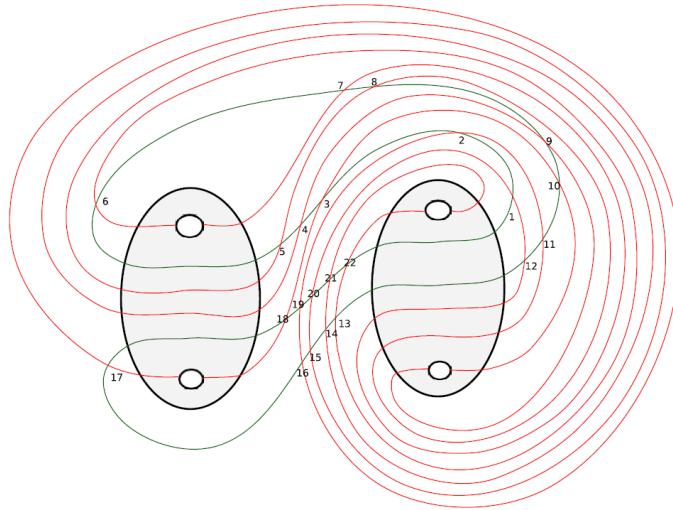**Figure 4.44** A model of the case when $n_2 = 4$ and $s = 7$ for γ'.

Some cases when there could be bypasses c along γ' in Figure 4.44 are represented as the result of attaching bypass in Figure 4.45 (a) and (b). We see that U_2 destabilizes in all these cases. If we attach a bypass along $1-2-3$, $3-4-5$, $5-6-7$, $7-8-9$, $8-9-10$, $10-11-12$, $12-13-14$, and $14-1-2$, then we would obtain a convex sphere S with disconnected dividing set, contradicting tightness. If we attach a bypass along $2-3-4$, $4-5-6$, $9-10-11$, and $11-12-13$ which are the cases when $c \cap (P_1' \cup P_2')$ has no components, then we would obtain a destabilization of U_2 and after the destabilization we would see that the n_2 becomes 3 and s becomes 5. If we attach a bypass along $6-7-8$ and $13-14-1$ which are the subcase mirror of 7, then we obtain a destabilization of U_2 and after the destabilization we see that the n_2 becomes 3 and s becomes 1.
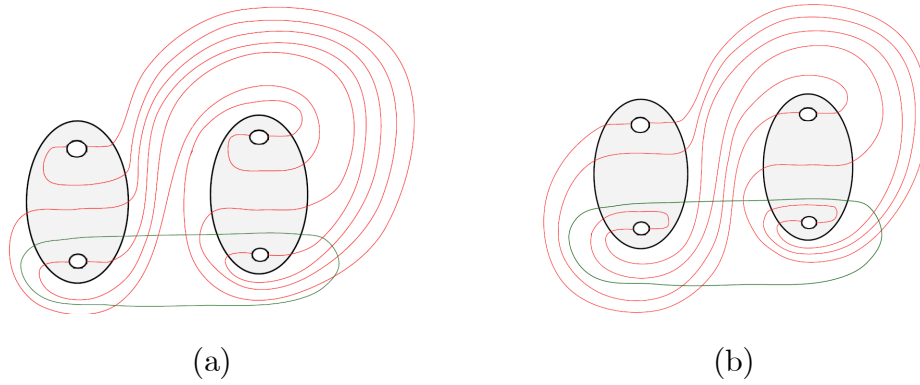
Figure 4.45 a) Γ_A after bypass along $2 - 3 - 4$, b) Γ_A after bypass along $6 - 7 - 8$ and $13 - 14 - 1$.

1.5 Let $s = -1$.

Figure 4.46 (a) illustrates a model of the case when $n_2 = 4$ and $s = -1$ for γ and Figure 4.46 (b) illustrates a model of the case when $n_2 = 4$ and $s = -1$ for γ' which we do not see any destabilization because of intersection number of Γ_A and γ'.

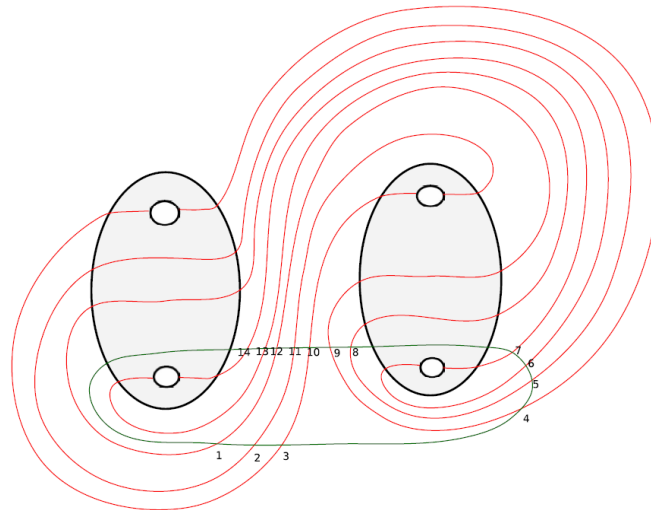**Figure 4.46** a) A model of the case when $n_2 = 4$ and $s = -1$ for γ, b) A model of the case when $n_2 = 4$ and $s = -1$ for γ'.

All cases when there could be bypasses c along γ in Figure 4.46 (a) are represented as the result of attaching bypass in Figure 4.47 (a), (b), (c) and (d). We see that U_2 destabilizes in all these cases. If we attach a bypass along $1 - 2 - 3$ and $7 - 8 - 9$ then we would obtain a convex sphere S with disconnected dividing set, contradicting tightness. If we attach a bypass along $5 - 6 - 7$, $10 - 11 - 12$, and $6 - 7 - 8$ which are the cases when $c \cap (P'_1 \cup P'_2)$ has no components, then we would obtain a destabilization of U_2 and after the destabilization we would see that the n_2 becomes 2 and s becomes -1 for $5 - 6 - 7$,

52

$10 - 11 - 12$ and n_2 becomes 3 and s becomes -1 for $6 - 7 - 8$. If we attach a bypass along $3 - 4 - 5$ which are the cases when $c \cap (P_1' \cup P_2')$ has two components, then we would obtain a destabilization of U_2 and after the destabilization we would see that the n_2 becomes 2 and s is still -1. If we attach a bypass along $2 - 3 - 4$ and $12 - 1 - 2$ which are the subcase 3, then we obtain a destabilization of U_2 and after the destabilization we see that the n_2 becomes 3 and s is still -1. If we attach a bypass along $4 - 5 - 6$ and $11 - 12 - 1$ which are the subcase 4, then we obtain a destabilization of U_2 and after the destabilization we see that the n_2 becomes 2 and s is still -1. If we attach a bypass along $8 - 9 - 10$ which are the subcase 7, then we obtain a destabilization of U_2 and after the destabilization we see that the n_2 becomes 3 and s is still -1. If we attach a bypass along $9 - 10 - 11$ which are the subcase 8, then we obtain a destabilization of U_2 and after the destabilization we see that the n_2 becomes 2 and s is still -1.

(a)　　　　　　(b)　　　　　　(c)　　　　　　(d)

Figure 4.47 a) Γ_A after bypass along $2 - 3 - 4$, b) Γ_A after bypass along $8 - 9 - 10$, c) Γ_A after bypass along $4 - 5 - 6$, $5 - 6 - 7$, $9 - 10 - 11$, $10 - 11 - 12$ and $11 - 12 - 1$, d) Γ_A after bypass along $12 - 1 - 2$.

1.6 Let $s = -3$.

1. Figure 4.48 illustrates a model of the case when $n_2 = 4$ and $s = -3$ for γ.

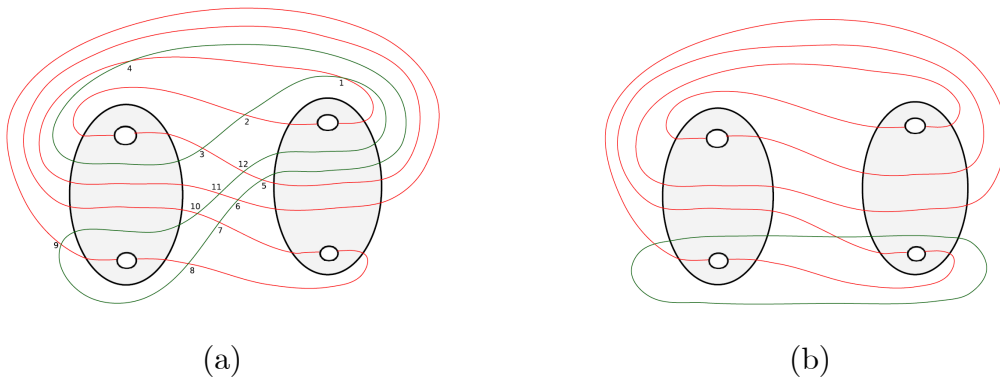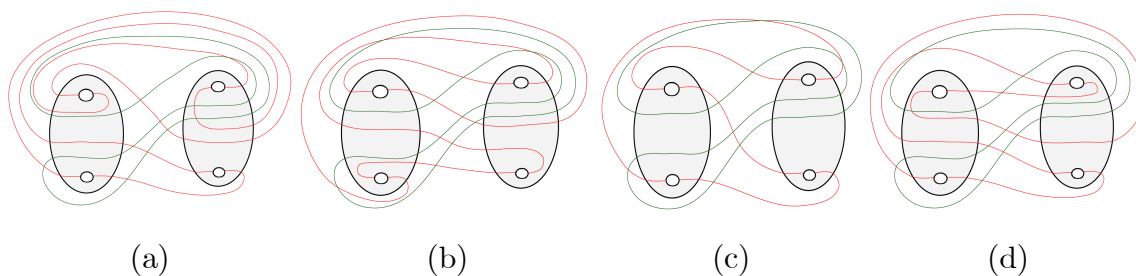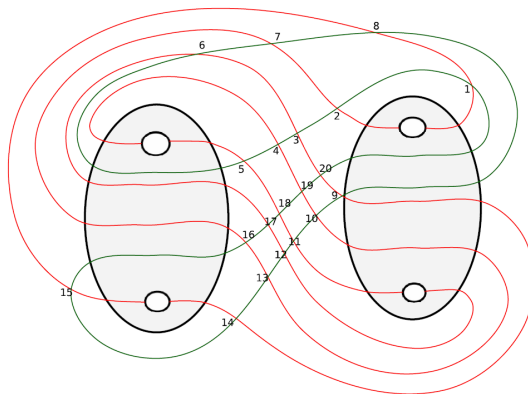**Figure 4.48** A model of the case when $n_2 = 4$ and $s = -3$ for γ.

Some cases when there could be bypasses c along γ in Figure 4.48 are represented as the result of attaching bypass in Figure 4.49 (a), (b), (c) and (d). We see that U_2 destabilizes in all these cases. If we attach a bypass along $1-2-3$, $3-4-5$, $5-6-7$, $6-7-8$, $8-9-10$, $9-10-11$, $11-12-13$, $13-14-15$, $15-16-17$, $16-17-18$, $18-19-20$, $19-20-21$ then we would obtain a convex sphere S with disconnected dividing set, contradicting tightness. If we attach a bypass along $2-3-4$, $10-11-12$, $12-13-14$, $14-15-16$, $17-18-19$ which are the cases when $c \cap (P_1' \cup P_2')$ has no components, then we obtain a destabilization of U_2 and after the destabilization we see that the n_2 becomes 3 and s is still -3. If we attach a bypass along $4-5-6$, $7-8-9$, $20-1-2$ which are the subcase 3 and $14-15-16$ which is the subcase 7, then we obtain a destabilization of U_2 and after the destabilization we see that the n_2 becomes 3 and s is still -3.

(a)   (b)   (c)   (d)

Figure 4.49 a) Γ_A after bypass along $2-3-4$, b) Γ_A after bypass along $4-5-6$, c) Γ_A after bypass along $7-8-9$ and $20-1-2$, d) Γ_A after bypass along $14-15-16$.

2. Figure 4.50 illustrates a model of the case when $n_2 = 4$ and $s = -3$ for γ'.

Figure 4.50 A model of the case when $n_2 = 4$ and $s = -3$ for γ'.

All the cases when there could be bypasses c along γ' in Figure 4.50 are represented as the result of attaching bypass in Figure 4.51 (a), (b), (c) and (d). We see that U_2 destabilizes in all these cases. If we attach a bypass along $3-4-5$ and $6-1-2$ then we would obtain a convex sphere S with disconnected dividing set, contradicting tightness. If we

attach a bypass along $2 - 3 - 4$ and $5 - 6 - 1$ which are the mirror of subcase 5, then we obtain a destabilization of U_2 and after the destabilization we see that the n_2 becomes 3 and s is still -3. If we attach a bypass along $1 - 2 - 3$ and $4 - 5 - 6$ which are the cases when $c \cap (P_1' \cup P_2')$ has no components, then we obtain a destabilization of U_2 and after the destabilization we see that the n_2 becomes 3 and s becomes -1.

(a) (b) (c) (d)

Figure 4.51 a) Γ_A after bypass along $1 - 2 - 3$, b) Γ_A after bypass along $2 - 3 - 4$, c) Γ_A after bypass along $4 - 5 - 6$, d) Γ_A after bypass along $5 - 6 - 1$.
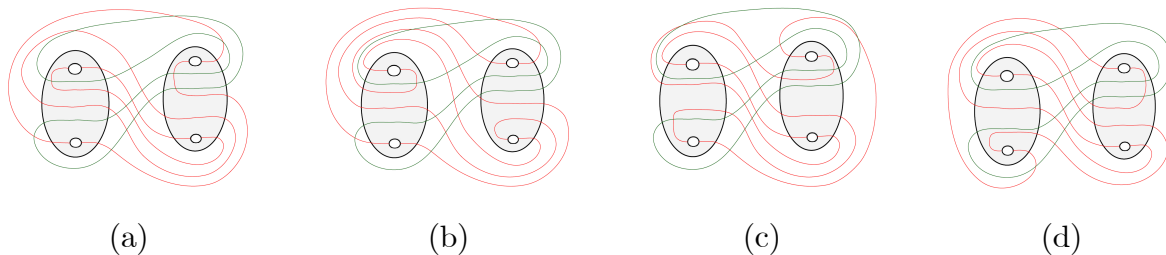
1.7 Let $s = -5$.

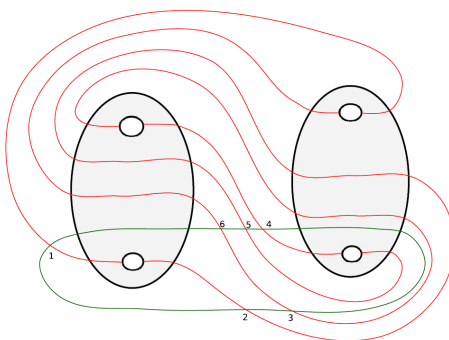**1.** Figure 4.52 illustrates a model of the case when $n_2 = 4$ and $s = -5$ for γ.
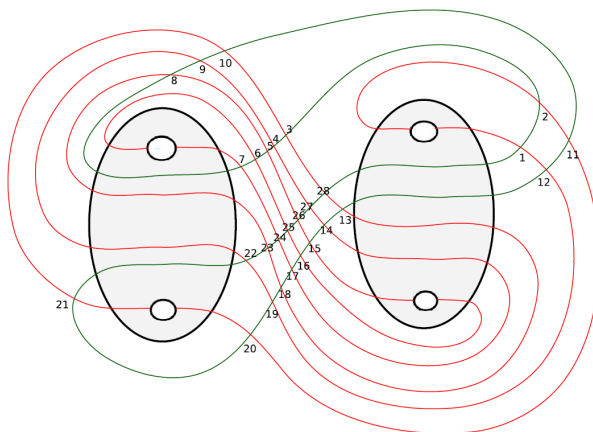
Figure 4.52 A model of the case when $n_2 = 4$ and $s = -5$ for γ.

Some cases when there could be bypasses c along γ in Figure 4.52 are represented as the result of attaching bypass in Figure 4.53 (a), (b), (c) and (d). We see that U_2 destabilizes in all these cases. If we attach a bypass along $1 - 2 - 3$, $5 - 6 - 7$, $10 - 11 - 12$, $15 - 16 - 17$, $19 - 20 - 21$ and $24 - 25 - 26$ then we would obtain a convex sphere S with disconnected dividing set, contradicting tightness. If we attach a bypass along $6 - 7 - 8$, $11 - 12 - 13$ and $28 - 1 - 2$ which is the subcase 3, then we obtain a destabilization of U_2 and after the destabilization we see that the n_2 becomes 3 and s becomes -3. If we attach a bypass along $7 - 8 - 9$, $12 - 13 - 14$ and $27 - 28 - 1$ which is the subcase 4 and $21 - 22 - 23$ which is the subcase 8, then we obtain a destabilization of U_2 and after the destabilization we see

that the n_2 becomes 2 and s becomes -3. If we attach a bypass along $20 - 21 - 22$ which is the subcase 7, then we obtain a destabilization of U_2 and after the destabilization we see that the n_2 becomes 3 and s is still -5.

(a)　　　　　　(b)　　　　　　(c)　　　　　　(d)

Figure 4.53 a) Γ_A after bypass along $6 - 7 - 8$, b) Γ_A after bypass along $7 - 8 - 9$, $12 - 13 - 14$, $21 - 22- 23$ and $27 - 28 - 1$, c) Γ_A after bypass along $11 - 12 - 13$ and $28 - 1 - 2$, d) Γ_A after bypass along $20 - 21 - 22$.
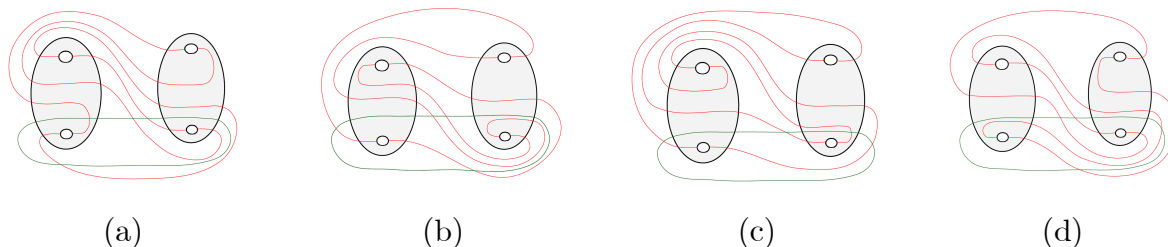
2. Figure 4.54 illustrates a model of the case when $n_2 = 4$ and $s = -5$ for γ'.

Figure 4.54 A model of the case when $n_2 = 4$ and $s = -5$ for γ'.

One case when there could be bypasses c along γ' in Figure 4.54 is represented as the result of attaching bypass in Figure 4.55. We see that U_2 destabilizes in this case. If we attach a bypass along $2 - 3 - 4$, $4 - 5 - 6$, $5 - 6 - 7$, $7 - 8 - 9$, $9 - 10 - 1$ and $10 - 1 - 2$ then we would obtain a convex sphere S with disconnected dividing set, contradicting tightness. If we attach a bypass along $1 - 2 - 3$, $3 - 4 - 5$, $6 - 7 - 8$ and $8 - 9 - 10$ which are the cases when $c \cap (P'_1 \cup P'_2)$ has no components, then we obtain a destabilization of U_2 and after the destabilization we see that the n_2 becomes 3 and s becomes -3.
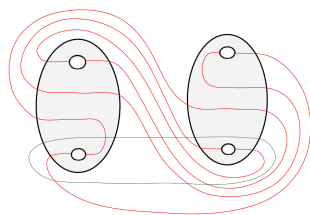
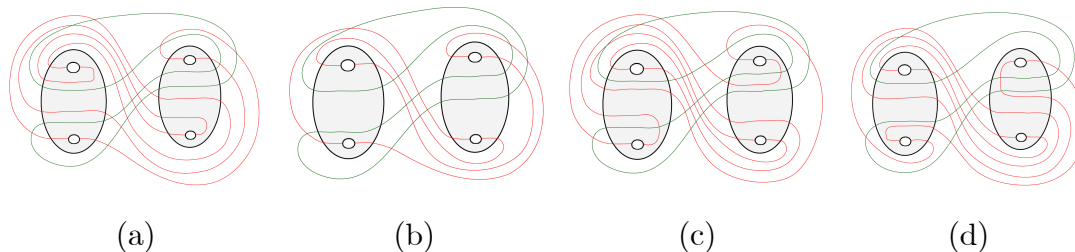**Figure 4.55** Γ_A after bypass along $1 - 2 - 3$.

1.8 Let $s = -7$.

1. Figure 4.56 illustrates a model of the case when $n_2 = 4$ and $s = -7$ for γ.

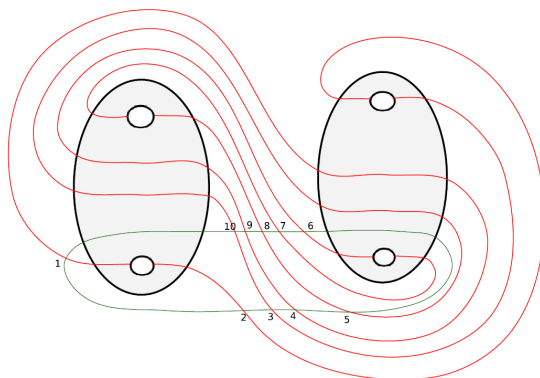**Figure 4.56** A model of the case when $n_2 = 4$ and $s = -7$ for γ.

Some cases when there could be bypasses c along γ in Figure 4.56 are represented as the result of attaching bypass in Figure 4.57 (a), (b) and (c). We see that U_2 destabilizes in all these cases. If we attach a bypass along $8-9-10$, $15-16-17$ and $36-1-2$ which are the subcase 3, then we obtain a destabilization of U_2 and after the destabilization we see that the n_2 becomes 3 and s becomes -5. If we attach a bypass along $26-27-28$ which is the subcase 7, then we obtain a destabilization of U_2 and after the destabilization we see that the n_2 becomes 3 and s becomes -5.

| (a) | (b) | (c) |
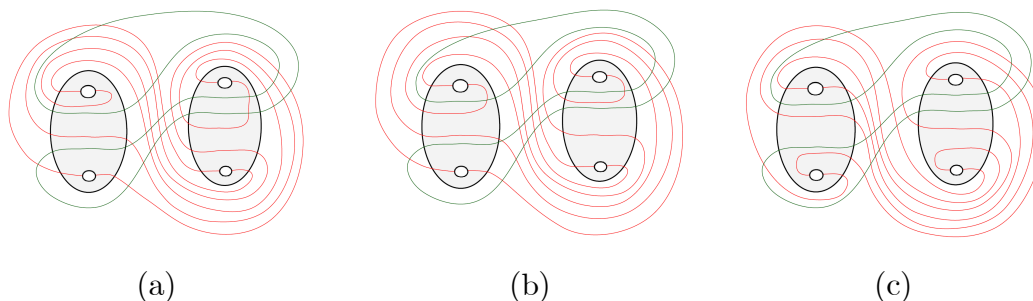
Figure 4.57 a) Γ_A after bypass along $8-9-10$, b) Γ_A after bypass along $15-16-17$ and $36-1-2$, c) Γ_A after bypass along $26-27-28$.

2. Figure 4.58 illustrates a model of the case when $n_2 = 4$ and $s = -7$ for γ'.

Figure 4.58 A model of the case when $n_2 = 4$ and $s = -7$ for γ'.

Some cases when there could be bypasses c along γ in Figure 4.58 are represented as the result of attaching bypass in Figure 4.59 (a), (b) and (c). We see that U_2 destabilizes in all these cases. If we attach a bypass along $4-5-6$, $7-8-9$, $11-12-13$ and $14-1-2$ then we would obtain a convex sphere S with disconnected dividing set, contradicting tightness. If we attach a bypass along $1-2-3$, $3-4-5$, $5-6-7$, $8-9-10$, $10-11-12$ and $12-13-14$ which are the cases when $c \cap (P_1' \cup P_2')$ has no components, then we obtain a destabilization of U_2 and after the destabili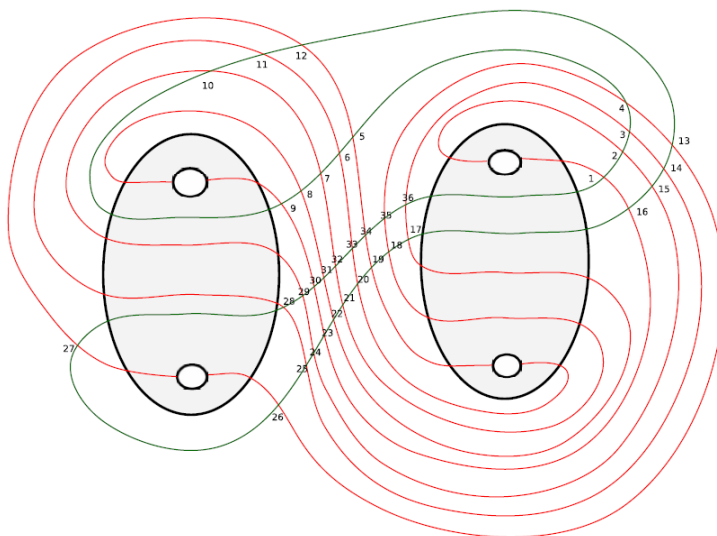zation we see that the n_2 becomes 3 and s becomes -5. If we attach a bypass along $2-3-4$ and $9-10-11$ which are the cases when $c \cap (P_1' \cup P_2')$ has no components, then we obtain a destabilization of U_2 and after the destabilization we see that the n_2 becomes 2 and s becomes -3. If we attach a bypass along $6-7-8$ and $13-14-1$ each of which is the subcase mirror of 5, then we obtain a destabilization of U_2 and after the destabilization we see that the n_2 becomes 3 and s becomes -5.

(a)   (b)   (c)
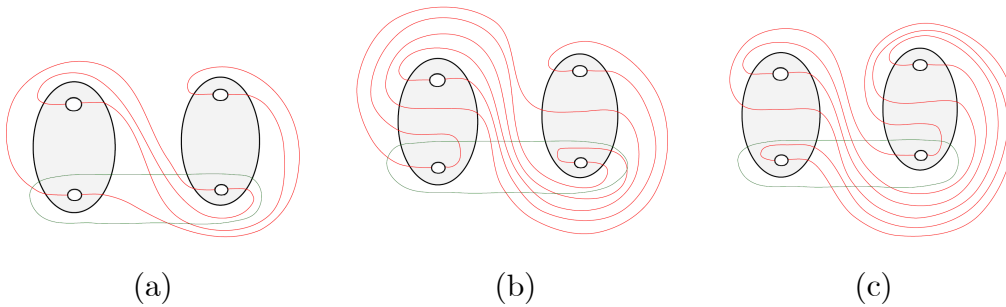
Figure 4.59 a) Γ_A after bypass along $2-3-4$ and $9-10-11$, b) Γ_A after bypass along $6-7-8$, c) Γ_A after bypass along $13-14-1$.

Proof of the Claim 4.2 In the case when $n_2 = 3$ and $|s| > 5$ there will be a bypass c along γ and along γ'. We need to see how attaching it will affect the dividing curves on S. If $c \cap (P_1' \cup P_2') = \emptyset$, then when attaching the bypass to $A \subset S$, we can destabilize U_2 in the complement of U_1. If $c \cap (P_1' \cup P_2')$ has one component, the possibilities of c are shown in Figure 4.60. For $s > 5$, we must consider the 1st, 2nd, 5th, and 6th configurations in Figure 4.60. If c is a subset of γ we see that in cases 2 and 6 that the dividing set on S is disconnected after attaching the bypass. This contradicts the tightness of the contact structure so such bypasses never exist. In cases 1 and 5 there exists a bypass c along γ, but we do not see a destabilization of U_2 after bypass attachment. However, if c is a subset of γ' then in cases 2 and 6, U_2 destabilizes for all slopes and also in cases 1 and 5 we have a convex sphere with disconnected dividing set for some slopes and a destabilization of U_2 for the other slopes. For $s < -5$ we must consider the 3rd, 4th, 7th and 8th configurations in Figure 4.60. If c is a subset of γ' we see that in cases 3 and 7 that the dividing set on S is disconnected after attaching the bypass. This contradicts the tightness of the contact structure so such bypasses never exist. In cases 4 and 8 there exists a bypass c along γ' for some slopes, but we do not see a destabilization of U_2 after bypass attachment and there does not exist any bypass for the other slopes for contradicting the tightness. However, if c is a subset of γ then in cases 3 and 7, U_2 destabilizes for all slopes and also in cases 4 and 8 we have a convex sphere with disconnected dividing set for some slopes and a destabilization of U_2 for the other slopes. To sum up, for $s > 5$, when we attach a bypass c along γ' we see that U_2 destabilizes and for $s < -5$, when we attach a bypass c along γ we see that U_2 destabilizes.

We are left to consider the case when $n_2 = 3$ and $s = 1, 2, 4, 5, -1, -2, -4,$ or -5. We will do a case by case analysis of these.

**Figure 4.60** The 8 subcases if $c \cap (P_1' \cup P_2')$ has one component when $n_2 = 3$.

2.1 Let $s = 1$.

1. Figure 4.61 illustrates a model of the case when $n_2 = 3$ and $s = 1$ for γ.
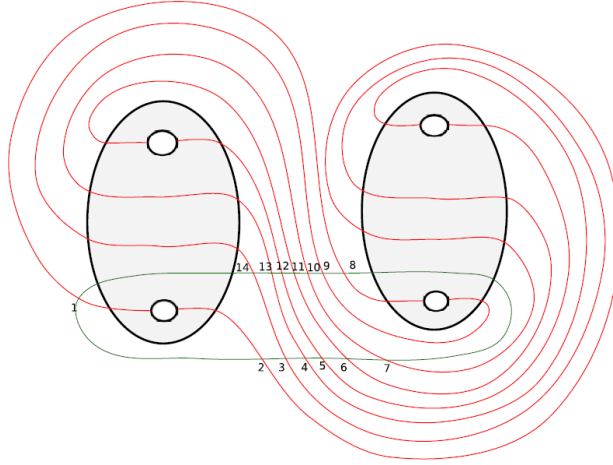

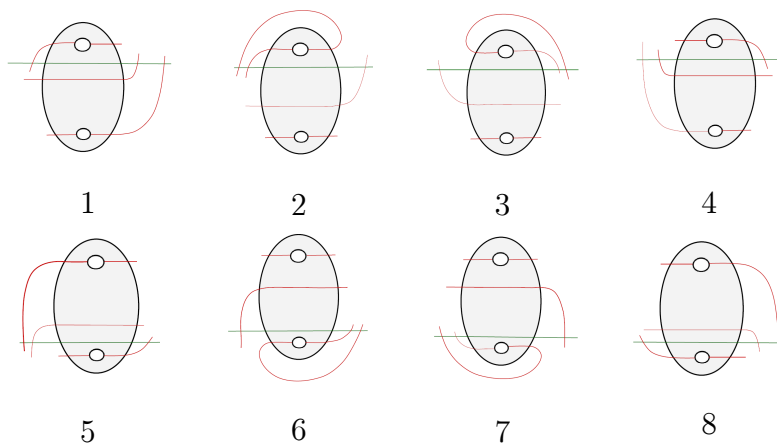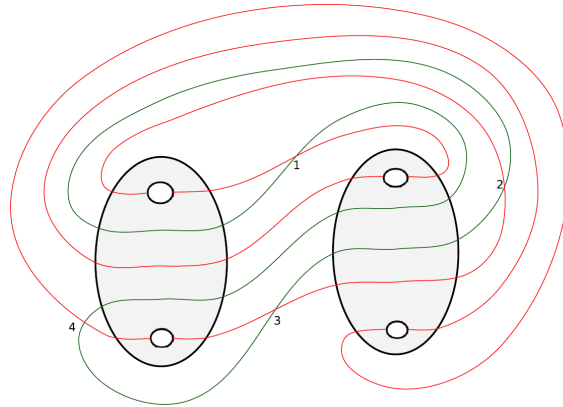**Figure 4.61** A model of the case when $n_2 = 3$ and $s = 1$ for γ.

All the cases when there could be bypasses c along γ in Figure 4.61 are represented as the result of attaching bypass in Figure 4.62 (a) and (b). If we attach a bypass along $2 - 3 - 4$ and $4 - 1 - 2$, then we would obtain a convex sphere S with disconnected dividing set, contradicting tightness. It is clearly seen that U_2 was not destabilized since it has still $tb = -3$ as seen in Figure 4.62 (a) and (b).

(a)

(b)

Figure 4.62 a) Γ_A after bypass along $1 - 2 - 3$, b) Γ_A after bypass along $3 - 4 - 1$.

2. Figure 4.63 illustrates a model of the case when $n_2 = 3$ and $s = 1$ for γ'.

Figure 4.63 A model of the case when $n_2 = 3$ and $s = 1$ for γ'.

Only one case when there could be bypass c along γ' in Figure 4.63 giving the destabilization of U_2 is represented as the result of attaching bypass in Figure 4.64 (a). If we attach a bypass along $1-2-3$ and $3-4-1$, then we would obtain a convex sphere S with disconnected dividing set, contradicting tightness. If we attach a bypass along $4-1-2$, then we do not have a destabilization of U_2 as seen in the Figure 4.64 (b). We meet the subcase mirror of 7 for a bypass along $2-3-4$. After the destabilization we see that the n_2 becomes 2 and s is still 1.

(a)   (b)

Figure 4.64 a) Γ_A after bypass along $2-3-4$, b) Γ_A after bypass along $4-1-2$.

2.2 Let $s = 2$.

1. Figure 4.65 illustrates a model of the case when $n_2 = 3$ and $s = 2$ for γ.

Figure 4.65 A model of the case when $n_2 = 3$ and $s = 2$ for γ.
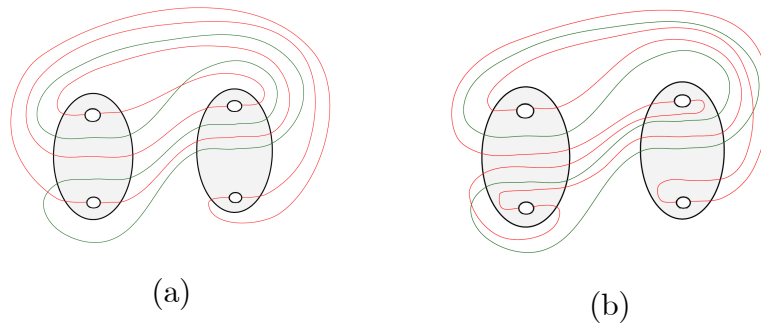
All the cases when there could be bypasses c along γ in Figure 4.65 are represented as the result of attaching bypass in Figure 4.66 (a) and (b). If we attach a bypass along $2-3-4$ and $4-1-2$, then we would obtain a convex sphere S with disconnected dividing set, contradicting tightness. It is clearly seen that U_2 was not destabilized as seen in the Figure 4.66 (a) and (b).

(a) (b)

Figure 4.66 a) Γ_A after bypass along $1-2-3$, b) Γ_A after bypass along $3-4-1$.

2. Figure 4.67 illustrates a model of the case when $n_2 = 3$ and $s = 2$ for γ'.
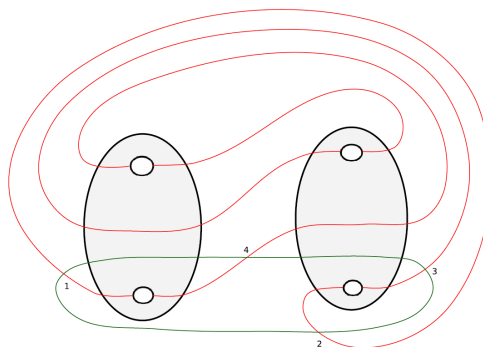

Figure 4.67 A model of the case when $n_2 = 3$ and $s = 2$ for γ'.

All the cases when there could be bypasses c along γ' in Figure 4.67 are represented as the result of attaching bypass in Figure 4.68 (a) and (b). We see that U_2 destabilizes in all these cases. If we attach a bypass along $2-3-4$ and $4-1-2$ then we would obtain a convex sphere S with disconnected dividing set, contradicting tightness. If we attach a bypass along $1-2-3$ and $3-4-1$ which are the mirror of subcase 7, then we obtain a destabilization of U_2 and after the destabilization we see that the n_2 becomes 2 and s is 1.

(a) (b)

Figure 4.68 a) Γ_A after bypass along $1-2-3$, b) Γ_A after bypass along $3-4-1$.
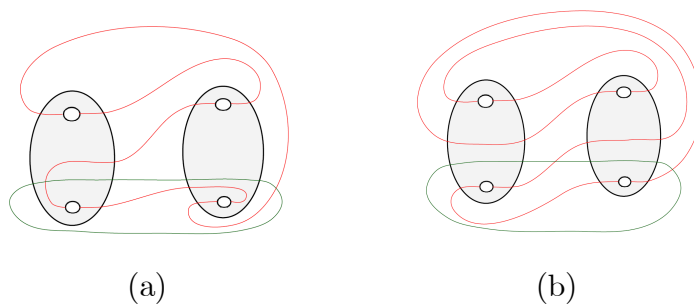
2.3 Let $s = 4$.

1. Figure 4.69 illustrates a model of the case when $n_2 = 3$ and $s = 4$ for γ.

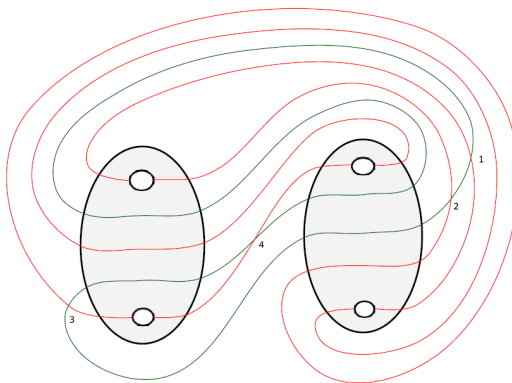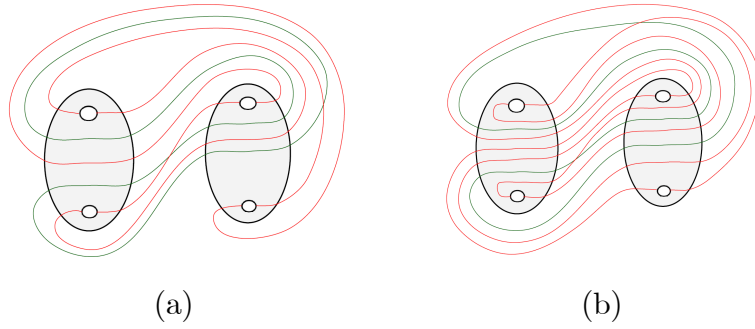**Figure 4.69** A model of the case when $n_2 = 3$ and $s = 4$ for γ.

All the cases when there could be bypasses c along γ in Figure 4.69 are represented as the result of attaching bypass in Figure 4.70 (a) and (b). If we attach a bypass along a curve except $3 - 4 - 5$ and $8 - 9 - 10$, then we would obtain a convex sphere S with disconnected dividing set, contradicting tightness. If we attach a bypass along $3 - 4 - 5$ and $8 - 9 - 10$ which are the cases when $c \cap (P_1' \cup P_2')$ has no components, then we obtain a destabilization of U_2 and after the destabilization we see that the n_2 becomes 2 and s becomes 3.

(a)   (b)
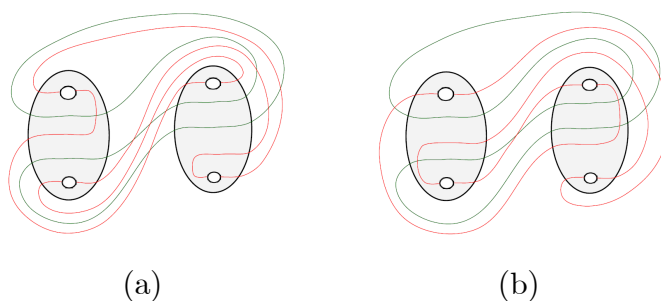
Figure 4.70 a) Γ_A after bypass along $3 - 4 - 5$, b) Γ_A after bypass along $8 - 9 - 10$.

2. Figure 4.71 illustrates a model of the case when $n_2 = 3$ and $s = 4$ for γ'.
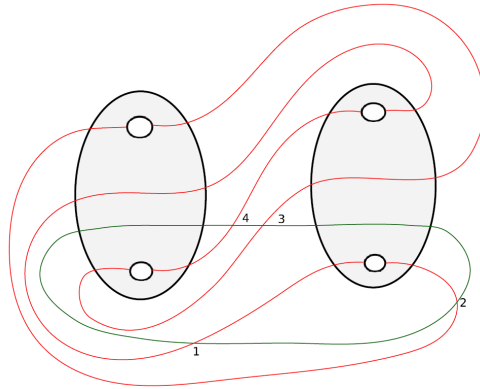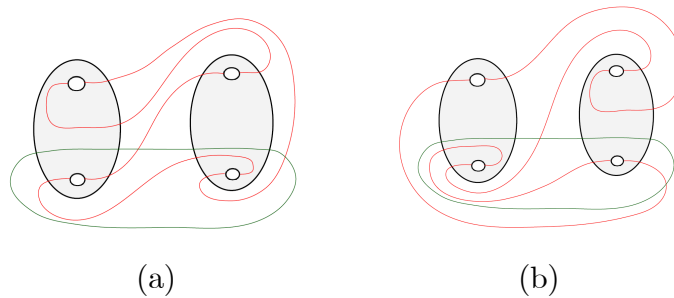

Figure 4.71 A model of the case when $n_2 = 3$ and $s = 4$ for γ'.

All the cases when there could be bypasses c along γ' in Figure 4.71 are represented as the result of attaching bypass in Figure 4.72 (a) and (b). If we attach a bypass along a curve $2-3-4$ and $6-7-8$, then we would obtain a convex sphere S with disconnected dividing set, contradicting tightness. If we attach a bypass along $1-2-3$ and $5-6-7$ which are the cases when $c \cap (P'_1 \cup P'_2)$ has no components, then we obtain a destabilization of U_2 and after the destabilization we see that the n_2 becomes 2 and s becomes 2. If we attach a bypass along $3-4-5$ and $7-8-1$ which is the subcase mirror of 7, then we obtain a destabilization of U_2 and after the destabilization we see that the n_2 becomes 2 and s becomes 3.

(a) (b)

Figure 4.72 a) Γ_A after bypass along $3-4-5$, b) Γ_A after bypass along $7-8-1$.

2.4 Let $s = 5$.

1. Figure 4.73 illustrates a model of the case when $n_2 = 3$ and $s = 5$ for γ'.

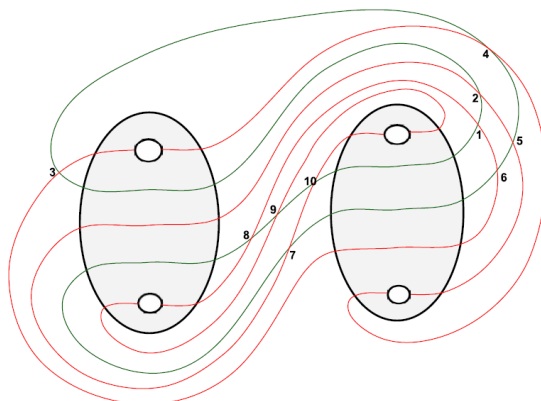**Figure 4.73** A model of the case when $n_2 = 3$ and $s = 5$ for γ'.

All the cases when there could be bypasses c along γ' in Figure 4.73 are represented as the result of attaching bypass in Figure 4.74 (a), (b), (c), (d) and (e). If we attach a bypass along a curve $1-2-3$, $2-3-4$, $4-5-6$, $5-6-7$, $7-8-9$, $9-10-11$, $10-11-12$, and $11-12-1$, then we would obtain a convex sphere S with disconnected dividing set,

contradicting tightness. If we attach a bypass along $3 - 4 - 5$ and $8 - 9 - 10$ which are the cases when $c \cap (P_1' \cup P_2')$ has no components, then we obtain a destabilization of U_2 and after the destabilization we see that the n_2 becomes 2 and s becomes 3. If we attach a bypass along $6 - 7 - 8$ which is the subcase mirror of 7, then we obtain a destabilization of U_2 and after the destabilization we see that the n_2 becomes 2 and s is still 5. After attaching a bypass along $12 - 1 - 2$, we obtain the dividing curves as in Figure 4.74 (d) and then if we attach again a bypass along $i - j - a$ which is the subcase mirror of 7, then we obtain a destabilization of U_2 as seen in Figure 4.74 (e) and after the destabilization we see that the n_2 becomes 2 and s is still 5.

(a)   (b)   (c)   (d)   (e)
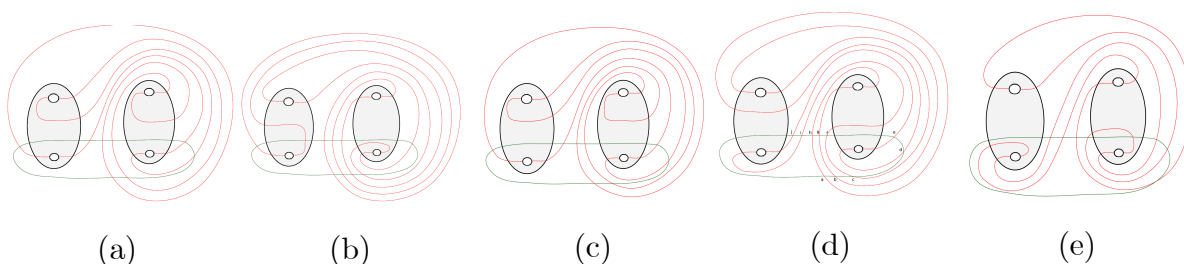
Figure 4.74 a) Γ_A after bypass along $3 - 4 - 5$, b) Γ_A after bypass along $6 - 7 - 8$, c) Γ_A after bypass along $8 - 9 - 10$, d) Γ_A after bypass along $12 - 1 - 2$, e) Γ_A after bypass along $i - j - a$ in (d).

2.5 Let $s = -1$.

Figure 4.75 (a) illustrates a model of the case when $n_2 = 3$ and $s = -1$ for γ' which we do not see any destabilization because of intersection number of Γ_A and γ'. Figure 4.75 (b) illustrates a model of the case when $n_2 = 3$ and $s = -1$ for γ.

(a)   (b)

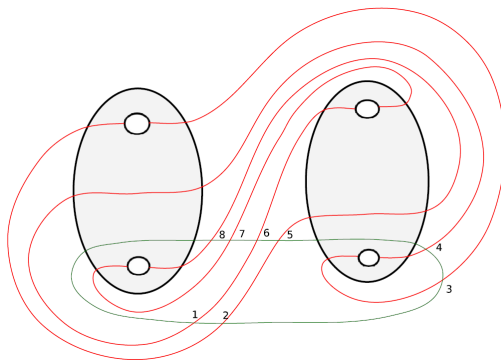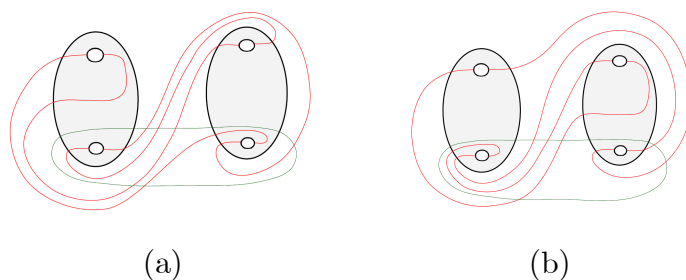**Figure 4.75** a) A model of the case when $n_2 = 3$ and $s = -1$ for γ', b) A model of the case when $n_2 = 3$ and $s = -1$ for γ.
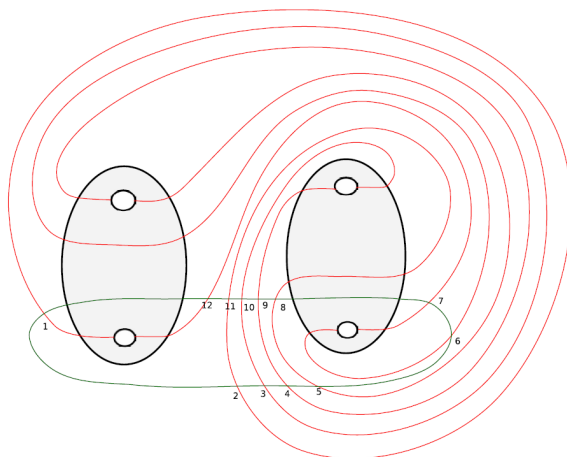
65

All the cases when there could be bypasses c along γ in Figure 4.75 (b) are represented as the result of attaching bypass in Figure 4.76 (a), (b), (c), (d), (e) and (f). If we attach a bypass along a curve $1-2-3$ and $6-7-8$, then we would obtain a convex sphere S with disconnected dividing set, contradicting tightness. If we attach a bypass along $5-6-7$ which is the case when $c \cap (P_1' \cup P_2')$ has no components, then we obtain a destabilization of U_2 and after the destabilization we see that the n_2 becomes 2 and s is still -1. If we attach a bypass along $2-3-4$ and $10-1-2$ which is the subcase 3, then we obtain a destabilization of U_2 and after the destabilization we see that the n_2 becomes 2 and s is still -1. If we attach a bypass along $3-4-5$ and $4-5-6$ which is the case when $c \cap (P_1' \cup P_2')$ has two components, then we obtain a destabilization of U_2 and after the destabilization we see that the n_2 becomes 1 and s becomes -1. If we attach a bypass along $8-9-10$ which is the subcase 8 and $9-10-1$ which is the subcase 4, then we obtain a destabilization of U_2 and after the destabilization we see that the n_2 becomes 1 and s is still -1.

(a)   (b)   (c)

(d)   (e)   (f)
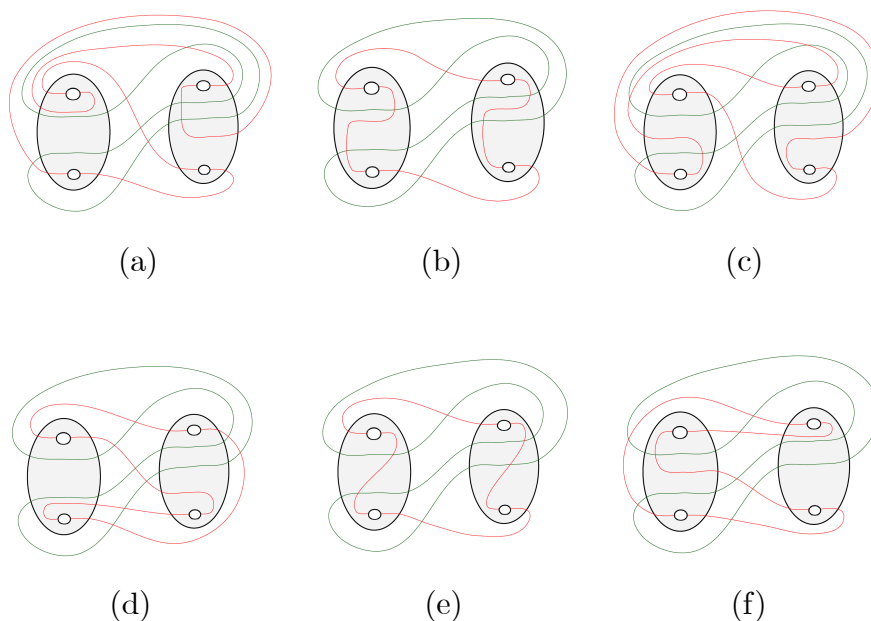
Figure 4.76 a) Γ_A after bypass along $2-3-4$, b) Γ_A after bypass along $3-4-5$ and $4-5-6$, c) Γ_A after bypass along $5-6-7$, d) Γ_A after bypass along $7-8-9$, e) Γ_A after bypass along $8-9-10$ and $9-10-1$, f) Γ_A after bypass along $10-1-2$.

2.6 Let $s = -2$.

1. Figure 4.77 illustrates a model of the case when $n_2 = 3$ and $s = -2$ for γ.

Figure 4.77 A model of the case when $n_2 = 3$ and $s = -2$ for γ.

All the cases when there could be bypasses c along γ in Figure 4.77 are represented as the result of attaching bypass in Figure 4.78 (a), (b), (c), (d) and (e). If we attach a bypass along a curve $1-2-3$, $2-3-4$, $4-5-6$, $6-7-8$, $8-9-10$, $9-10-11$, $11-12-13$ and $13-14-1$, then we woul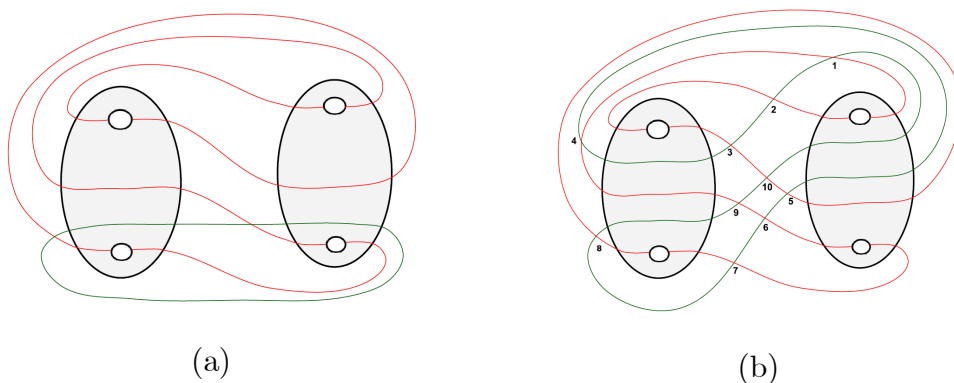d obtain a convex sphere S with disconnected dividing set, contradicting tightness. If we attach a bypass along $7-8-9$ and $12-13-14$ which is the case when $c \cap (P_1' \cup P_2')$ has no components, then we obtain a destabilization of U_2 and after the destabilization we see that the n_2 becomes 2 and s is -1. If we attach a bypass along $3-4-5$, $5-6-7$ and $14-1-2$ which is the subcase 3, then we obtain a destabilization of U_2 and after the destabilization we see that the n_2 becomes 2 and s is -1. If we attach a bypass along $10-11-12$ which is the subcase 7, then we obtain a destabilization of U_2 and after the destabilization we see that the n_2 becomes 2 and s is -1.

Figure 4.78 a) Γ_A after bypass along $3-4-5$, b) Γ_A after bypass along $5-6-7$, c) Γ_A after bypass along $7-8-9$, d) Γ_A after bypass along $10-11-1$, e) Γ_A after bypass along $14-1-2$.

2. Figure 4.79 illustrates a model of the case when $n_2 = 3$ and $s = -2$ for γ'.

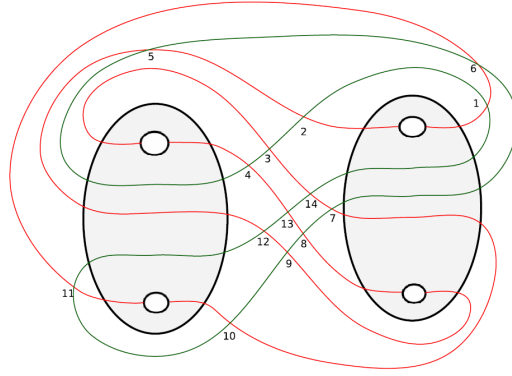**Figure 4.79** A model of the case when $n_2 = 3$ and $s = -2$ for γ'.

All the cases when there could be bypasses c along γ' in Figure 4.79 are represented as the result of attaching bypass in Figure 4.80 (a) and (b). If we attach a bypass along $2-3-4$ and $4-1-2$, then we would obtain a convex sphere S with disconnected dividing set, contradicting tightness. It is clearly seen that U_2 was not destabilized since it has still $tb = -3$ as seen in Figure 4.81 (a) and (b).

(a)   (b)
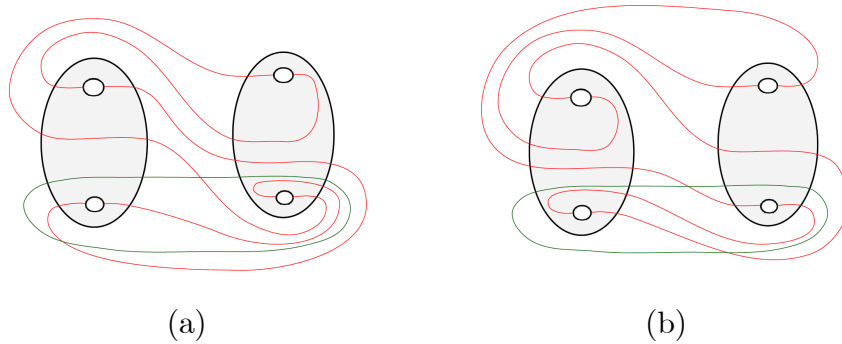
Figure 4.80 a) Γ_A after bypass along $1-2-3$, b) Γ_A after bypass along $3-4-1$.
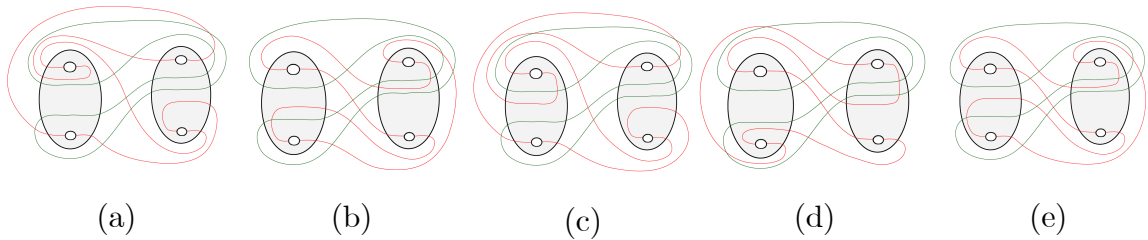
2.7 Let $s = -4$.

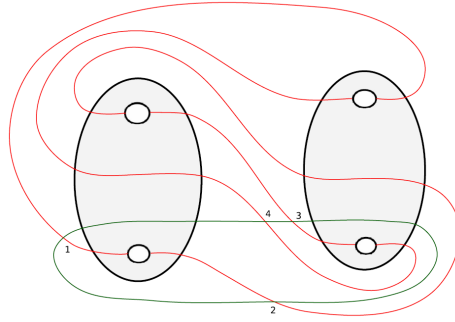**1.** Figure 4.81 illustrates a model of the case when $n_2 = 3$ and $s = -4$ for γ.

Figure 4.81 A model of the case when $n_2 = 3$ and $s = -4$ for γ.

All the cases when there could be bypasses c along γ in Figure 4.81 are represented as the result of attaching bypass in Figure 4.82 (a), (b), (c), (d) and (e). If we attach a bypass along a curve $1-2-3$, $4-5-6$, $8-9-10$, $12-13-14$, $15-16-17$ and $19-20-21$, then we would obtain a convex sphere S with disconnected dividing set, contradicting tightness. If we attach a bypass along $2-3-4$, $3-4-5$, $11-12-13$, $13-14-15$, $14-15-16$, $18-19-20$ and $20-21-22$ which is the case when $c \cap (P'_1 \cup P'_2)$ has no components, then we obtain a destabilization of U_2 and after the destabilization we see that the n_2 becomes 2 and s is still -2. If we attach a bypass along $3-4-5$, $5-6-7$ and $14-1-2$ which is the subcase 3, then we obtain a destabilization of U_2. If we attach a bypass along $5-6-7$, $9-10-11$ and $22-1-2$ which is the subcase 3, then we obtain a destabilization of U_2 and after the destabilization we see that the n_2 becomes 2 and s is still -3. If we attach a bypass along $10-11-12$ and $21-22-1$ which is the subcase 4, then we obtain a destabilization of U_2 and after the destabilization we see that the n_2 becomes 1 and $s = -1$. If we attach a bypass along $16-17-18$ which is the subcase 7, then we obtain a destabilization of U_2 and after the destabilization we see that the n_2 becomes 2 and s is still -3. If we attach a bypass along $17-18-19$ which is the subcase 7, then we obtain a destabilization of U_2 and after the destabilization we see that the n_2 becomes 1 and $s = -1$.

(a) (b) (c)

(d) (e)

Figure 4.82 a) Γ_A after bypass along $5-6-7$, b) Γ_A after bypass along $9-10-11$ and $22-1-2$, c) Γ_A after bypass along $10-11-12$ and $21-22-1$, d) Γ_A after bypass along $16-17-18$, e) Γ_A after bypass along $17-18-19$.

2. Figure 4.83 illustrates a model of the case when $n_2 = 3$ and $s = -4$ for γ'.

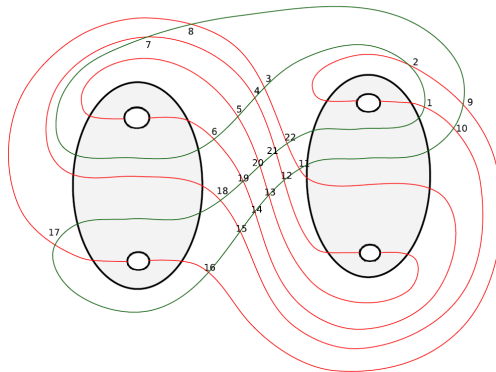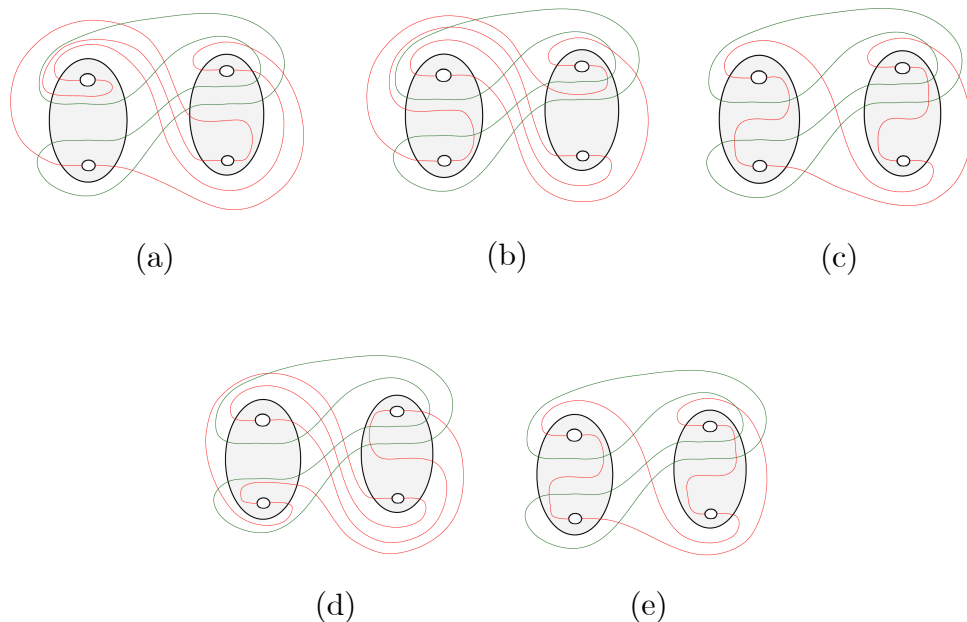**Figure 4.83** A model of the case when $n_2 = 3$ and $s = -4$ for γ'.

All the cases when there could be bypasses c along γ' in Figure 4.84 (a) and (b). If we attach a bypass along $2 - 3 - 4$, $4 - 5 - 6$, $6 - 7 - 8$ and $8 - 1 - 2$, then we would obtain a convex sphere S with disconnected dividing set, contradicting tightness. If we attach a bypass along $1 - 2 - 3$ and $5 - 6 - 7$ which is the case when $c \cap (P_1' \cup P_2')$ has no components, then we obtain a destabilization of U_2 and after the destabilization we see that the n_2 becomes 2 and s is -1.

(a)   (b)

Figure 4.84 a) Γ_A after bypass along $1 - 2 - 3$, b) Γ_A after bypass along $5 - 6 - 7$.

2.8 Let $s = -5$.

1. Figure 4.85 illustrates a model of the case when $n_2 = 3$ and $s = -5$ for γ.

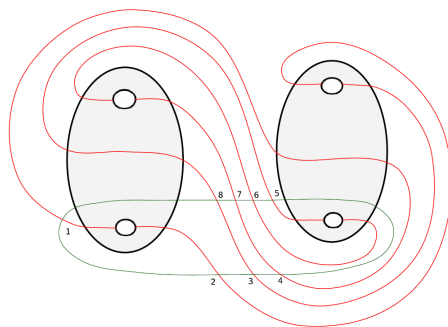**Figure 4.85** A model of the case when $n_2 = 3$ and $s = -5$ for γ.

Some cases when there could be bypasses c along γ in Figure 4.85 are represented as the result of attaching bypass in Figure 4.86 (a), (b) and (c). If we attach a bypass along $6-7-8$, $11-12-13$ and $26-1-2$ which is the subcase 3, then we obtain a destabilization of U_2 and after the destabilization we see that the n_2 becomes 2 and s becomes -3. If we attach a bypass along $19-20-21$ which is the subcase 7, then we obtain a destabilization of U_2 and after the destabilization we see that the n_2 becomes 2 and s becomes -1.
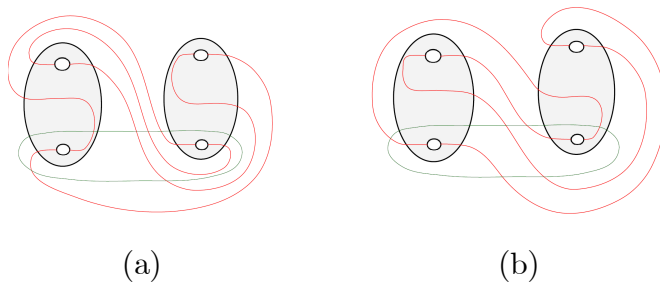

(a) (b) (c)

Figure 4.86 a) Γ_A after bypass along $6-7-8$, b) Γ_A after bypass along $11-12-13$ and $26-1-2$, c) Γ_A after bypass along $19-20-21$.

2. Figure 4.87 illustrates a model of the case when $n_2 = 3$ and $s = -5$ for γ'.

Figure 4.87 A model of the case when $n_2 = 3$ and $s = -5$ for γ'.

All the cases when there could be bypasses c along γ' in Figure 4.87 are represented as the result of attaching bypass in Figure 4.88 (a), (b), (c) and (d). If we attach a bypass along $3-4-5$, $5-6-7$, $8-9-10$ and $10-1-2$, then we would obtain a convex sphere S with disconnected dividing set, contradicting tightness. If we attach a bypass along $1-2-3$, $2-3-4$, $6-7-8$ and $7-8-9$ which is the case when $c \cap (P_1' \cup P_2')$ has no components, then we obtain a destabilization of U_2 and after the destabilization we see that the n_2 becomes 2 and s becomes -3.
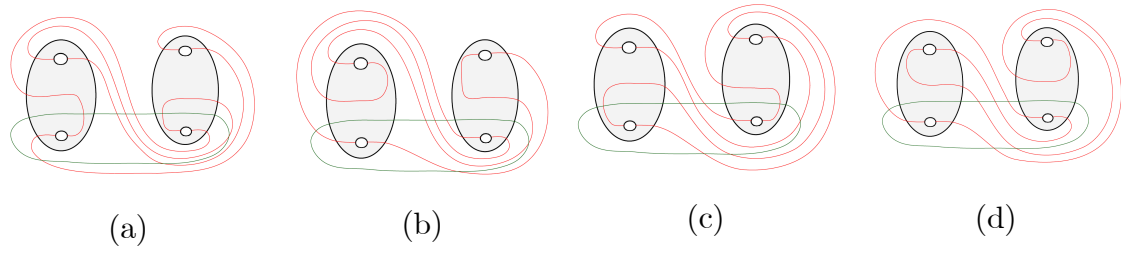
Figure 4.88 a) Γ_A after bypass along $1 - 2 - 3$, b) Γ_A after bypass along $2 - 3 - 4$, c) Γ_A after bypass along $6 - 7 - 8$, d) Γ_A after bypass along $7 - 8 - 9$.

Proof of the Claim 4.3 In the case when $n_2 = 2$ and $|s| > 5$ there will be a bypass c along γ and along γ'. We need to see how attaching it will affect the dividing curves on S. If $c \cap (P_1' \cup P_2') = \emptyset$, then when attaching the bypass to $A \subset S$, we can destabilize U_2 in the complement of U_1. If $c \cap (P_1' \cup P_2')$ has one component, the possibilities of c are shown in Figure 4.89. For $s > 5$, we must consider the 1st, and 3rd configurations in Figure 4.89. If c is a subset of γ we see that in all cases that the dividing set on S is disconnected after attaching the bypass. This contradicts the tightness of the contact structure so such bypasses never exist. If c is a subset of $\gamma\prime$ then we see that U_2 destabilizes for all cases. For $s < -5$ one can similarly see that either a bypass attachment leads to a disconnected dividing set for S, and so does not exist, or destabilizes U_2.

We are left to consider the case when $n_2 = 2$ and $s = 1, 3, -1$, or -3. We will do a case by case analysis of these.

Figure 4.89 The 4 subcases if $c \cap (P_1' \cup P_2')$ has one component when $n_2 = 2$.

Now, in the case when $n_2 = 2$, we will do case by case analysis for the slopes $s = 1, 3, -1$ and -3, respectively as follows.

3.1 Let $s = 1$.

1. Figure 4.90 illustrates a model of the case when $n_2 = 2$ and $s = 1$ for γ.

72

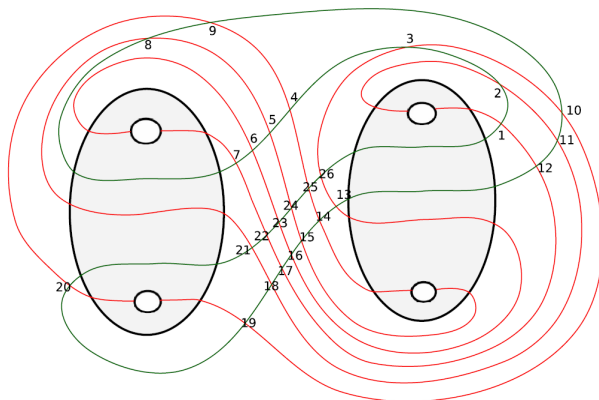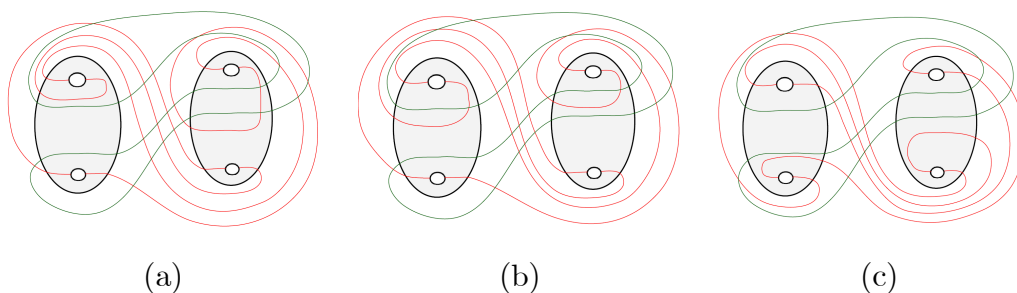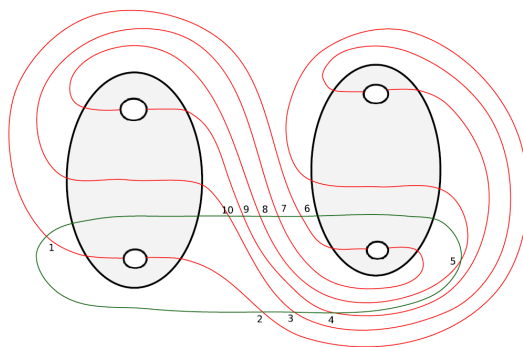**Figure 4.90** A model of the case when $n_2 = 2$ and $s = 1$ for γ.
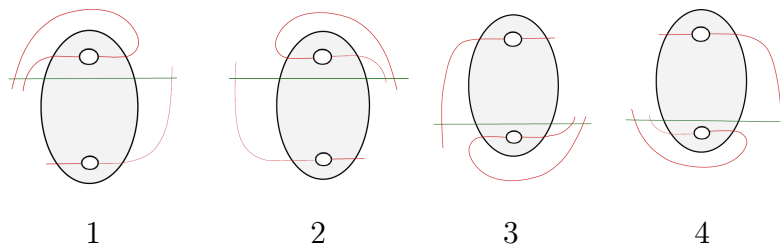
All the cases when there could be bypasses c along γ in Figure 4.90 are represented as the result of attaching bypass in Figure 4.91 (a) and (b). If we attach a bypass along $2 - 3 - 4$ and $4 - 1 - 2$, then we would obtain a convex sphere S with disconnected dividing set, contradicting tightness. It is clearly seen that U_2 was not destabilized since it has $tb = -3$ as seen in Figure 4.91 (a) and (b).

(a)   (b)

Figure 4.91 a) Γ_A after bypass along $1 - 2 - 3$, b) Γ_A after bypass along $3 - 4 - 1$.

2. Figure 4.92 illustrates a model of the case when $n_2 = 2$ and $s = 1$ for γ'.

Figure 4.92 A model of the case when $n_2 = 2$ and $s = 1$ for γ'.

All the cases when there could be bypasses c along γ' in Figure 4.92 are represented as the result of attaching bypass in Figure 4.93 (a) and (b). If we attach a bypass along $1 - 2 - 3$ and $3 - 4 - 1$, then we would obtain a convex sphere S with disconnected dividing set, contradicting tightness. If we attach a bypass along $2 - 3 - 4$, then we obtain a destabilization of U_2 and after the destabilization we see that the n_2 becomes 1 and $s = 0$. If we attach a bypass along $4 - 1 - 2$, then we do not see a destabilization of U_2 since it has still $tb = -2$ as seen in the Figure 4.93 (b).

(a)   (b)
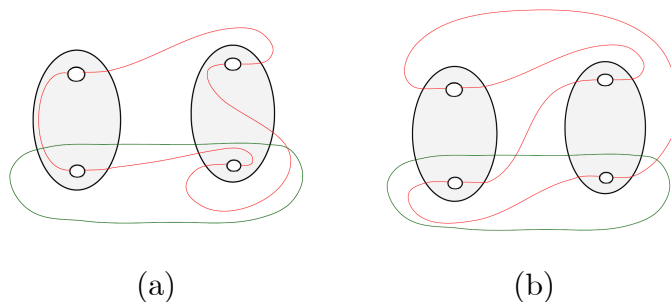
Figure 4.93 a) Γ_A after bypass along $2 - 3 - 4$, b) Γ_A after bypass along $4 - 1 - 2$.

3.2 Let $s = 3$.

1. Figure 4.94 illustrates a model of the case when $n_2 = 2$ and $s = 3$ for γ.

Figure 4.94 A model of the case when $n_2 = 2$ and $s = 3$ for γ.

All the cases when there could be bypasses c along γ in Figure 4.94 are represented as the result of attaching bypass in Figure 4.95 (a) and (b). If we attach a bypass along $1 - 2 - 3$, $3 - 4 - 5$, $4 - 5 - 6$, $5 - 6 - 7$, $7 - 8 - 1$ and $8 - 1 - 2$, then we would obtain a convex sphere $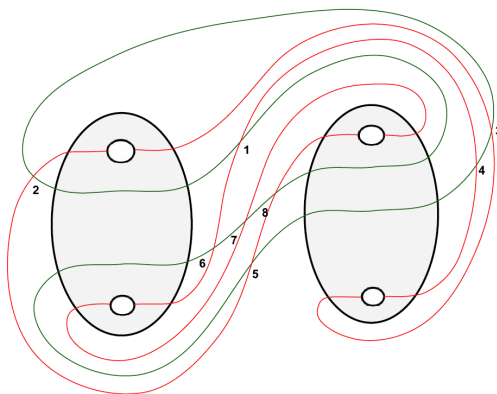S$ with disconnected dividing set, contradicting tightness. If we attach a bypass along $2 - 3 - 4$ and $6 - 7 - 8$ which is the case when $c \cap (P_1' \cup P_2')$ has no components, then we obtain a destabilization of U_2 and after the destabilization we see that the n_2 becomes 1. In Figure 4.95 (a) and (b), s, the slope of Γ_A becomes 1.

74

(a)   (b)

Figure 4.95 a) Γ_A after bypass along $2-3-4$, b) Γ_A after bypass along $6-7-8$.

2. Figure 4.96 illustrates a model of the case when $n_2 = 2$ and $s = 3$ for γ'.

Figure 4.96 A model of the case when $n_2 = 2$ and $s = 3$ for γ'.

All the cases when there could be bypasses c along γ' in Figure 4.96 are represented as the result of attaching bypass in Figure 4.97 (a), (b) and (c). If we attach a bypass along $1-2-3$, $3-4-5$, $4-5-6$, $5-6-7$, $7-8-1$ and $8-1-2$, then we would obtain a convex sphere S with disconnected dividing set, contradicting tightness. If we attach a bypass along $2-3-4$ and $6-7-8$ which is the case when $c \cap (P_1' \cup P_2')$ has no components, then we obtain a destabilization of U_2.

(a)   (b)   (c)

Figure 4.97 a) Γ_A after bypass along $2-3-4$, b) Γ_A after bypass along $4-5-6$, c) Γ_A after bypass along $5-6-7$.
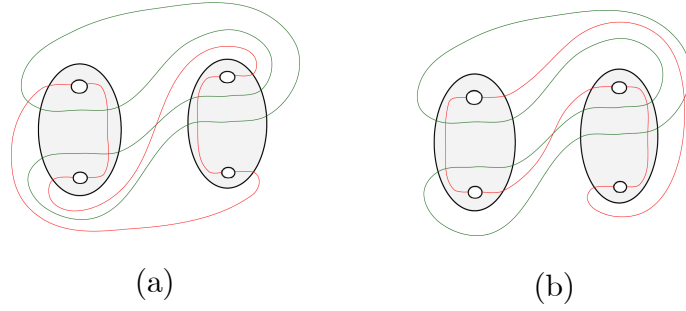
75

3.3 Let $s = -1$.

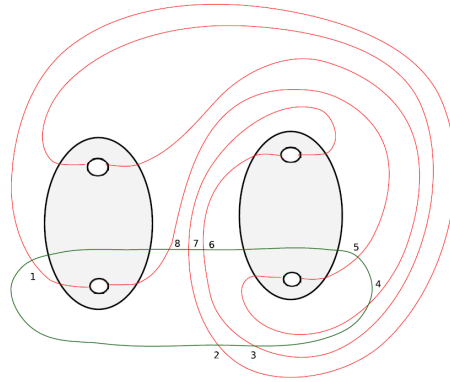**1.** Figure 4.98 illustrates a model of the case when $n_2 = 2$ and $s = -1$ for γ.
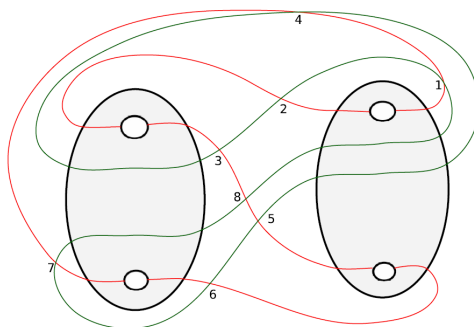
Figure 4.98 A model of the case when $n_2 = 2$ and $s = -1$ for γ.

All the cases when there could be bypasses c along γ in Figure 4.98 are represented as the result of attaching bypass in Figure 4.99 (a), (b), (c) and (d). If we attach a bypass along $1 - 2 - 3$ and $5 - 6 - 7$, then we would obtain a convex sphere S with disconnected dividing set, contradicting tightness. If we attach a bypass along $2 - 3 - 4$ and $8 - 1 - 2$ which are the subcase 2 and along $4 - 5 - 6$, $6 - 7 - 8$ which are the subcase 4, then we obtain a destabilization of U_2 and after the destabilization we see that the n_2 becomes 1 and $s = 0$.

Figure 4.99 a) Γ_A after bypass along $2 - 3 - 4$, b) Γ_A after bypass along $4 - 5 - 6$, c) Γ_A after bypass along $6 - 7 - 8$, d) Γ_A after bypass along $8 - 1 - 2$.
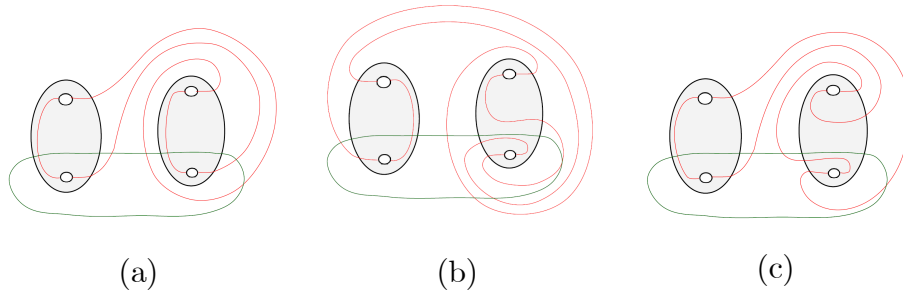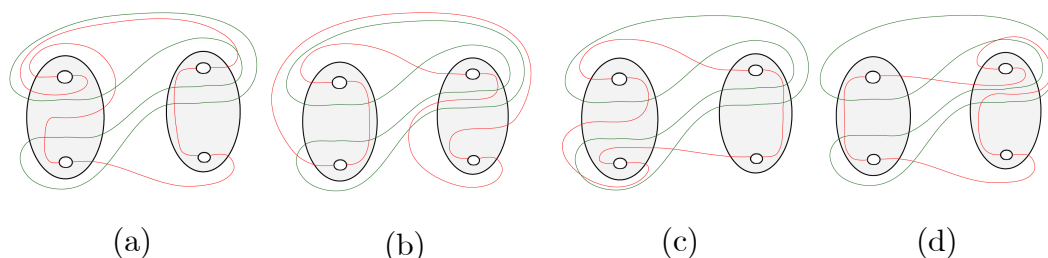
2. Figure 4.100 illustrates a model of the case when $n_2 = 2$ and $s = -1$ for γ'.

Figure 4.100 A model of the case when $n_2 = 2$ and $s = -1$ for γ'.

There does not exist any bypass c along γ', so we can not use γ' to destabilize U_2.

3.4 Let $s = -3$.

1. Figure 4.101 illustrates a model of the case when $n_2 = 2$ and $s = -3$ for γ.
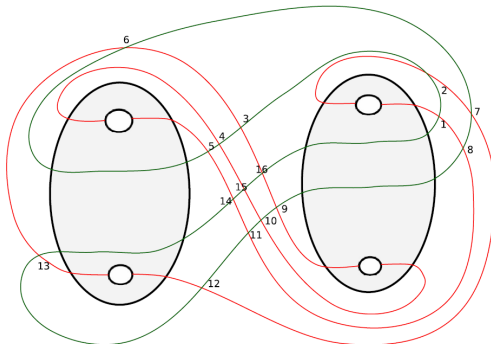
Figure 4.101 A model of the case when $n_2 = 2$ and $s = -3$ for γ.

If we attach a bypass along $4 - 5 - 6$, $7 - 8 - 9$, $13 - 14 - 15$, $16 - 1 - 2$ which are the subcase 3 and along $8 - 9 - 10$, $12 - 13 - 14$ and $15 - 16 - 1$ which are the subcase 4, then we obtain a destabilization of U_2 and after the destabilization we see that the n_2 becomes 1 and $s = -1$.

2. Figure 4.102 illustrates a model of the case when $n_2 = 2$ and $s = -3$ for γ'.
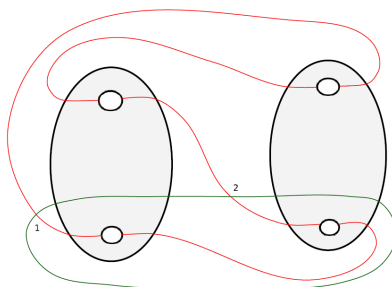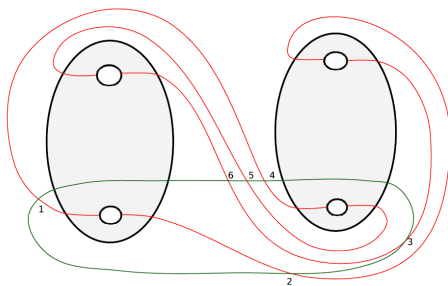

Figure 4.102 A model of the case when $n_2 = 2$ and $s = -3$ for γ'.

All the cases when there could be bypasses c along γ' in Figure 4.102 are represented as the result of attaching bypass in Figure 4.103 (a) and (b). If we attach a bypass along $2 - 3 - 4$, $3 - 4 - 5$, $5 - 6 - 1$ and $6 - 1 - 2$, then we would obtain a convex sphere S with disconnected dividing set, contradicting tightness. If we attach a bypass along $1 - 2 - 3$ and $4 - 5 - 6$ which is the case when $c \cap (P'_1 \cup P'_2)$ has no components, then we obtain a destabilization of U_2 and after the destabilization we see that the n_2 becomes 1 and $s = -1$.
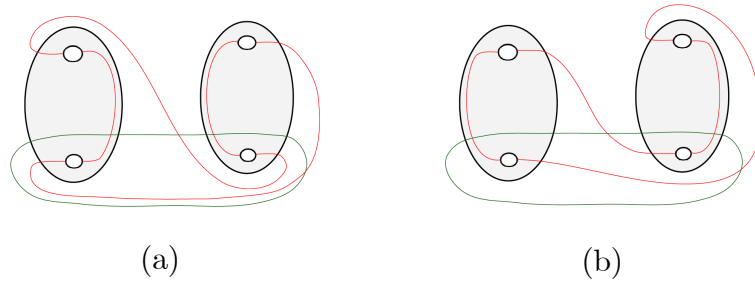
Figure 4.103 a) Γ_A after bypass along $1 - 2 - 3$, b) Γ_A after bypass along $4 - 5 - 6$.

After all, we classified the Legendrian Positive Whitehead links up to Legendrian isotopy and see that this link type is not Legendrian simple because of the fact that there are two Legendrian representatives with the maximal Thurston-Bennequin invariant and the same rotation number.

CHAPTER 5

FUTURE PLANS

The (Negative) Whitehead Link W_- is topologically isotopic to the link $O_1 \cup O_2$, with O_1 being the twist knot K_m when $m = -1$ and O_2 be the topological unknot B illustrated in Figure 4.7. See Figure 5.1. Take the Legendrian class of W_- as $U_1 \cup U_2$, such that U_1 and U_2 are a Legendrian representative of O_1 and O_2, respectively.

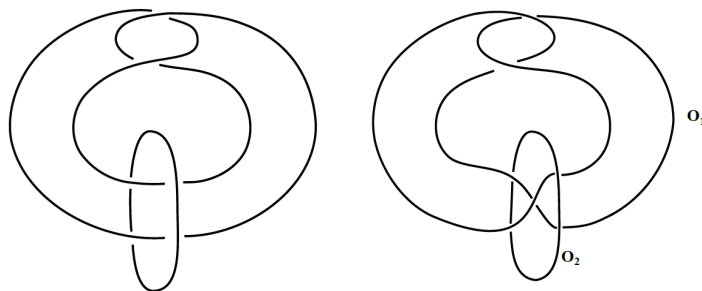**Figure 5.1** Whitehead Link W_- (left) is isotopic to $O_1 \cup O_2$ (right).

We cannot realize W_- with components consisting of Legendrian unknots with maximal tb since we have the inequality that $tb(W_-) \le -5$ by [**21**] for any Legendrian representative of W_-. In Figure 1.3, we see two Legendrian representatives of the Whitehead link W_- with maximal tb such that the components have Thurston-Bennequin number -1 and -4 for one of the Legendrian resspresentative of the link, and the components have Thurston-Bennequin number -3 and -2 for the other one. One can ask whether each of these two Legendrian representations of the Whitehead link W_- with maximal tb are unique representation or not. The other problem waiting an answer is a given Legendrian W_- say $U_1 \cup U_2$, then this link can be destabilized until each component has tb equal to $-4, -3, -2,$ or -1. We have shown the following.

Proposition 5.1 *A Legendrian realization of the (negative) Whitehead link W_- may be destabilized unless $(tb(U_1), tb(U_2))$ equals $(-4, -1)$, $(-3, -2)$, $(-2, -3)$, or $(-1, -4)$.*

This proposition will be proven in a forthcoming paper.

79

The other problems below whose answers we are looking for in future research are steps for the classification of the Legendrian negative Whitehead links in (S^3, ξ_{std}) giving as a conjecture below. The above proposition which we have proved is the other step for the classification.

Problem 5.1 *Let $U_1 \cup U_2$ be a Legendrian realization of the (negative) Whitehead link W_- having maximal $tb = -5$ such that $(tb(U_1), tb(U_2))$ equals $(-4, -1)$, $(-3, -2)$, $(-2, -3)$, or $(-1, -4)$. Is there a unique representation of each $U_1 \cup U_2$ with maximal $tb = -5$ for each $(tb(U_1), tb(U_2))$?*

Problem 5.2 *Let $U_1 \cup U_2$ be a Legendrian realization of the (negative) Whitehead link W_-. Can U_1 be destabilized if U_2 is stabilized once when $(tb(U_1), tb(U_2)) = (-4, -1)$? Can U_2 be destabilized if U_1 is stabilized once when $(tb(U_1), tb(U_2)) = (-3, -2)$? If U_2 is stabilized so its rotation number is 0 then is there a Legendrian isotopy interchanging U_1 and the stabilized U_2.*

To summarize for classification we should prove the next conjecture.

Conjecture 5.2 *The Legendrian (negative) Whitehead link W_- in (S^3, ξ_{std}) is Legendrian simple and every Legendrian representative of W_- is a stabilization of one of the links indicated in Problem 5.1 that is to one whose components have Thurston-Bennequin invariant and rotation numbers (tb, r) either $(-1, 0)$ and $(-4, \pm 1)$ or $(-3, 0)$ and $(-2, \pm 1)$.*

REFERENCES

[1] **Bennequin D** (1983) Entrelacements et equations de Pfaff. *Asterisque*, 107-108: 87–161.

[2] **Chekanov Y** (2002) Differential algebra of Legendrian links. *Inventiones mathematicae*, 150 (3): 441–483.

[3] **Chmutov S and Goryunov V** (1997) Polynomial invariants of Legendrian links and their fronts. *Proceedings of Knots '96, World Scientific Publishing Co.*, 239–256.

[4] **Dalton J** (2008) Legendrian torus links. *Ph. D. thesis*, Bryn Mawr College, Bryn Mawr, Pennsylvania, United States.

[5] **Ding F and Geiges H** (2007) Legendrian knots and links classified by classical invariants. *Communications in Contemporary Mathematics*, 9 (2): 135–162.

[6] **Eliashberg Y** (1992) Contact 3−manifolds twenty years since J. Martinet's work. *Annales de l'Institut Fourier,* 42: 165–192.

[7] **Eliashberg Y** (1998) Invariants in contact topology. *Documenta Mathematica*, 2: 327–338.

[8] **Eliashberg Y and Fraser M** (1998) Classification of topologically trivial Legendrian knots. *CRM Proc. Lecture Notes, Amer. Math. Soc., Providence, RI*, 15: 17–51.

[9] **Epstein J, Fuchs D and Meyer M** (2001) Chekanov-Eliashberg invariants and transverse approximations of Legendrian knots. *Pacific Journal of Mathematics,* 201 (1): 89–106.

[10] **Etnyre J B** (2003) Introductory Lectures on Contact Geometry. *Proc. Sympos. Pure Math.*, 71: 81–107.

[11] **Etnyre J B** (2005) Legendrian and transversal knots. *In Handbook of knot theory*, Elsevier B. V., Amsterdam, 105–185

[12] **Etnyre J B and Honda K** (2001) Knots and contact geometry I: Torus knots and the Figure Eight Knot. *Journal of Symplectic Geometry*, 1 (1): 63–120.

[13] **Etnyre J B and Vertesi V** (2017) Legendrian satellites. *International Mathematics Research Notices*, 2018 (23): 7241–7304.

[14] **Etnyre J B, LaFountain D and Tosun B** (2012) Legendrian and transverse cables of positive torus knots. *Geometry&Topology*, 16: 1639–1689.

[15] **Etnyre J B, Ng L L and Vertesi V** (2013) Legendrian and transverse twist knots. *Journal of the European Mathematical Society (JEMS),* 15 (3): 451–512.

[16] **Fuchs D and Tabachnikov S** (1997) Invariants of Legendrian and transverse knots in the standard contact space. *Topology*, 36 (5): 1025–1053.

[17] **Tabachnikov S** (1997) Estimates for the Bennequin number of Legendrian links from state models for knot polynomials. *Math. Res. Let.* 4: 143–156.

[18] **Geiges H** (2008) *An introduction to Contact Topology.* ISBN: 978-0-521-86585-2, Cambridge Studies in Advanced Mathematics, 109, Cambridge University Press, Cambridge, 458 pp/s.

[19] **Geiges H and Onaran S** (2020) Legendrian Hopf Links. T*he Quarterly Journal of Mathematics*, 71: 1419–1459.

[20] **Honda K** (2002) Gluing tight contact structures. *Duke Mathematical Journal*, 115 (3): 435–478

[21] **Mohnke K** (2001) Legendrian links of topological unknots. *Contemporary Mathematics*, American Mathematical Society, Providence, RI, 279: 209–211.

[22] **Giroux E** (1991) Convexite en topologie de contact. *Commentarii Mathematici Helvetici*, 66: 637–677.

[23] **Kanda Y** (1998) On the Thurston-Bennequin invariant of Legendrian knots and non-exactness of Bennequin's inequality. *Inventiones mathematicae.* 133: 227–242.

[24] **Honda K** (2000) On the Classification of tight contact structures I. *Geometry & Topology,* 4(1): 309–368.

[25] **Honda K, Kazez W H and Matic G** (2007) Right-veering diffeomorphisms of compact surfaces with boundary. *Inventiones mathematicae*, 169 (2): 427–449.

[26] **Ng L L** (2003) Computable Legendrian Invariants. *Topology*, 42 (1): 55–82.

[27] **Rudolph L** (1990) A congruence between link polynomials. *Mathematical Proceedings of the Cambridge Philosophical Society,* 107 (2): 319–327.

[28] **Onaran S (**2018) Legendiran torus knots in Lens spaces. *Turkish Journal of Mathematics,* 42: 936–948.

[29] **Özbağcı B and A I Stipsicz** (2004) *Surgery on Contact 3−manifolds and Stein Surfaces.* ISBN 978-3-540-22944-5, Bolyai Society Mathematical Studies, 13. Springer-Verlag, Berlin; J´anos Bolyai Mathematical Society, Budapest, 284 pp/s.

[30] **Tosun B** (2013) On the Legendrian and transverse classification of cablings. *Mathematical Research Letters,* 20 (4): 787–803.

CURRICULUM VITAE

PERSONAL INFORMATION

Name, Surname: Ece Gülşah ÇOLAK

Nationality: Turkish (T.C.)

EDUCATION

Degree	Institution	Year of Graduation
MSc	Bülent Ecevit University, Mathematics	2009-2011
MSc	Uludağ University, Pedagogical Formation	2007-2008
BS	Anadolu University, Mathematics	2002-2007
High School	Bursa Anadolu Lisesi	1998-2002

FOREIGN LANGUAGE

English

FIELD OF STUDY

Major Field: Contact Topology, Knot Theory, Geometry and Topology of Manifolds